Modeling the Thermal Diffusion Coefficients

Gonzales Bagnoli, Mariana G.

Publication date:
2004

Document Version
Publisher's PDF, also known as Version of record

Modeling the Thermal Diffusion Coefficients

Mariana Gabriela Gonzalez Bagnoli

2004

Ph.D. Thesis

DTU

TECHNICAL UNIVERSITY OF DENMARK
DEPARTMENT OF CHEMICAL ENGINEERING
CENTER FOR PHASE EQUILIBRIA AND SEPARATION PROCESSES (IVC-SEP)

Modeling the Thermal Diffusion Coefficients

Mariana Gabriela González Bagnoli

Ph.D. Thesis, September 2004

Center for Phase Equilibria and Separation Processes (IVC-SEP)
Department of Chemical Engineering
Technical University of Denmark
DK-2800 Lyngby, Denmark

ISBN 87-91435-14-5

Printed by Book Partner, Nørhaven Digital.

Copenhagen, Denmark.

Dedicated to

My family, my recently born niece and all my friends around the world

Preface

This thesis is submitted in partial fulfillment of the requirements for the Ph.D. degree at the Technical University of Denmark (Danmarks Tekniske Universitet).

This work has been conducted at the Department of Chemical Engineering (Institut for Kemiteknik) from August 2001 to September 2004 under the supervision of Associate Professor Alexander A. Shapiro and Professor Erling H. Stenby. The Danish Technical Research Council is kindly acknowledged for financial support.

I would like to thank Professor Stenby for providing me the opportunity to work with such a scientifically interesting project in the IVC-SEP group. I would like to express my gratitude to Professor Shapiro for his help and guidance through this project. Also in this regard, I would like to thank Guillaume Galliero for his help, his inspiring discussions and his huge enthusiam. Additionally, I greatly appreciate the help of Francois Montel for his fruitful discussions and making my stay in Pau (France) very pleasant. I would also like to thank Professor Jean Claude Legros for making my stay in Université Libre de Bruxelles very pleasant and Professor Stefan Van Vaerenbergh for his contributions and suggestions. Also I would like to thank all the colleagues as well as friends in the IVC-SEP group for the nice time we had together. My gratitude and appreciation go also to Mrs. Annelise Kofod and Mrs. Anne Louise Biede for being very supportive and helpful with the administrative work.

Last -but definitely not least- I would like to express my deepest gratitude to my beloved family and to my friend Maria Dolores Campos Velarde for their endless moral support, patience and understanding.

Kongens Lyngby, September 2004

Mariana G. González Bagnoli

(Author)

Synopsis

The thermal diffusion effect has been studied intensely during the past 150 years. Many researchers have developed different techniques to measure this effect and deduced theories to explain it. However, only recently, there has been an agreement on the values of the thermal diffusion coefficients measured by different techniques. Theoretically, there exists a rigorous approach based on the kinetic gas theory which explains the thermal diffusion effect for ideal gas mixtures. For liquids, the theories developed are not that accurate and still there is a lack of understanding the basis of the effect for these mixtures. The situation becomes more complicated when considering multicomponent mixtures. The background and main goal of this project is presented in Chapter 1.

In Chapter 2 we present a comprehensive review of different thermodynamic models proposed along the years to estimate the thermal diffusion factor. Most of these models are based on the theoretical explanation given by Denbigh. He introduced the concept of the heats of transport to explain the thermal diffusion effect. The theories that followed his work present mainly different approaches to estimate the heats of transport.

In Chapter 3 we present description of the different setup used to measure the thermal diffusion effect. Advantages and disadvantages of each technique are discussed and a global conclusion is made. Only in the past years researchers have come to an agreement on the value for the thermal diffusion coefficient for three binary mixtures measured by different setups.

Chapter 4 presents wide comparison between the existing thermodynamic models for the thermal diffusion factor and the available experimental data. Different equations of state are used for evaluation of the thermodynamic properties. The thermal diffusion factor is highly sensitive to the values of the partial molar properties and to the chosen model.

In Chapter 5 we present a new model for estimating the thermal diffusion coefficient. This new approach is based on statistical mechanics and the

fluctuation theory. A solid basis for modeling the transport coefficients is introduced by this new approach.

In Chapter 6 we evaluate the thermal diffusion factor for multicomponent mixtures of ideal gases. Approach to such mixtures based on the kinetic gas theory. The expressions for estimating the thermal diffusion ratio give excellent results for binary mixtures. However, in the case of multicomponent systems the results are not so promising.

Evaluation of the thermal diffusion factor for multicomponent mixtures was extended onto non-ideal systems, in Chapter 7. We present general formulae for the thermal diffusion factor in multicomponent mixtures which different expressions may be derived. Comparison between the models and molecular dynamics simulations is presented.

In Chapter 8, conclusions and suggestions for future work are presented.

Dansk Resumé

Termodiffusionseffekten er blevet intenst studeret i de sidste 150 år. Mange forskere har udviklet forskellige teknikker til måling af denne effekt og udledt teorier for at forklare den. Imidlertid er det først for nylig, at der har været enighed med hensyn til værdierne af de termodiffusionskoefficienter, der er målt ved hjælp af forskellige teknikker. Der er teoretisk en rigoristisk fremgangsmåde, baseret på den kinetiske gasteori, som forklarer termodiffusionseffekten for ideale gasblandinger. For væsker er de udviklede teorier ikke så nøjagtige, og der mangler stadig forståelse af grundlaget for effekten for disse blandinger. Situationen kompliceres yderligere, når multikomponentblandinger tages i betragtning. Baggrunden og hovedformålet med dette projekt præsenteres i kapitel 1.

I kapitel 2 præsenterer vi en omfattende oversigt over forskellige termodynamiske modeller, der er blevet foreslået i årenes løb til beregning af termodiffusionsfaktoren. De fleste af disse modeller er baseret på Denbighs teoretiske forklaring. Han indførte konceptet med transportvarme for at forklare termodiffusionseffekten. De teorier, der fulgte hans arbejde, præsenterer hovedsageligt forskellige fremgangsmåder til beregning af transportvarme.

I kapitel 3 giver vi en beskrivelse af forskellige opstillinger, der er anvendt til målinger af termodiffusionseffekten. Fordele og ulemper ved hver teknik diskuteres, og en overordnet konklusion drages. Først i de sidste år er forskerne nået til enighed om værdien for termodiffusionskoefficienten for tre binære blandinger målt ved forskellige opstillinger.

Kapitel 4 præsenterer en vidtspændende sammenligning mellem de eksisterende termodynamiske modeller for termodiffusionsfaktoren og de foreliggende eksperimentelle data. Forskellige tilstandsligninger anvendes til vurdering af de termodynamiske egenskaber. Termodiffusionsfaktoren er særdeles følsom over for værdierne af partielle molære egenskaber og den valgte model.

I kapitel 5 fremlægger vi en ny model til beregning af termodiffusionskoefficienten. Denne nye fremgangsmåde er baseret på statistisk mekanik og fluktuationsteorien.

Et solidt grundlag for modellering af transportkoefficienterne indføres med denne nye fremgangsmåde.

I kapitel 6 vurderer vi termodiffusionsfaktoren for ideale gassers multikomponentblandinger. Fremgangsmåden for sådanne blandinger er baseret på den kinetiske gasteori. Udtrykkene for beregning af termodiffusionsratioen giver udmærkede resultater for binære blandinger. Imidlertid er resultaterne ikke så lovende for multikomponentsystemer.

Vurderingen af termodiffusionsfaktoren for multikomponentblandinger bliver udvidet til ikke-ideale systemer i kapitel 7. Vi fremlægger generelle formler for termodiffusionsfaktoren i multikomponentblandinger, hvoraf forskellige udtryk kan udledes. Der gives en sammenligning mellem modellerne og molekylære dynamiksimuleringer.

I kapitel 8 gives konklusioner og forslag til kommende arbejde.

Contents

List of Figures

List of Tables

Chapter 1

Introduction

The thermal diffusion effect was first observed by Ludwig in 1856, and later studied by Soret in 1880. It is also known as the Ludwig-Soret effect. It can simply be described as the relative motion of species in a uniform mixture due to temperature gradient. It is an important cross coupling phenomenon observed in non-isothermal systems. The Dufour effect is inverse: A heat flux is created due to an isothermal diffusion process. Both the Soret and the Dufour effects are directly connected to isothermal diffusion.

Many transport processes induced by temperature gradient take place in situations of basic and practical interest. Diffusion effects are much slower than the heat transport. The isothermal diffusion and the Soret effects are of fundamental importance for description of natural convection. It has been observed that thermal convection decreases due to the Soret effect, since concentration gradients are relaxed by diffusion. It is therefore important to know the whole set of isothermal and thermal diffusion coefficients to correctly describe the transport processes in a system exhibiting convection. A particular example of thermodiffusion is the thermohaline convection in oceans [33]. Salinity gradients are studied in connection with the temperature differences and water circulation in oceans. Other studies of the thermohaline convection were carried out for aqueous lithium chloride solutions [17].

The thermal diffusion effect may play an important role in metallic alloys. The physical parameters as well as the morphological stability of solidification front and the hydrodynamic stability are strongly dependent on the thermal diffusion effect,

even under small temperature gradients [127, 128]. Hydrodynamic instabilities and Rayleigh convection make it difficult to measure the thermal diffusion effect on the Earth and, therefore, several microgravity experiments have been carried out on the international space station [90, 126]. Further studies on the effect of thermodiffusion in solids and in condensed systems were carried out in connection with the electrical properties of conductors and semiconductors [4, 15, 61] and, in particular, with the problems of damage of the metal-oxide-semiconductor [79]. The thermal diffusion effect was taken into account to describe water fluxes on the surface of Mars [58]. In geology, the Ludwig-Soret effect was studied in connection to the origin of the deformed Proterozoic anorthositic massif [95].

The thermal diffusion effect in gases has been largely studied. Theoretically, Chapmann and Enskog [14] derived a rigorous mathematical approach for estimating the thermal diffusion ratio, based on the gas kinetic theory. Excellent approximations were obtained for binary ideal gas mixtures. Experimentally, the thermal diffusion effect was studied in relation to the influence on the soot formation for ethylene-air flames [43]. It was observed that the addition of Helium to the air stream increases the thermal diffusion velocity, exceeding ordinary diffusion velocities. Dunlop [29] estimated the isothermal diffusion coefficients for gas mixtures by means of the thermal diffusion effect. Thermodiffusion works as a separation effect in industrial processes relevant to gases. In particular, gas separators were used in the fuel cycle of fusion nuclear reactors [56, 129].

A special area of thermodiffusion is thermophoresis: movement of particles due to the temperature gradient. Several important applications were developed in this particular area, as cleaning of particles from gas streams. Thermophoresis may also have a negative effect as, for example, in nuclear reactors, where transport of radioactive aerosols may cause serious accidents and may contribute to ambient pollution through airborne particle deposition [131].

A more recent application of thermodiffusion was related to macromolecules like DNA. The Soret coefficient was measured for this type of molecules. It was observed that a temperature difference may lead to DNA depletion. However, due to convection, depletion can be turned into accumulation. This suggests a possibility for

designing Soret-driven bio-reactors [10]. Special interest was given to the study of the thermal diffusion for polymers solutions [22, 89], asphaltenes [11] and other organic compounds [50], in connection to the thermal field-flow fractionation (ThFFF). This method employs the thermal diffusion effect in order to separate macromolecules and colloids [13, 82]. For example, one of its applications was determination of the molecular weights of asphaltenes. In the area of protein crystallization, the influence of the thermal diffusion effect on crystal growth was studied under microgravity conditions [81].

The present study was initiated in connection to chemical and, mainly, petroleum industry. The Soret effect may have a significant impact on the composition gradients in thick petroleum reservoirs. Its neglection may result in incorrect estimation for the GOC (gas-oil-contact) location and inaccurate evaluation of oil and gas in place [38]. Several methods are available for calculating the compositional gradient in the reservoir taking into consideration the gravity and the thermal gradient. However, in many cases, it was observed that the calculated profile differs from the actual one. Thus, it is important to estimate the thermodiffusion accurately. A detailed description of the reservoir, fundamental for petroleum industry, is required, as well as knowledge of all the phenomena occurring in the field [76–78].

One of the first theoretical approaches for calculation of the thermal diffusion effect in condensed phases was presented by Denbigh in 1951, who introduced the concept of heat of transport. After his publication, many researchers presented different approaches to estimate the heats of transport. An intensive literature review was carried out and the different models for estimating the thermal diffusion factor are presented in Chapter 2.

There are many experimental methods for measuring the thermal diffusion effect. We present these methods in Chapter 3. There are many inconsistencies in the available experimental data. The reported thermal diffusion coefficients for the same mixture may exhibit large deviations in the absolute values and even different sign. Only in the past years, researchers seemed to come to agreement in the measurement techniques. However, the reliable experimental data is still very scarce.

Comparison of the models with experimental data available shows that neither

of the models is capable of correct determining the thermal diffusion factor, not even the sign of the effect. A new theory for estimating the thermal diffusion coefficients is presented. The transport properties are described on the basis of statistical mechanics and the fluctuation theory. We show that the theory presents a solid basis for modeling the transport coefficients and in particular the thermal diffusion coefficient.

Normally, the transport processes deal with multicomponent mixtures and calculations for binary systems are not sufficient. Several thermodynamic models for prediction of the thermal diffusion factors, both for liquids and gases, have been proposed along the years. The majority of these models is applicable only to binary mixtures and, even if formulas to determine these coefficients in multicomponent systems exist, no results based on these formulae have been presented. In this area, we first evaluated the thermal diffusion effect in ideal gas ternary mixtures. We tested different approaches presented by Hirschfelder et al. [47] for estimating this coefficient. No experimental data has been reported in the literature. Hence we compared different theoretical approaches. We incorporated the corresponding states law, according to which the ternary mixture is considered as a binary mixture of a component and a pseudo-component. The properties of the pseudo component are estimated from the properties of the rest of the substances in the mixture. For non-ideal mixtures, we evaluated available thermodynamic models for estimation of the thermal diffusion factors. The experimental data available for this type of systems are very scarce and deal only with associated fluids and/or polymer solutions. Recently some measurements were carried out for ternary organic mixtures of heavy molecules [88]. Additionally, molecular dynamic simulations for an alcane ternary system were published [37]. We compared the results obtained by thermodynamic modeling with these data.

The thermal diffusion ratio in this thesis is defined as $k_i^T = -\nabla(\ln(z_i))/\nabla(\ln(T))$ where z_i is the mole fraction of component i and T the temperature. The common convention on the sign of the thermal diffusion factor is such that the component with the positive sign concentrates in the colder region.

150 years had passed since the thermodiffusion effect was first observed. A lot of

research has been carried out in this area. However this effect has not yet been fully understood. Investigations on thermodiffusion are currently being carried out in wide variety of fields. It is the intention of this work to provide one more mile-stone to the progress towards the general physical understanding of thermodiffusion and to contribute into building the theoretical scheme necessary for future prediction of the thermodiffusion coefficients.

Chapter 2

Existing models

This chapter presents the theory involved in the description of the thermal diffusion effect by means of thermodynamics of irreversible processes. Further, we will describe the approach developed by Denbigh, who introduced the heats of transport to describe the thermal diffusion effect. Finally, we present a summarized explanation of different models for estimation of the thermal diffusion factor.

2.1 Thermodynamics of irreversible processes

The thermal diffusion coefficient D^T, ratio k^T, factor α^T and Soret coefficient S^T are defined by means of the thermodynamics of irreversible processes, as presented by de Groot [23]. When diffusion is coupled with heat conduction, cross-phenomena appear, called the thermal diffusion (Soret effect in condensed phase) and the Dufour effect. The thermal diffusion represents the concentration gradient rised due to the temperature difference. The Dufour effect represents the heat flux created as the result of the diffusion process. Therefore, the Dufour effect is considered to be inverse to the Soret effect.

Equations developed from the thermodynamics of irreversible processes and definitions given for the coefficients will be presented according to the book of de Groot [23]. Let us consider a mixture of n components in a non-uniform temperature field. The second law of thermodynamics has the form of

$$T\frac{dS}{dt} = \frac{dU}{dt} + P\frac{dV}{dt} - \sum_k \mu_k \frac{dm_k}{dt} \tag{2.1}$$

where S is the total entropy of the system, U the total energy, μ_k the chemical potential of substance k. This equation is valid both for open and for closed systems. It can be writen in terms of intensive variables: specific entropy $s = S/M$, specific energy $u = U/M$, specific volume $v = V/M$, and concentrations $c_k = m_k/M$, M being the total mass of the system.

$$T\frac{ds}{dt} = \frac{du}{dt} + P\frac{dv}{dt} - \sum_k \mu_k \frac{dc_k}{dt} \tag{2.2}$$

It is shown [23] that equations (2.1) and (2.2) are equivalent if one keeps in mind Eurler relation and the specific Gibbs function (mean specific chemical potential) is:

$$g = \sum_k \mu_k c_k = \frac{\sum_k \mu_k \rho_k}{\rho} = u - Ts + Pv \tag{2.3}$$

De Groot stresses that equation (2.16) is supposed to be corrected when working with material derivatives. In this way, it is established that entropy s

does not explicitly depend on space and time coordinates but only through the variables u, v, and $c_k (k = 1, ..., n-1)$. For detailed proof of this postulate please refer to [23] .

The energy equation can be writen as

$$\rho\frac{d\left(\frac{1}{2}\mathbf{v}^2 + u\right)}{dt} = -\nabla\left(P\mathbf{v} + \mathbf{J}_q\right) + \sum_{k=1}^{n} \mathbf{F}_k \bullet \mathbf{v}_k \rho_k \tag{2.4}$$

where u is the internal energy per unit mass, v_k the velocity of k, $\mathbf{J}_q$ is called the flow of heat.

The force equation has the form of

$$\rho\frac{d\mathbf{v}}{dt} = -\nabla P + \sum_{k=1}^{n} \mathbf{F}_k \rho_k \tag{2.5}$$

where $\mathbf{v}$ is the center of mass velocity, P is the pressure and $\mathbf{F}_k$ is the external force per unit of mass acting on substance k. Viscous forces are neglected.

By multiplying equation (2.5) by $\mathbf{v}$ and then substracting it from the energy equation (2.4), the equation for change of energy u is obtained

$$\rho\frac{du}{dt} = -P\nabla\mathbf{v} - \nabla\mathbf{J}_q + \sum_k \mathbf{F}_k \bullet \mathbf{J}_k \tag{2.6}$$

The mass conservation law can be writen as

$$\rho\frac{dc_k}{dt} = -\nabla\mathbf{J}_k + \nu_k \mathsf{J}_c \tag{2.7}$$

where ρ is the density of the system, c_k the concentration of component k in the system, t is the time variable, $\mathbf{J}_k$ the flux of component k, J_c mass exchange due to chemical reactions and ν_k the rate of reaction. We will neglect chemical reactions, therefore $\mathsf{J}_c = 0$.

Introducing equation (2.6) and (2.7) into equation (2.16) together with the continuity equation results in the entropy balance equation

$$\rho T\frac{ds}{dt} = -\nabla\mathbf{J}_q + \sum_k \mathbf{F}_k \bullet \mathbf{J}_k + \sum_k \mu_k \nabla\mathbf{J}_k \tag{2.8}$$

It can be rewriten in the following way

$$\rho\frac{ds}{dt} = -\nabla\left(\frac{\mathbf{J}_q - \sum_k \mu_k\mathbf{J}_k}{T}\right) + \frac{\mathbf{J}_q + \sum_k \mathbf{J}_k \bullet \mathbf{X}_k}{T} = -\nabla\mathbf{J}_s + \sigma \tag{2.9}$$

where

$$\mathbf{X}_u = -\frac{\nabla T}{T} \tag{2.10}$$

$$\mathbf{X}_k = \mathbf{F}_k - T\nabla\frac{\mu_k}{T} \tag{2.11}$$

From equation (2.9) it may be noticed that the change of entropy of the system has two main contributions: the negative divergence of the entropy flow $\mathbf{J}_s$ and the entropy production σ. This last term is the sum of the products of "fluxes" $\mathbf{J}_k$ and $\mathbf{J}_q$ and the corresponding "forces" $\mathbf{X}_u$ and $\mathbf{X}_k$.

Linear relations between fluxes and forces can be assumed, as a first approxima-

tion. The so-called Onsager phenomenological relations are

$$\mathbf{J}_i = \sum_{k=1}^{n} L_{ik}\mathbf{X}_k + L_{iu}\mathbf{X}_u \tag{2.12}$$

$$\mathbf{J}_q = \sum_{k=1}^{n} L_{uk}\mathbf{X}_k + L_{uu}\mathbf{X}_u \tag{2.13}$$

The Onsager reciprocal relations are: $L_{ik} = L_{ki}$ and $L_{iu} = L_{ui}$.

The entropy production can be writen in terms of the fluxes and forces as

$$T\sigma = \sum_{i=1}^{n} \mathbf{J}_i\mathbf{X}_i + \mathbf{J}_q\mathbf{X}_u \tag{2.14}$$

The mass conservation equation (2.7) can be written with respect to the center of mass movement, assuming the form $\sum_{k=1}^{n} \mathbf{J}_k = 0$. Introducing this last expression into equation (2.14) we obtain

$$T\sigma = \sum_{i=1}^{n} \mathbf{J}_i \left(\mathbf{X}_i - \mathbf{X}_n\right) + \mathbf{J}_q\mathbf{X}_u \tag{2.15}$$

The following realations exist between the phenomenological coefficients

$$\sum_{k=1}^{n} L_{ik} = 0 \quad , \quad \sum_{k=1}^{n} L_{uk} = 0 \tag{2.16}$$

$$\sum_{i=1}^{n} L_{ik} = 0 \quad , \quad \sum_{i=1}^{n} L_{iu} = 0 \tag{2.17}$$

Introducing these relations into the expressions (2.23) and (2.13), we obtain:

$$\mathbf{J}_i = \sum_{k=1}^{n-1} L_{ik} \left(\mathbf{X}_k - \mathbf{X}_n\right) + L_{iu}\mathbf{X}_u \qquad (i = 1, ..., n-1) \tag{2.18}$$

$$\mathbf{J}_q = \sum_{k=1}^{n-1} L_{uk} \left(\mathbf{X}_k - \mathbf{X}_n\right) + L_{uu}\mathbf{X}_u \tag{2.19}$$

In equation (2.18) we have only $n-1$ independent fluxes. Taking into consideration Onsager relations, we find that there are $\frac{1}{2}(n+1)n$ independent coefficients. The coefficients L_{iu} are then replaced by new coefficients, Q_k^*. They are defined as

solutions of the system of equations

$$L_{iu} = \sum_{k=1}^{n-1} L_{ik} Q_k^* \tag{2.20}$$

Substituting them into equation (2.18) we obtain:

$$\mathbf{J}_i = \sum_{k=1}^{n-1} L_{ik} \left(\mathbf{X}_k - \mathbf{X}_n + Q_k^* \mathbf{X}_u \right) \tag{2.21}$$

Q_k^* represent the heat transported with the unity of mass k at uniform temperature ($\mathbf{X}_u = 0$).

Replacing X_k and X_u in equation (2.21) by their definitions, (2.10) and (2.11), we get

$$\mathbf{J}_i = \sum_{k=1}^{n-1} L_{ik} \left(\mathbf{F}_k - \mathbf{F}_n - T\nabla \left(\frac{\mu_k - \mu_n}{T} \right) - Q_k^* \frac{\nabla T}{T} \right) \tag{2.22}$$

The chemical potentials are functions of both temperature, pressure and composition. Therefore

$$\nabla \mu_i = -s_k \nabla T + v_k \nabla P + \sum_{k=1}^{n} \frac{\partial \mu}{\partial c_i} \nabla c_i \tag{2.23}$$

where s_k is the specific entropy and v_k is the specific volume of component k. The flux can be writen now as

$$\mathbf{J}_i = \sum_{k=1}^{n-1} L_{ik} \left(\mathbf{F}_k - \mathbf{F}_n - (v_k - v_n)\nabla P - \sum_{j=1}^{n-1} \frac{\partial \left(\mu_k - \mu_n \right)}{\partial c_j} \nabla c_j - (Q_k^* - h_k + h_n) \frac{\nabla T}{T} \right) \tag{2.24}$$

where $h_k = \mu_k + T s_k$ is the partial specific enthalpy of component k.

The definitions for the different coefficients describing the thermal diffusion effect are given only for binary mixtures.

For a binary mixture the flux equation becomes

$$\mathbf{J}_1 = -\mathbf{J}_2 = L_{11}\left(\mathbf{F}_1 - \mathbf{F}_2 - (v_1 - v_2)\nabla P - \frac{1}{c_2}\frac{\partial \mu_1}{\partial c_1}\nabla c_1 - (Q_1^* - h_1 + h_2)\frac{\nabla T}{T}\right) \tag{2.25}$$

The diffusion coefficient D_{12} is defined by the following relation

$$\rho D_{12} = \frac{L_{11}}{c_2}\frac{\partial \mu_k}{\partial c_1} \tag{2.26}$$

Similarly, the thermal diffusion coefficient D_{12}^T is defined by

$$\rho D_{12}^T c_1(1 - c_1) = \frac{L_{11}(Q_1^* - h_1 + h_2)}{T} \tag{2.27}$$

Analogous definitions can be given using the mole fraction z_i instead of the weight fractions c_i. However this is valid only for binary systems and cannot be directly extended onto multicomponent mixtures. This is further discussed in Chapter 7.

Three possible combinations of the ordinary and thermal diffusion coefficients have been given by specific names:

1. The Soret Coefficient: $S_T = D_{12}^T/D_{12}$
2. The thermal diffusion factor: $\alpha = D_{12}^T T/D_{12}$
3. The thermal diffusion ratio: $k_T = D_{12}^T T c_1 c_2/D_{12}$

If no external forces exist and the system is under mechanical equilibrium (equation (2.25)) we obtain the expression for $\mathbf{J}_i$ only in terms of ∇c_i and ∇T. For binary mixture,

$$\mathbf{J}_1 = -\mathbf{J}_2 = -D_{12}\rho\nabla c_1 - D_{12}^T \rho c_1(1 - c_1)\nabla T \tag{2.28}$$

A particular case to be considered is a stationary state where all diffusion flows vanish, $\mathbf{J}_i$ =0, but a heat flow still exists $\mathbf{J}_q \neq 0$. Equation (2.25) becomes

$$D_{12}\nabla c_1 - D_{12}^T c_1(1 - c_1)\nabla T = 0 \tag{2.29}$$

From this equation, the relations between the thermal diffusion coefficients, ratio, factor and Soret coefficient, and the gradients of concentration and temperature are obtained

$$S_T = -\frac{\nabla c_j}{c_1(1-c_1)\nabla T} \tag{2.30}$$

$$\alpha = -\frac{T\nabla c_j}{c_1(1-c_1)\nabla T} \tag{2.31}$$

$$k_T = -\frac{T\nabla c_j}{\nabla T} \tag{2.32}$$

2.2 The Denbigh theory

To estimate the thermal diffusion effect, many authors have proposed different correlations. Denbigh [25] was the first to describe in a clear way this effect by means of thermodynamics of the steady state. He introduced the concept of heat of transport. After his work many authors proposed different correlations to estimate the heats of transport. A review of this models and correlations is presented here. We will start by presenting the theory of Denbigh.

Denbigh defined the steady state as a simplification of a real state where the processes involved are considered to be in pseudo-equilibrium and no spontaneous evolution takes place. This meant, for Denbigh, that macroscopic parameters such as temperature, pressure and composition are time independent at every point of the system, despite occurrence of the dissipative processes. The second law of thermodynamics postulates that the total change in entropy of a system and its surroundings resulting from a reversible process is zero whereas it is positive for irreversible process: $\sum S_i \geq 0$. Denbigh applied Thompson hypothesis to describe the thermal diffusion effect. Thompson used $\sum S_i = 0$ for the system at steady state, even if this is rigorously only valid for a system in equilibrium.

Figure 2.1 shows the imaginary setup used by Denbigh to describe the thermal diffusion effect. In this setup the temperatures in vessels I and II are held constant at

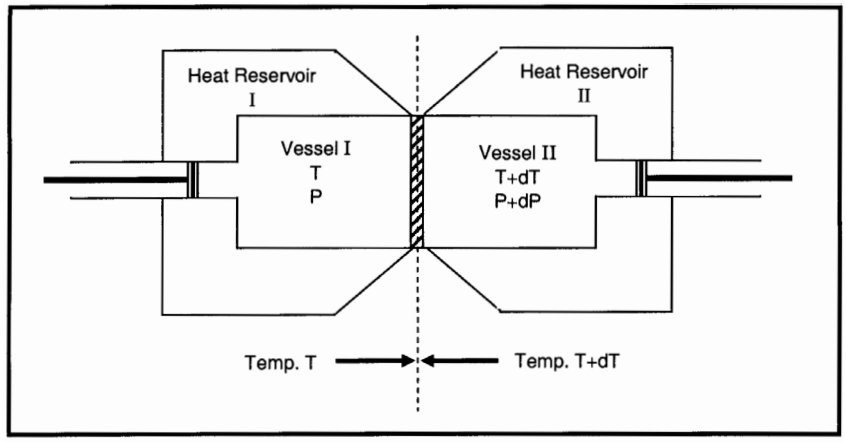

Figure 2.1: The Denbigh imaginary system used to describe the thermal diffusion effect

T and $T+dT$ by contact with infinite heat reservoirs, and each layer is separated by a purely imaginary plane. A heat flow is created due to existence of the temperature gradient. Let us assume that the system is a homogeneous mixture of n components, and flows of various components relative to each other may exist. We are dealing with a "virtual" displacement at the steady state comparable to the "virtual" changes in equilibrium theory. Considering the displacement of one mole of substance i from I to II, where both pressures and temperatures remain constant, we get an unchanged thermodynamic state. We can now consider different entropy changes in the system:

1- dS_{r1}= Entropy change due to the absorption of heat by the fluid from the reservoirs:

$$dS_{r1} = -\frac{H}{T} = -\frac{1}{T}\left(\frac{dH_i}{dT}dT + \frac{dH_i}{dP}dP + \sum_j \frac{dH_i}{dn_j}dn_j\right)$$

2- dS_{r2}= Entropy change in the reservoir due to transport of component i. Let us denote by Q_i^* the heat provided in reservoir I and removed from II (apart from the heat absorption by the enthalpy change) in order that a mole of this component may pass from I to II at constant temperature and pressure:

$$dS_{r2} = -\frac{Q_i^*}{T} + \frac{Q_i^*}{T+dT} = -\frac{Q_i^*}{T^2}dT$$

3- dS_f= Entropy change in the mole transferred due its change of state from (T, P) to $(T + \Delta T, P + \Delta P)$

$$dS_f = \frac{\partial S_i}{\partial T}dT + \frac{\partial S_i}{\partial P}dP + \sum_j \frac{\partial S_i}{\partial n_j}dn_j$$

Applying the Thompson hypothesis then the sum of dS_{r1}, $dS_{r2}$and dS_f is equal to zero and we obtain:

$$v_i dP + \sum_j \frac{\partial \mu_i}{\partial n_j}dn_j + \frac{Q_i^*}{T^2}dT = 0 \tag{2.33}$$

In a system in absence of rigid barriers the variation of pressure is negligible, so that the first term in the last equation vanishes. Further, in the case of an ideal system, the chemical potential of component i is:

$$\mu_i = \mu_i^0(T, P) + RT \ln z_i$$

Therefore, equation (2.33) results in the following expression for the thermal diffusion effect:

$$\frac{d \ln z_i}{dT} = -\frac{Q_i^*}{RT}$$

That is, the compositional variation per temperature difference is given as a function of a heat of transport of the particular component. Further, together with $\sum z_i = 1$, we get:

$$\sum n_i Q_i^* = 0$$

When considering a binary mixture, it is convenient to express the relative separation of species as:

$$-\frac{d \ln \left(\frac{z_1}{z_2}\right)}{dT} = \frac{Q_1^* - Q_2^*}{RT} \tag{2.34}$$

From equation (2.34) it follows that:

$$\alpha^T = \frac{Q_2^* - Q_1^*}{RT}$$

A more general expression is:

$$\alpha^T = \frac{a_1 Q_2^* - a_2 Q_1^*}{a\, z_1 \left(\frac{\partial \mu_i}{\partial z_1}\right)_{T,P}} \tag{2.35}$$

That is the thermal diffusion factor which depends on the "system of coordinates" with regard to which the relative motion of the species of the mixture is considered: whether it is associated with the center of masses, of volumes, or of molar amounts. Correspondingly $a_i = (i = 1, 2)$ are the partial molar properties corresponding to the system of coordinates selected: partial molar volumes V_i for the system associated with the center of volumes, molar masses M_i for the center of masses, and unities for the center of molar amounts. The value of a is an average determined as $a = a_1 z_1 + a_2 z_2$.

Denbigh explains the nature of the heats of transport by the analysis of energetic molecular motion. He declares that the total flux of energy differs from the flow of molecules multiplied by the average energy, since it may occur that the particles in various energy states do not pass through the cross-section at a proportional rate as the fluxes, as for example in processes where the particles have to exceed a certain energy before changing state. The heat of transport Q^* takes into consideration the difference between the energy per mole of transported fluid and the energy per mole of the fluid on either side.

2.3 Existing models for the thermal diffusion coefficient

After the work of Denbigh, several approaches to describe the heats of transport were developed. In earlier works the authors often proposed a thermodynamic model for the chemical potential along with an expression for the thermal diffusion factor. In

the following sections we will present different models found in the literature.

2.3.1 Rutherford and Drickamer

Rutherford and Drickamer [98] presented an approach to evaluate the heats of transport based on a molecular model. The mixture was considered to be a random distribution of molecules. Transport was represented as a process of filling and emptying the "holes" between the molecules. When the mixture was composed of molecules of approximately the same size and shape, the relative probabilities of a hole being filled by a molecule of type 1 or 2 were supposed to be related as (z_1/z_2), while the heats of filling and leaving a hole were expressed in terms of the partial molar enthalpies. Consequently, the thermal diffusion factor was found to be

$$\alpha_T^D = \frac{\left(z_1 h_1^{\frac{1}{2}} + z_2 h_2^{\frac{1}{2}}\right)\left(h_2^{\frac{1}{2}} - h_1^{\frac{1}{2}}\right)}{2\left(RT - z_1 z_2 \left(h_1^{\frac{1}{2}} - h_2^{\frac{1}{2}}\right)^2\right)} \tag{2.36}$$

The authors extended the theory to be applied to binary mixtures composed by particles of different sizes or shapes. Different modifications were proposed:

1- It was considered that not only one, but several molecules can move into a hole. Therefore, factor ψ_1 was incorporated, as the number of molecules moving into a hole left by molecule 1, with similar definition for ψ_2. An extra term was obtained, additional to the right-hand side of equation (2.36)

$$\alpha_T = \alpha_T^D + \frac{\left(\psi_1 - \psi_2\right)\left(z_1 h_1^{\frac{1}{2}} + z_2 h_2^{\frac{1}{2}}\right)}{2\left(RT + z_1 z_2 \left(\frac{\Delta V}{V}\right)^2 - z_1 z_2 \left(h_1^{\frac{1}{2}} - h_2^{\frac{1}{2}}\right)^2\right)} \tag{2.37}$$

2. A second approach was in taking into account different expressions for f_i (fraction of nearest neighbor) and CN_i (coordination number) when considering molecules of different size and shapes. In this case the results were presented in the two forms:

2.a. If $f_1 = f_2$ and $CN_1 \neq CN_2$

$$\alpha_T = \alpha_T^D + (h_1 h_2)^{\frac{1}{2}} \left(z_2 \left(\delta - 1\right) - z_1 \left(\frac{1}{\delta} - 1\right)\right) \tag{2.38}$$

where $\delta = (CN_1/CN_2)^{\frac{1}{2}}$. The results are discussed in terms of the ratio of the coordination numbers even if they can not be individually calculated. The authors claim that this second equation is physically less likely than equation (2.37).

2.b. For the case where $f_1 \neq f_2$ and $CN_1 = CN_2$ the authors give only the expression for the difference $f_1 - f_2$, see (2.39), and do not specify how it affects to the thermal diffusion factor.

$$f_1 - f_2 = \frac{h_2^{\frac{1}{2}}}{\left(z_1 h_1^{\frac{1}{2}} + z_2 h_2^{\frac{1}{2}}\right)} (\psi_2 - \psi_1) \tag{2.39}$$

3- Finally the third expression is given to take into account the interaction between unlike molecules, like in the case of the associated fluids. The equation for the thermal diffusion factor becomes

$$\alpha = \alpha^D = \frac{(z_2 z_1)\,\Delta + (\psi_1 - \psi_2)\left(\left(z_1 h_1^{\frac{1}{2}} + z_2 h_2^{\frac{1}{2}}\right)^2 + 2 z_1 z_2 \Delta\right)}{2\left(RT\left(1 + z_1 z_2 \left(\frac{\Delta V}{V}\right)^2\right) - z_1 z_2 \left(h_1^{\frac{1}{2}} - h_2^{\frac{1}{2}}\right)^2 - 2 z_1 z_2 \Delta\right)}$$

where $\Delta = h_{mix} - (h_1 h_2)^{\frac{1}{2}}$.

2.3.2 Dougherty and Drickamer

The following year Dougherty and Drickamer [27] presented an approach based on the previous work of Rutherford and Drickamer [98]. In this new theory the energies involved in the transport process were expressed in terms of partial molal cohesive energies of the components in solution. These energies, in turn, were expressed as functions of the internal energies of the mixtures and of the solution. The resulting expression for the thermal diffusion factor in case of the molecules of similar sizes is:

$$\alpha^T = \frac{1}{\tau} \frac{\left(u_1 - u_2 - \frac{\partial U_e}{\partial z_1}\right)}{z_1 \left(\frac{\partial \mu_1}{\partial z_1}\right)_{T,P}} \tag{2.40}$$

The coefficient $1/\tau$ is equivalent to assuming that the supplied energy by molecule

motion is $1/\tau$ times the cohesive energy of the liquid. According to the authors the value τ may be set to 4. The approach of Dougherty and Drickamer was extended onto molecules of different sizes, similar to Rutherford and Drickamer [98], obtaining the following expression:

$$\alpha_T = \frac{1}{\tau}\frac{\left(u_1 - u_2 - \frac{\partial U_e}{\partial x_1}\right)}{z_1\left(\frac{\partial \mu_1}{\partial z_1}\right)_{T,P}} + (\psi_1 - \psi_2)\frac{1}{\tau}\frac{(z_1 u_1 + z_2 u_2 + U_e)}{z_1\left(\frac{\partial \mu_1}{\partial z_1}\right)_{T,P}} \tag{2.41}$$

Coefficients ψ_1 and ψ_2 are expressed as functions of the molar volumes and of the correction factor η_i. They represent the excess (or deficiency) of volume resulting in the region when a certain amount of molecules type 1 is replaced by the two other quantities: one of the same type of molecules and the second amount of molecules of the type 2. The resulting expression is

$$\psi_i = \frac{v_i}{V}\left(1 + \frac{\eta_i}{v_i}\right)$$

The authors observed pressure and temperature dependency of ψ_i.

In the same year, Dougherty and Drickamer [28] presented a second approach where the heats of transport, Q_i^*, were calculated from viscosity measurements and the solution thermodynamic data. They expressed the thermal diffusion factor in terms of the activation energies $U_{a,i}$:

$$\alpha_T = \frac{(M_1 v_2 + M_2 v_1)}{2M}\frac{\left(\frac{U_{a,2}}{v_2} - \frac{U_{a,1}}{v_1}\right)}{z_1\left(\frac{\partial \mu_1}{\partial z_1}\right)_{T,P}} \tag{2.42}$$

Instead of the activation energies of the components in the mixture, Dougherty and Drickamer proposed to use individual activation energies of pure components, which may be determined from the viscosity data by the known Eyring formula

$$\eta_i = \frac{Nah}{V}\exp\left(\frac{\Delta F}{RT}\right) \tag{2.43}$$

The authors compared their formula with experimental data. In the calculations they were forced to make three mayor approximations, which are not inherent from the theory. Firstly, the pure component volumes were used instead of the partial

molar volumes. Secondly, the derivative of the chemical potential with respect to composition was assumed to be as for an ideal mixture. This second assumption may create large deviations. Finally, activation energies of the pure components were used instead of the activation energies in the mixture. The authors were not able to predict the error of this approximation. From the plots presented in the paper, one can see that the theoretical curves and the experimental one in most of the cases do not agree satisfactorily. However, some of them seem to predict the sign and the behavior of the thermal diffusion factor.

2.3.3 Tichacek et al.

In 1956 Tichacek et al. [121] presented a new approach the heats of transport. They based their theory on thermodynamics of irreversible processes and the steady state. In this new theory the heats of transport were described as functions of the activation energy, as was proposed by Dougherty and Drickamer in their second approach [28]. A difference with the previous model was that the model of Tichacek et al. depends only on the partial molar volumes and the activation energies and is independent of the molecular weights of the components as the previous model did. The thermal diffusion was expressed as

$$\alpha_T = \frac{1}{V} \frac{(v_1 U_{a,2} - v_2 U_{a,1})}{z_1 \left(\frac{\partial \mu_1}{\partial z_1}\right)_{T,P}} \tag{2.44}$$

The authors neglected non-ideality contributions, and they replaced the derivative of the chemical potential by RT. The activation energies were calculated in the same way, as for the previous model, applying equation (2.43).

2.3.4 Shieh

In 1969 Shieh [115] presented a new model for estimating the thermal diffusion factor. The author proposed to use unperturbed terms for the heats of transport in the equation given by Denbigh. Based on the Bearman-Kirkwood-Fixman theory [5], the thermal diffusion factor was represented as a function of the partial molar heats

of vaporization and the partial molar volumes, and the derivatives of the chemical potential

$$\alpha_T = \frac{v_1 E_2^{vap} - v_2 E_1^{vap}}{2V z_1 \left(\frac{\partial \mu_1}{\partial z_1}\right)_{T,P}} \tag{2.45}$$

In the reference paper, the author used experimental data for the heats of vaporization. Here we will determine the energies of vaporization by means of the Riedel method given in [96]. This method was tested for several types of mixtures and the errors were almost always less than 2 percent.

$$E^{vap} = 1.093 R T_c \left(T_{br} \frac{\ln P_c - 1.013}{0.930 - T_{br}}\right) \tag{2.46}$$

where R is the gas constant, T_c is the critical temperature, P_c the critical pressure and $T_{br} = T_b/T_c$ the reduced boiling temperature. In order to take into account the variations of the energy of vaporization with temperature the Watson relation may be applied

$$E_{T2}^{vap} = E_{T1}^{vap} \left(\frac{1 - T_{r2}}{1 - T_{r1}}\right)^{Exp^{vap}} \tag{2.47}$$

where Exp^{vap} was calculated according to Viswanath and Kuloor [96] recomendation

$$Exp^{vap} = \left(0.00264 \frac{E_{T1}^{vap}}{R T_b} + 0.8794\right)^{10}$$

2.3.5 Haase

In 1969 Haase [44] suggested a new expression for the thermal diffusion factor by exploiting analogy with baro-diffusion, where particle motion is studied due to pressure gradient in an isothermal system. According to Haase, the baro-diffusion factor for a binary mixture has the form of

$$\alpha_P = \frac{P M_1 \left(v_2 - v_2^0\right) - P M_2 \left(v_1 - v_1^0\right)}{\left(z_1 M_1 + z_2 M_2\right) z_1 \left(\frac{\partial \mu_1}{\partial z_1}\right)_{T,P}} + \alpha_P^0 \frac{RT}{z_1 \left(\frac{\partial \mu_1}{\partial z_1}\right)_{T,P}} \tag{2.48}$$

According to this equation, the baro diffusion factor α_P can be determined from the thermodynamic properties of the (real) gas mixture. α_P^0 is the barodiffusion factor corresponding to the pressure tending to zero.

Haase stated that in the case of thermal diffusion, the thermodynamics of irreversible processes produces no analogous relation as for baro-diffusion because there does not exist a general connection between diffusion and thermal diffusion (We will see later in section 2.3.7 that still there is a way to theoretically obtain the Haase expression [52, 53]). Nevertheless, Haase compares the relation between α_T and α_P. By substitution of the partial molar volumes by the partial molar enthalpies, a resulting expression for the thermal diffusion factor was obtained

$$\alpha_T = \frac{M_1\left(h_2 - h_2^0\right) - M_2\left(h_1 - h_1^0\right)}{\left(z_1 M_1 + z_2 M_2\right) z_1 \left(\frac{\partial \mu_1}{\partial z_1}\right)_{T,P}} + \alpha_T^0 \frac{RT}{z_1 \left(\frac{\partial \mu_1}{\partial z_1}\right)_{T,P}} \tag{2.49}$$

The limiting value α_T^0 can be obtained from the gas kinetic theory [47]. Similarity of equation (2.49) to the general expression (2.35) may be observed. The values of a_i for this case are equal to the molecular weights M_i and the heats of transport Q_i^* equal to the difference between the real and the ideal partial molar enthalpies $(h_i - h_i^0)$. The extra term, which computes the effect of the thermal diffusion in ideal gas state, does not change the main form of equation (2.35).

2.3.6 Shukla and Firoozabadi

Shukla and Firoozabadi [116] based their theory on the approach of Dougherty and Drickamer [28]. Their modified expression incorporates more accurate thermodynamic properties of a mixture expressed by means of the Peng-Robinson equation of state (PR EoS). Further, the non-equilibrium part in the model is accounted by incorporating the energy of viscous flow. The expression obtained for the thermal diffusion factor in a binary mixture has the form of:

$$\alpha_T = \frac{\left(\frac{u_1}{\tau_1} - \frac{u_2}{\tau_2}\right)}{z_1 \left(\frac{\partial \mu_1}{\partial z_1}\right)_{T,P}} + \frac{\left(v_2 - v_1\right)\left(z_1 \frac{u_1}{\tau_1} + z_2 \frac{u_2}{\tau_2}\right)}{\left(z_1 v_1 + z_2 v_2\right) z_1 \left(\frac{\partial \mu_1}{\partial z_1}\right)_{T,P}} \tag{2.50}$$

For practical calculations the authors use the values of $\tau_1 = \tau_2 = 4$. The authors

stated that these coefficients can be calculated by the relation between the energy of viscous flow and the energy of vaporization and viscosity, but they did not succeed to rigorously define them. Let us note that for the case where $\tau_1 = \tau_2 = 4$ equation (2.50) is reduced to equation (2.35) with a_i equal to partial molar volumes v_i and Q_i^* equal to $u_i/4$.

This approach has been extended onto multicomponent mixtures, as it is shown in Chapter 7.

2.3.7 Kempers

Kempers [52, 53] introduced a new way of calculating the thermal diffusion factor. Although his theory was developed for multicomponent mixtures, we would like to describe it first for the binary case. We will give the corresponding multicomponent formulations in Chapter 7.

The approach of Kempers consists in extending statistical mechanics onto a non-equilibrium two-bulb system (Figure 2.1). This is similar to the old Thompson approach, as described by Denbigh.

A single assumption was made that a non-equilibrium steady state is the macroscopic state accomplished by the maximum number of microstates with respect to the ideal gas state. The canonical partition function for the whole system was expressed as the product of the canonical partition functions of each bulb, and maximized under two constrains. In the first paper [52] the constrains were:

1. The material conservation $n_i^A + n_i^B = n_i^T (i = 1, ..., n)$.

2. Pressure equality in the whole system $P^A = P^B$.

The final expression for binary thermal diffusion factor was similar to equation (2.35):

$$\alpha_T = \frac{v_1 h_2 - v_2 h_1}{(z_1 v_1 + z_2 v_2)\, z_1 \left(\frac{\partial \mu_1}{\partial z_1}\right)_{T,P}} \tag{2.51}$$

Later, Kempers [53] in 2001 modified his model. The main difference with his

previous work was the constrains. Instead of the equality of pressure, he applied the following constrains

1. The material conservation $n_i^A + n_i^B = n_i^T (i = 1, ..., n)$
2. The material conservation of the components in the ideal gas state $n_i^{A0} + n_i^{B0} = n_i^A + n_i^B \ (i = 1, ..., n)$.
3. Invariability of the reference frame in which the process takes place (Center-of-volume or center-of-mass). For example, for the center of volume case, the constraint had the form of: $\sum n_i^A v_i^A = \sum n_i^B v_i^B$.

The constraint of mechanical equilibrium is not applied in the second approach. The final expression for the thermal diffusion factor with volume frame of reference was

$$\alpha_T = \frac{v_1 (h_2 - h_2^0) - v_2 (h_1 - h_1^0)}{(z_1 v_1 + z_2 v_2) z_1 \left(\frac{\partial \mu_1}{\partial z_1}\right)_{T,P}} + \alpha_T^0 \frac{RT}{z_1 \left(\frac{\partial \mu_1}{\partial z_1}\right)_{T,P}} \tag{2.52}$$

Kempers made an extensive comparison between his model and the model presented by Haase shown by equation (2.49). When the center of mass frame is used instead of the center of volume, equation (2.52) is reduced to that of Haase. As was mentioned previously, Haase obtained his expression purely by analogy with baro-diffusion, but Kempers could obtain the same expression applying thermodynamics of irreversible processes and statistical mechanics.

The ideal state is normally considered as a state at a small pressure, where the mixture becomes an ideal gas. In this case the value of α_T^0 is computed on the basis of the Boltzmann gas kinetic theory. The formula for the thermal diffusion ratios for binary mixtures, in the first approximation of the Chapman-Enskog expansion, may be found in Hirshfelder et al. [47]. In some cases it is assumed that the first term in the last equation is negligible compared to the second term. However, our experience indicates that this assumption is not always correct.

Although the authors of the papers cited above presented some comparison of their results with experimental data, this comparison usually was not very extensive. A more or less extensive comparison may only be found in Shukla and Firoozabadi

[116], and Kempers [53]. For simulation of partial molar properties the authors used available experimental data or the simplest equations of state, such like the Soave-Redlich-Kwong (SRK) and Peng-Robinson (PR) EoS [96]. It was noticed [53] that the thermal diffusion factors are extremely sensitive to the values of the partial molar properties and, thus, to an EoS selected. A systematic comparison of all the existing models on the same sets of experimental data and with different equations of state was presented in our publication [42]. This comparison is further extended to other types of mixtures and will be presented in Chapter 4.

Chapter 3

Measuring the thermal diffusion factor

150 years have passed since the thermal diffusion effect was firstly observed by Ludwig. Along these years researches have imagined, designed and created a wide variety of setup for measuring this effect. Measuring thermodiffusion is not an easy task. This effect is usually very small compared to convection and other transport phenomena. However, researchers have been very ingenious to develop setup in order to reduce, avoid or, in its worse, compute convection or other phenomena that may affect the measurements.

In this chapter we present a review of different methods used for measuring the thermal diffusion effect. The designations given for the techniques do not always agree. Hereby we propose a possible classification for the existing techniques. A complete list of the measured mixtures and the corresponding technique is given in table 4.1 of the next Chapter.

3.1 The thermogravitational column - TGC

Two types of geometries and three operational procedures were used for the thermogravitational columns. Further sub-classification can be made by the materials used for their construction. A concentric tube column and a parallel plate column are the two possible geometries for this type of apparatus. The second type of columns

may be operated in two different ways. In the classical technique, the system is closed. Once the steady state is reached the concentration gradients are measured. The second method was developed by Dutrieux et al. [30]. The Soret coefficients were estimated during the transient regime. This method was based on application of the Laser Doppler Velocimeter (LDV), as will be explained in section 3.2.

3.1.1 The concentric tube column

The Thermal diffusion column of Trevoy and Drickamer [124,125] is the oldest type of this setup we have found. It was used both to measure the diffusion and the thermal diffusion effects. This apparatus consists of two connected vessels mounted on a thermostat-tube inside a thermostat-bath. Water circulates through the thermostat-tube. The wall temperatures of the column are measured by thermocouples clamped against the wall. A typical run of the column starts by draining the bath. Then the column is filled with the mixture to be studied and, subsequently hermetically closed. It is important to prevent liking into the vessel. The bath is filled with water and its temperature is adjusted. Then water from the second thermostat starts circulating through the thermostat tube. The steady sate is reached in about 1 hour. The system evolves for a period between 4 to 10 hours. At the end of a run the thermostat bath is half drained and the content of the upper reservoir is taken out. The remaining water in the bath is then siphoned and the content of the second reservoir is extracted. The concentration is measured for each reservoir by refractive index, assuming a linear dependence between the concentration and the mole fraction. The original figure of the setup used by Trevoy and Drickamer [125] is shown in Figure 3.1.1.

The authors carried out several runs for small gradients of temperature $\Delta T \approx 5^oC$, in order to study the dependence of α^T on the temperature. It was therefore necessary to use relatively large annular space. As a consequence, small equilibrium separation ratios were obtained.

The authors used the separation ratio equation developed by Furry, Jones and Onsager. This equation is deduced from the Navier-Stokes system for the steady state separation in the thermal diffusion column and has the form of:

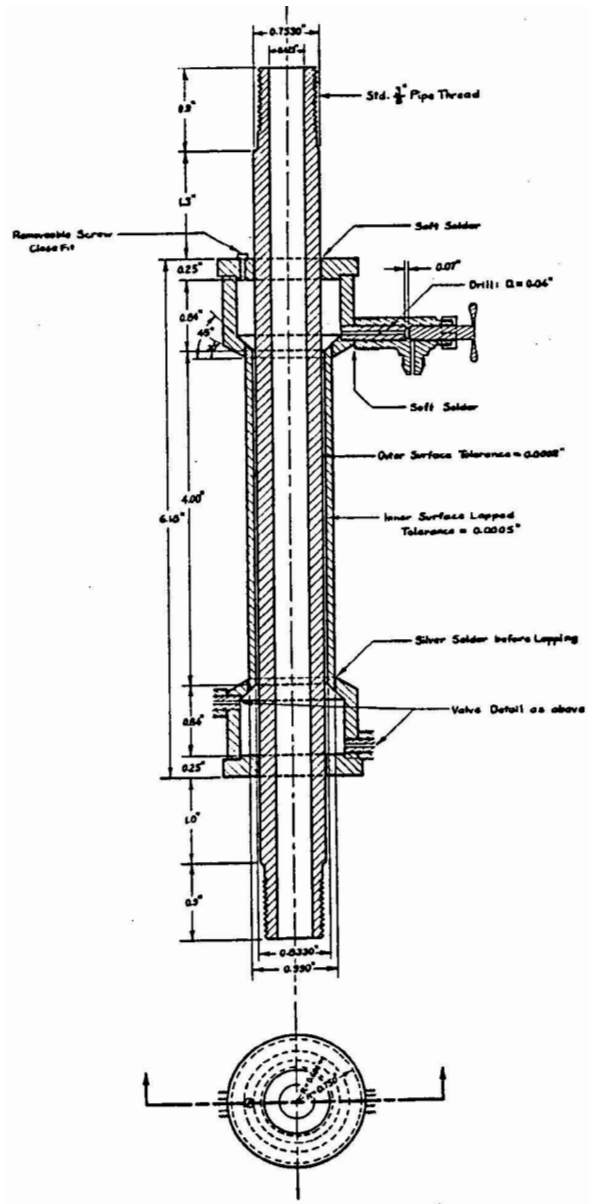

FIG. 1. Thermal diffusion column.

Figure 3.1: The original thermogravitational column of Trevoy and Drickamer [125]

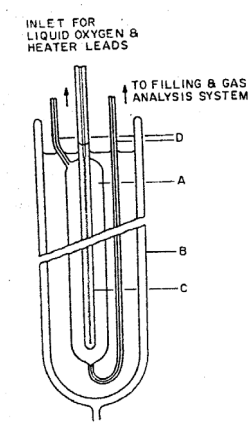

FIG. 1. Low-temperature thermal-diffusion column.

Figure 3.2: The original thermogravitational glass column of Humphreys and Mason [48]

$$\ln\left(\frac{(z_1/z_2)_{Top}}{(z_1/z_2)_{Bottom}}\right) = \left(\frac{63\alpha^T D_{12}\eta L}{2T\omega^4\beta}\right)\left(\frac{1}{1+5670\,(\eta D_{12}\,g\omega^3\beta\Delta T)^2}\right)$$

where z_1, z_2 are the mole fractions of component 1 and 2, D_{12} is the binary diffusion coefficient, η is the viscosity of the fluid, β is the thermal expansion coefficient, g is the gravity acceleration. Both the diffusion coefficients and the viscosity data were measured by the authors, while the density data were taken from standard tables [49]. The geometrical variables are: L the length of the column and ω half of the annular spacing.

The low-temperature thermogravitational column constructed in glass was used by Humphreys and Mason [48] in 1970 to measure the thermal diffusion effect in gas mixtures. The original sketch of the column is shown in Figure 3.2. The temperature gradient is obtained by using liquefied nitrogen at $77K$ and liquified oxygen at $90K$. The liquified nitrogen is contained in a special vessel (B) where the whole column is immersed. The oxygen is contained in tube (C) maintaining the proper temperature of the inner-wall. Capillary sampling tubes (D) are located at the top and at the bottom of the column. The experiments were performed at 0.5 atmospheres for various time periods, between 2 to 10 hours. Trace amounts of a radioactive substance are incorporated in the mixture before the run starts, in order to measure the composition at the top and at the bottom of the column.

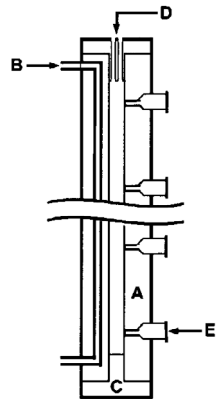

Figure 3.3: The parallel thermogravitational column

3.1.2 The parallel plate column

This type of setup is slightly different from the previous one. The liquid mixture to be studied is enclosed in a vertical slot and the upper and the lower reservoirs are eliminated. The two vertical walls are maintained at two different temperatures, so that the required ΔT is obtained. A sketch of this type of column is shown in Figure 3.3.

Once the steady state is reached, about 30 minutes after start, the concentration at the top and at the bottom of the column are measured by refractive index. The Soret coefficient is determined by the following relation:

$$\frac{\Delta c}{c_0(1-c_0)} = \Psi \frac{S_T \eta D_{12}}{\rho \beta}$$

where c_0 is the initial concentration, Δc is the steady-state separation between the column ends, Ψ is a parameter that depends on the geometrical dimensions of the column given by $\Psi = 504 L/g\,\omega^4$, where L is the distance between the sampling ports and ω is the gap width. The values for density, ordinary diffusion and viscosity were obtained from the literature. Other researchers [8] measured the isothermal diffusion coefficient by the "Open-ended capillary" (OEC) technique.

3.2 The Laser Doppler Velocimeter - LDV

Dutrieux et al. [30] presented a new technique for measuring the Soret coefficient utilizing modification of the velocity field under the influence of the Soret effect. The setup was the parallel thermogravitational column, where the hot and cold walls were connected by a glass strip, allowing optical access (Figure 3.3). With the help of the nozzles incorporated along the column it was possible to evaluate the concentration gradients as functions of the height.

The LDV technique is based on the fact that during the transient time the concentration gradient can be thought as mainly caused by the Soret effect. In other words, it has been observed that during the steady state the concentration gradient depends mainly on the vertical coordinate, and therefore the horizontal contribution may be neglected. On the other hand, in the transient regime the concentration gradient is mainly function of the horizontal coordinate, in the direction of the temperature gradient. This initial horizontal concentration gradient is mainly induced by the Soret effect. When the temperature gradient is established, the light substance migrates to the hot region in order to lower the local density. The LDV technique takes these phenomena into consideration and measures the Soret coefficient during the transient time. The maximum horizontal density gradient appears in diffusive regime, indicated by a larger velocity amplitude transient in time. This velocity amplitude inside the column is measured by Laser Doppler Velocimetry (LDV).

The thermal diffusion coefficient is determined by the following relation:

$$\Delta c \approx 504 \frac{\nu}{\beta g} D^T c_0 (1 - c_0) \frac{L}{\omega^4}$$

where c is the mass fraction and ν is the kinematic viscosity. The authors measured the kinematic viscosity and the thermal expansion coefficient themselves.

3.3 The two-chamber apparatus

The design of a two-chamber apparatus may be different, but the concept behind this technique is the same. The pressure cell used by Rutherford and Drickamer [98] and the cell used by Shashkov et al. [107] are based on the idea that a large volume difference between the chambers avoids convection. The difference between these two setups is in their construction and in the method used to change pressure in the system. In the two-chamber cell of Trengove et al. [122, 123] used for gas systems the volume of the chambers may vary by attaching the bulbs of different sizes. A different type of the two-chamber setup is a diaphragm cell where the volume of each chamber is equal and they are separated by a fine-grade porous diaphragm. In the cell apparatus used by Longree et al. [71] the top and the bottom chambers are connected by a section constructed of 125 stainless tubes, as a sort of diaphragm, in order to avoid convection.

3.3.1 The two-chamber pressure apparatus of Rutherford and Drickamer

Figure 3.4 shows the original setup used by Rutherford and Drickamer [98]. The thermal diffusion pressure cell consists of the two chambers constructed of thin stainless steel. They are separated by a piece of the fine porous fritted glass. The chambers are mounted in a mercury cup, with which pressure may be regulated. A brass cap is mounted on the upper part of the cell constituting the cold chamber with a volume of 0.15 cm^3. The rest of the cell constitutes the hot chamber, with a volume of 1.1 cm^3. The large volume difference between the chambers is deliberately designed to avoid remixing. Iron stirrers are located inside each chamber and activated every second by direct current pulse.

The lower chamber is heated by a wire in the lower part of the cell, so that it was possible to maintain a temperature difference of 10^oC between the chambers. Thermocouples are inserted in both chambers. Pressures up to 10000 atmospheres may be obtained by means of a pressure bomb mounted on the bottom plug of the cell. To avoid evaporation the cell was immersed into a water bath.

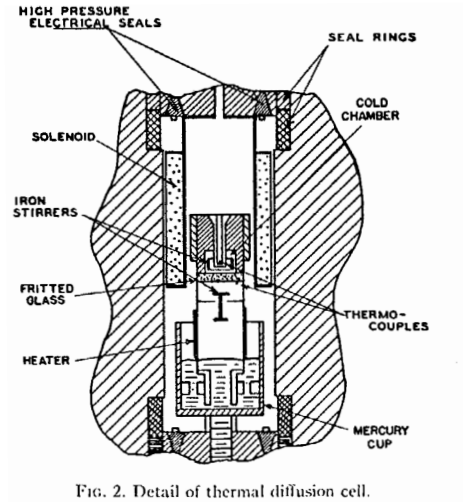

Figure 3.4: The original two chamber cell of Rutherford and Drickamer [98]

In a typical run of this setup the chambers are filled by the liquid under study. The cell is stabilized by standing several hours at constant temperature and low pressure. Concentration gradients inside the chambers are eliminated in this way before starting the run. The runs last between 3 and 20 hours to make sure that the steady state has been reached. The pressure bomb is removed at the end of the run and the composition of each chamber is analyzed in a refractometer. Corrections for the cold temperature chamber are needed, since the thermocouples in this section are in contact with the pressure transmitting fluid.

3.3.2 The the two-chamber gas apparatus of Shashkov et al.

The original cell apparatus developed by Shashkov et al. [107] is shown in Figure 3.5.

This type of apparatus, as the previous one, is constructed of the two chambers of largely different volumes. A metal jacket filled with an asbestos coating covers the top large chamber ($V_1 = 141.2\,cm^3$). The small bottom chamber ($V_2 = 2.45\,cm^3$) is drilled in a solid metal block. A second cavity drilled next to the small chamber is connected with the previous chamber by a valve. This second cavity acts as a

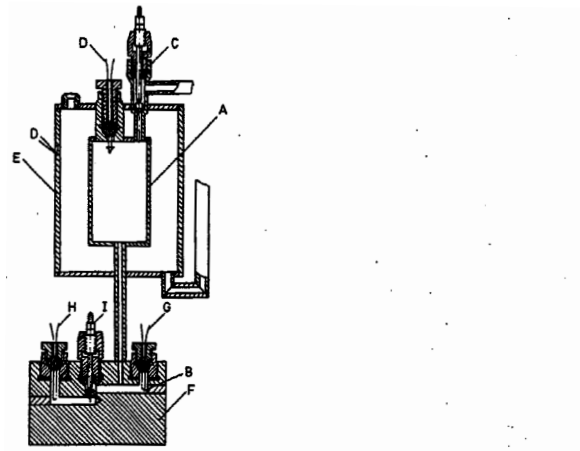

Figure 1. A schematic diagram of the two-bulb apparatus, A: top bulb; B: bottom bulb; C: gas inlet valve; D: thermocouple; E: metal jacket with asbestos insulation; F: metal block; G and H: thermistor elements, and I: isolation valve.

Figure 3.5: The original two-chamber gas apparatus of Shaskov et al. [107]

reference cell, to determine the compositional gradient. The lower and the upper chambers are connected by a thin-wall metal tube. The temperature of the top chamber is controlled by circulating a silicon organic liquid in the jacket. A thermostat bath is used to fix the temperature of the lower metal block containing the small chambers. The temperatures are measured and controlled by thermocouples installed in both chambers.

Due to the large volume difference, it can be assumed that almost all changes in the mixture composition occur in the small chamber. The katharometer method is used to determine the composition in the bottom chamber. This method consists in application of thermistors mounted in the bottom cell and in the reference cell. The difference in the values shown by the thermistors indicates the composition gradient. The thermal diffusion factor is determined by:

$$\alpha^T = \frac{\Delta z}{z_1 z_2} \ln\left(\frac{T_H}{T_c}\right)$$

where z_1 and z_2 are the initial concentrations of the mixture, Δz is the mole fraction gradient and T_H and T_C are the top-chamber (hot) and bottom-chamber (cold) temperatures. The resulting thermal diffusion factor corresponds to the average

temperature between the cells.

3.3.3 The two-chambers gas apparatus of Trengove et al.

A different chamber cell setup was designed by Trengove et al. [122] to measure the thermal diffusion factor in gas mixtures. The original sketch of the apparatus is shown in Figure 3.6.

The cell has cylindrical brass bulbs connected at either end, so that it is possible to change them. The relaxation times depend on the volumes of the attached bulbs. The valves located in ports (N) allow the gas mixture to enter the bulbs. The gas mixture in the bulbs is isolated from the gas in the long separating tube (S) by means of two stainless bellow valves (V) tolerating pressures up to 5 atmospheres.

The relaxation time for a particular pair of bulbs is measured by attaching a thermal conductivity cell (T) to the lower end of the apparatus. This cell is removed for the thermal diffusion experiments. The volumes of the cell bulbs are always adjusted for pressures less than 1 atmosphere, for which the steady state is reached within 12 hours.

A typical run starts by introducing the gas mixture in the cell through the valves (N). The cell is put in an upside down position. The canopy (C) is attached to the main cell frame through the holes (H). The cell is then turned into the right position and lowered into a water thermostat up to the level (L), so that the bottom bulb and the valve are immersed into the thermostat bath. After this, hot water from a second thermostat is pumped through the canopy entering at (W1) and exiting at (W2) by means of the oil pump attached at (P). The pressure of the jacket surrounding the water in the canopy is reduced to 10^{-5} Torr. The top valve can be closed, while the hot water is circulating by means of an adjustable connector (E). The gas samples in each bulb are isolated simultaneously once the steady state is reached. The cell is removed from the thermostat bath. The canopy is removed and the content of the top and bottom bulbs is analyzed. The concentration in each cell is determined by digital volumeter-thermal conductivity.

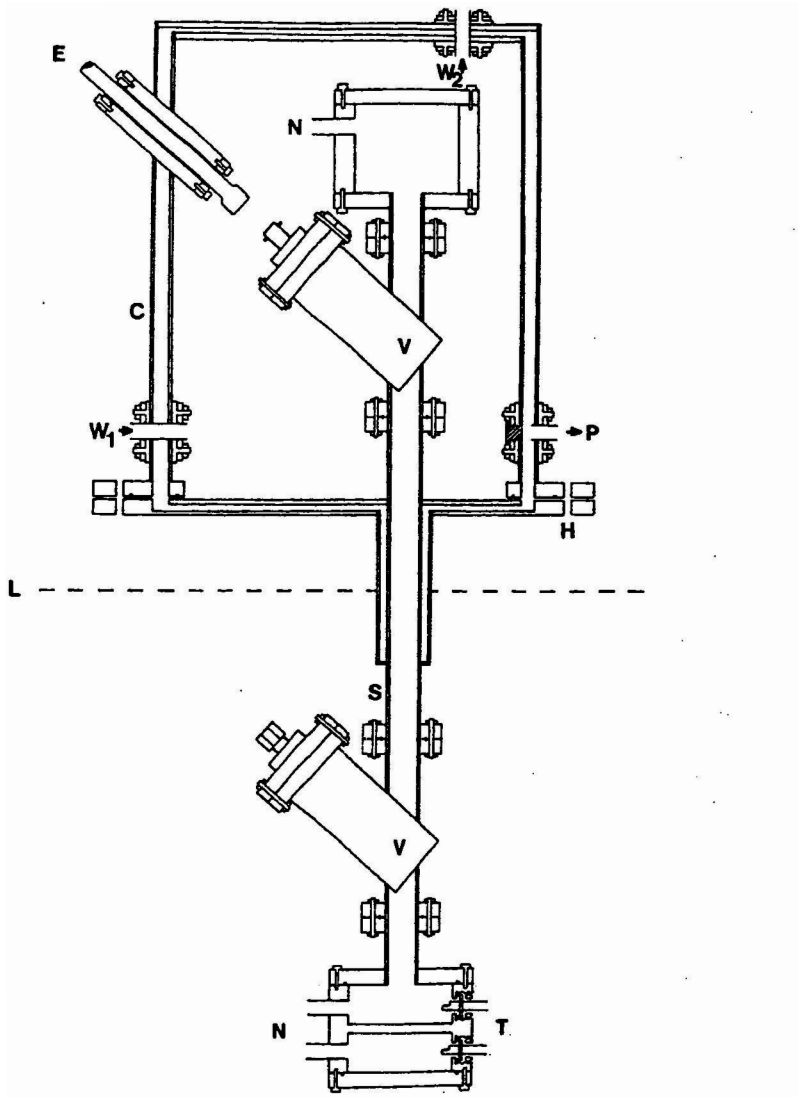

Fig. 1. Diagram of the thermal diffusion cell and canopy; see text for details.

Figure 3.6: The original two-chamber cell of Trengove et al. [122]

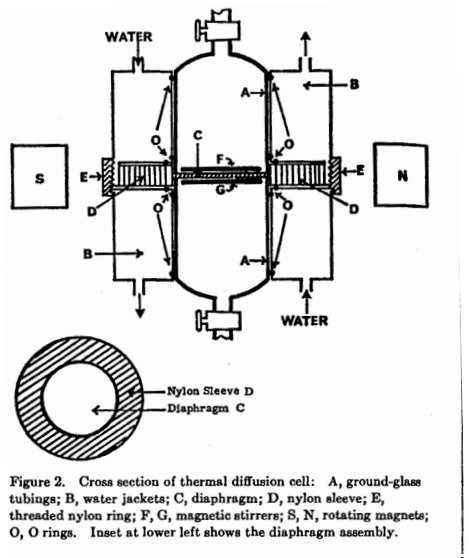

Figure 2. Cross section of thermal diffusion cell: A, ground-glass tubings; B, water jackets; C, diaphragm; D, nylon sleeve; E, threaded nylon ring; F, G, magnetic stirrers; S, N, rotating magnets; O, O rings. Inset at lower left shows the diaphragm assembly.

Figure 3.7: The original diaphragm cell of Shieh [115].

3.3.4 The diaphragm apparatus

This type of apparatus is also called the modified Stokes diaphragm cell. It was originally designed for study any kind of membrane transport. The original sketch of the setup used by Shieh [115] is shown in Figure 3.7.

The cell consists of one large glass tube (A) divided on two halves by a fine-grade diaphragm (C). Each chamber has a volume of 16 milliliters. The diaphragm is mounted in a nylon sleeve (D), so that it is simple to remove and to replace it. A cylindrical nylon ring (E) is used to tighten the two chambers together. Two stirrers, (F) and (G), are located inside each chamber and are rotated by cylindrical magnets. By means of the diaphragm and the stirrers convection is avoided. The temperature gradient is obtained by means of the two cylindrical water jackets (B). Each half is inserted inside the jackets circulating hot water in the top jacket and cold water in the bottom one. The temperatures of both chambers are measured and controlled constantly near the diaphragm region.

An ordinary run starts by cleaning the cell by acetone and then filling it by the mixture to be studied. The top stopcock is left open until the cell is finally mounted on a platform and then extra fluid is removed. The stopcock is then closed. It takes

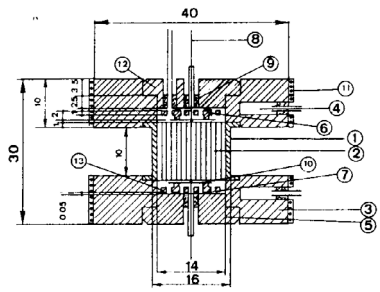

Figure 1. The cell: (1) lateral boundary, cylinder in stainless steel; (2) filling by 125 thin-walled stainless steel tubes; (3) lower plate; (4) methane thermometer; (5–12) supports of the capacitors; (6–13) plates of the capacitors; (7) quartz spacer: ϕ 0.05 mm; (8) stainless steel wire ϕ 0.1 mm acting on spring 10; (9) insulator; (10) stainless steel plates, 0.08 mm thick, used as spring; (11) heating wire.

Figure 3.8: The original 125 tubes cell of Longre et al. [71].

two days to reach steady state. The concentration in each chamber is determined by liquid scintillation spectrometry.

3.3.5 The gas cell of Longree et al.

An alternative cell for measuring the thermal diffusion effect in gas mixture was used by Longree et al. [71]. The original schema of the apparatus is shown in Figure 3.8.

The setup consists of a single chamber which is filled with 125 vertical thin-walled stainless steel tubes. These tubes are used in order to avoid convection. A liquid-nitrogen cryostat is used to work at various constant temperatures, obtaining the thermal gradient by controlled electrical heating. The concentration gradient obtained at the end of the run is measured by capacity variation using a liquid solution as a dielectric medium. The concentration is measured in situ and therefore the mole fraction can be studied as a function of time. The final concentration is determined when steady state has been reached.

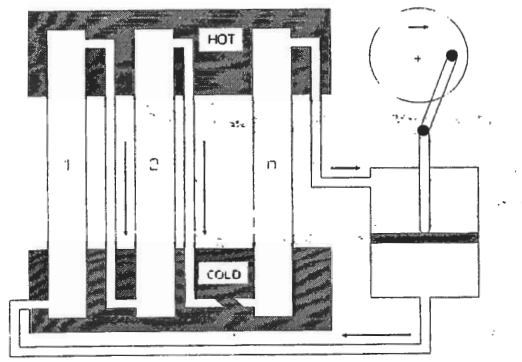

FIG. 1. Principle of the trennschaukel or swing separator. A given number of tube/capillary pairs is connected top to bottom and the contained gas mixture is swung to and fro by a pump. A temperature difference, $\Delta T = T_H - T_C$, is imposed across the n tubes by embedding the top approximately 1/3 of the tubes in an isothermal region at T_H and the bottom 1/3 in another isothermal region at T_C.

Figure 3.9: The swing separator cell of Clusius and Hubert [16].

3.4 The swing separator cell

This cell was developed by Clusius and Huber in 1955 [16]. The sketch of the cell is shown in Figure 3.9.

The cell consists of a number of tubes (n_{tubes}) connected in a series. The top part of each tube is immersed in the isothermal hot region and is connected by a capillary to the bottom part of the next tube, which, in turn, is immersed in the cold isothermal region. The gas mixture to be studied slowly circulates through the tubes by means of a pump. The top part of a tube has the same concentration as the bottom part of the next tube. The authors claim that convection is eliminated by setting the temperature gradient vertically with the hot end (T_H) at the top. The separation factor of the components is multiplicative, therefore separation increases with increase of the number of tubes. In the particular setup used by Taylor and Hurley [118] the apparatus consisted of 20 tubes. Two solid nickel blocks were used to transmit the temperature. A bellow pump was used to swing the gas mixture.

Explicit operational parameters were established by Taylor et al. [117] in order to operate the device in an optimal way. Even though the setup is very simple, careful considerations have to be made regarding operational times, pump period, pumped

volume and pressure. The operational time has to be sufficiently long in order to reach the steady state. Incorrect flow velocities can damage the experiments. If the velocity is too slow, backward diffusion in the capillaries may appear. On the other hand, if the velocity is too high, the thermal diffusion balance is perturbed. The compositions at the hot and the cold end of the cell are measured at the end of the experiment on a mass spectrometer. Corrections for back diffusion in capillaries and for disturbances due to pumping are applied. Further, a third correction is implemented taking into account approach to equilibrium. The final separation factor, *sp*, is:

$$sp = \frac{1 + (\Delta z_1(corr)/z_1(T_C))}{1 + (\Delta z_2(corr)/z_2(T_C))}$$

where $z_1$and z_2 are the mole fractions of the light and heavy component species, respectively. The experimental thermal diffusion facto is given by:

$$\alpha^T = \frac{1}{n_{tubes}} \frac{\ln(sp)}{\ln\left(\frac{T_H}{T_C}\right)}$$

where n_{tubes} is the number of stages (or tubes).

3.5 The thermal field-flow fractionation - ThFFF

This setup is employed nowadays as a separation technique similar to chromatography. It is especially useful for solutions of large molecules [82]. Average molecular weights of asphaltenes and their distribution in crude oil were investigated using this type of apparatus [11]. The original sketch of the setup used by Janca is shown in Figure 3.10.

The apparatus consists of two walls, the hot wall (1) and the cold wall (2), clamped together by a polymer foil (3). The mixture to be studied flows through a channel, which is cut in the foil. The lower plate is cooled by circulating thermostated liquid (5). The upper bar is either heated by an electric cartridge or by circulating liquid, as in the lower plate. Thermocouple holes (8) are located along the plates to control and to measure the temperature during the experiment. The

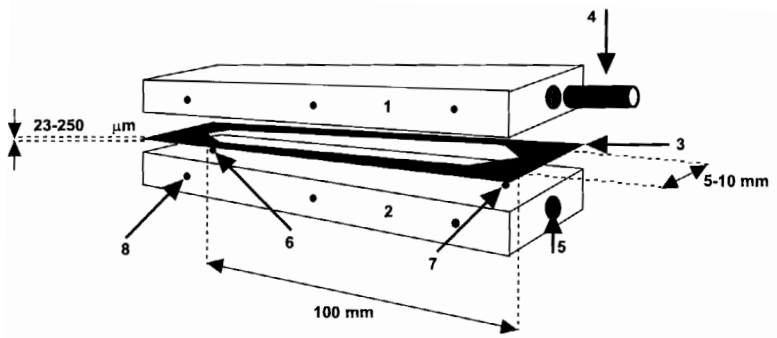

Figure 3. Schematic representation of the μ-TFFF channel: 1, hot bar; 2, cold bar; 3, polymer foil; 4, heating cartridge; 5, duct for cooling liquid; 6, inlet capillary; 7, outlet capillary; 8, thermocouple holes.

Figure 3.10: The thermal field-flow fractionation apparatus of Janca [51].

liquid mixture enters the channel from the inlet capillary (6) and leaves it through the outlet capillary (7). Two different types of exit capillary exist: a single nozzle as shown in figure (3.10) and two exit nozzles which split the upper from the lower part of the channel.

The principle of the ThFFF apparatus is that due to the temperature gradient compositional flow appears towards the walls of the channel. Heavier molecules will flow to the cold plate while lighter molecules will stay at the top. For the second type of exit nozzle, the upper and the lower sections are divided and the composition is determined by refractive index. When the exit nozzle is a single capillary, the composition is determined by fractogram. The concept lying behind this is that friction between large molecules and the walls slows down these molecules. The compositional gradient is determined by the difference in average velocity due to the spatial and temporal separation of different particles.

3.6 The thermal diffusion force Rayleigh scattering - TDFRS

The holographic grating technique was first suggested by Allain et al. [1] and was later developed by Köhler [57]. In the recent years this technique has become a reli-

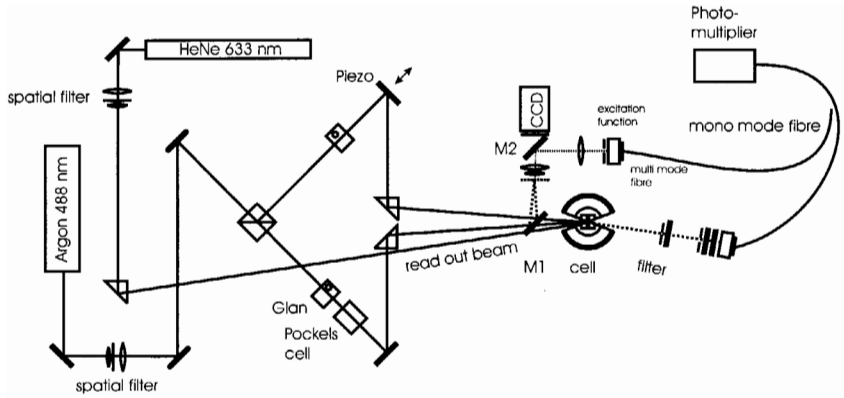

Figure 4. Schematic drawing of a thermal diffusion forced Rayleigh scattering (TDFRS) set-up.

Figure 3.11: The TDFRS setup of Köhler [57].

able method to measure the Soret coefficient. This method has several advantages: for example, neither external calibration is needed, no absolute intensity measurements are required. Convection is also eliminated due to low temperature gradients of several micro-Kelvin. Further, equilibration times are very short. A sketch of the set-up is shown in Figure 3.11.

By means of the interference of two laser beams intersecting on the sample, grating is created. The intensity of the laser light is converted into a temperature gradient due to small amounts of dye dissolved in the sample. In turn, the temperature gradient creates a concentration gradient due to the thermal diffusion effect. Grating of the refractive index shows both the temperature gradient and the compositional gradient, which is read out by diffraction of a third laser beam. Analyzing the time dependence, one can extract three transport coefficients: the thermal diffusion coefficient D^T, the translational diffusion $D = 1/q^2t$ and the thermal diffusivity $D_{th} = 1/q^2t_{th}$, where t and t_{th} are the the decay time of the thermal grating and the delay time of the concentration grating correspondingly, and q is the grating vector magnintude determined each time when a TDFRS experiment is performed. The Soret coefficient, S_T, is obtained as the ratio of the thermal diffusion coefficient and the translational diffusion coefficient. These coefficients are all simultaneously determined in one single measurement.

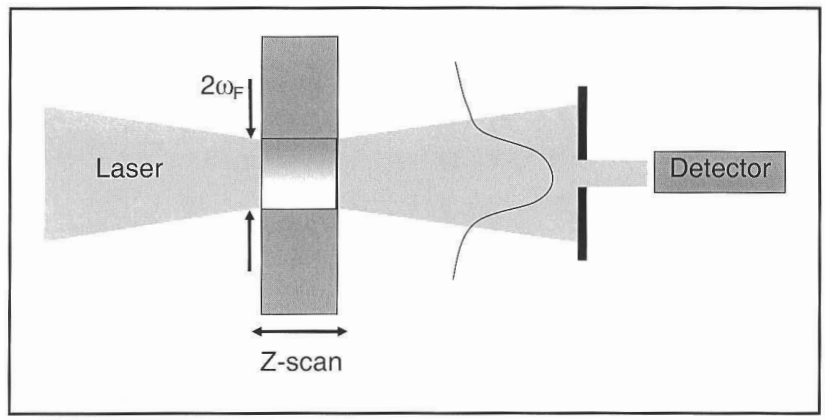

Figure 3.12: The thermal lens technique.

3.7 The single-beam Z-scan or the thermal lens technique

Figure 3.12 illustrates a typical thermal lens setup. In this type of technique a single laser beam is used for both heating and detecting. Any effect that creats variation of the refractive index can be studied with this setup.

Gliglio and Vendramini [40] noticed that, when an intense narrow laser beam is reflected in a liquid, beside the thermal expansion, the Soret effect appears. This work showed the effect of the laser beam in binary mixtures compared to pure liquids.

This technique for determination of the Soret coefficient is based on analyzing the optical nonlinearities of the laser light. The sample cell is located along a single focus gaussian laser beam (z axis). The light intensity is measured as a function of the sample position (z). The temperature difference is created by space modulation of the light intensity. In turn, due to the Soret effect, this temperature gradient generates a modulation of the nanograin volume fraction ϕ. The temperature and the volume fraction profiles are analyzed by the laser beam. It is possible to determine two different diffracted intensities: I_d^T only for volume fraction modulation and $I_d^{T+\phi}$ when both volume and temperature modulations take place at the same time, due to the different evolution times. Alves et al. [2] derived the following equation for

determining the Soret coefficient by this method:

$$\frac{1}{S^T} = \left(1 - \sqrt{\frac{I_d^{T+\phi}}{I_d^{\phi}}}\right) F\tau_{th} \frac{\partial n}{\partial \phi} \left(\frac{\partial n}{\partial T}\right)^{-1}$$

where n is the refractive index of the sample, τ_{th} is the relaxation time of the temperature grating and F is the pulse repetition rate.

3.8 The packed Soret cell and column

This technique was first used by Costeseque in 1982 [18]. It exists in two basic geometries: as a cell and as a column. In the first case, the glass - (ZrO_2) inert micro-balls are packed between the two horizontal walls, maintained at the temperature T_h (hot) for the lower plate and T_c (cold) for the upper plate. The second geometry is basically identical to the thermogravitational column, but in this case the gap between the hot and the cold walls is filled by the glass (ZrO_2) inert micro-balls. The original sketches presented by Costeseque et al. [19, 20] are shown in Figure 3.13.

The packed cell requires a perfect vertical temperature gradient for effective separation of the components. The cell is designed with lateral dimensions (b) and (L) much larger than the thickness of the gap (a) to avoid convection. Therefore, variations of the thermal gradient may be neglected in the center of the cell where sampling is performed. The stationary state is considered to be achieved after five times the characteristic time θ, which is estimated by:

$$\theta = \frac{a^2}{\psi^2 D^*}$$

where a is the thickness of the gap and D^* the isothermal diffusion coefficient. Concentration is measured by the refraction index technique.

In the vertical geometry, convection effects are important. Flux of light molecules going to the bottom (hot) is observed. Vice versa, heavy molecules flow to the top. Due to the denser fluid located in the upper part of the column, instability arises. However, a stationary state was achieved after 60 days.

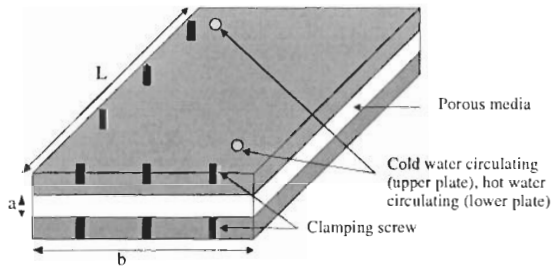

Figure 1: Packed Soret cell (vertical thermal gradient)

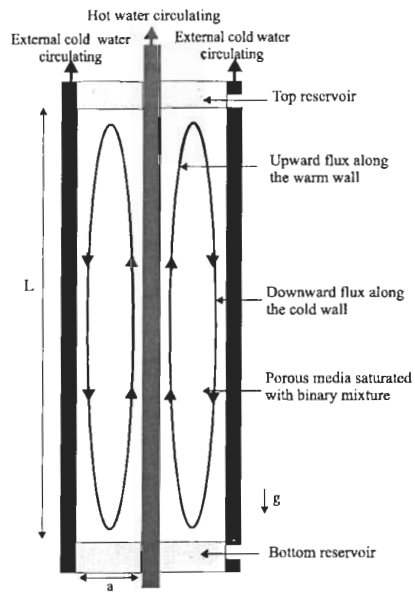

Figure 2: Packed thermogravitational column (horizontal thermal gradient)

Figure 3.13: The original packed cell and the original packed column of Costeseque et al. [19, 20].

This technique is of special interest to the petroleum industry, since it is a first approach to determine the thermal diffusion coefficient in porous media. It is important to emphasize that the actual Soret coefficient measured in the packed cell and/or the packed column corresponds to the thermal diffusion coefficient in porous media, but not in free space. However, Shaprio and Stenby [112] demostrated that the thermal diffusion coefficient in macro porous media should be the same as in bulk fluids. Desagreement existing between the theory and the experiments should further be studied.

3.9 The Benard-configuration cell

This type of cell consists of the two heat-conducting horizontal plates, which are made from a massive sapphire. Spacers and O-rings are used to form a gap between the two sapphires. The mixture is located in this gap. The sapphire walls present the advantages of optical access and good thermal conducting properties. The Peltier elements connected to the sapphire create the temperature gradient.

Stability of colloidal suspensions with negative Soret coefficient were studied with this apparatus [12]. Convective flow inside the cell was analyzed by means of the shadowgraph technique, which gets images of the mixture by an out-of-focus condition. Perturbations of the refraction index are observed as bright and dark zones, indicating oscilating behavior. No values for the thermal diffusion coefficient have been reported using this method yet.

3.10 Comparison of different methods

In measurements of the thermal diffusion coefficients, it is difficult to avoid convection. Discrepancies between different measurements have been attributed mainly to this effect. Convection depends on geometry, dimensions of the setup as well as the material of the cell walls. The Soret effect is very small compared to other transport phenomena. It is therefore necessary to apply large temperature gradients to be able to observe this effect experimentally. Density variations due to the

temperature gradient can induce thermo-solutal Rayleigh convection. The resulting re-mixing may be very effective, leading to no compositional gradient inside the cell like for example in some of the experiments performed by Prigogine [93, 94].

Several ways have been suggested to avoid convection. As was already seen in section 3.2, the LDV technique determines the Soret coefficient during the transient time before convection can influence the results. Several setups are designed with very small gaps between the hot and the cold wall. In this way convection is reduced significantly, and its effect may be neglected. The TDFRS technique works with thin cells under very small temperature gradients and, therefore, convection is also neglected. The diaphragm cell is used mainly because of the possibility to avoid remixing. However, it has been shown [24] that the porous medium has an active action on the separation process. The temperature dependence of the porous solid surface is not well known and it could be of the order of the Soret effect. A similar effect may be observed when using capillaries to connect the cells, since wall effects may affect the final value of the Soret coefficient.

Five different experimental setups were used to measure the thermal diffusion effect for three organic mixtures [87]. This project was called the Fountain bleau Benchmark test. It was shown that the results obtained by different methods differ from each other by at most, 8.5 percent. The largest difference was obtained with the TGC method by Bou-Ali et al. [9]. The results in that work were obtained as mean values for four different columns, with larger or smaller gaps between the cold and the hot wall. The authors observed differences in the value of the Soret coefficient, depending on the gap. Further, the LDV technique [86] failed for mixtures where the separation factor is small due to creation of enhanced buoyancy. It was also pointed out that the values obtained by application of the packed cell (porous medium) present uncertainties in the value of tortuosity. The thermal diffusion coefficient obtained by this technique presents high deviations from other results.

Many experimental setups have been used to measure the thermal diffusion effect. However there are still some disagreements between the results. A major poryect [24] is being conducted by the European Space Agency and several research groups to measure the thermal diffusion effect under microgravity conditions. It is believed

that performing the experiments under this condition, convection is totally avoided. Nevertheless, it is important to perform these measurements with a reliable setup to avoid perturbations during the flight. This project is being carried out at the present time and the flight is expected to be launch in 2005. We believe that as a result of these experiments it will be possible to establish, what corrections are needed (for convection perturbations), when measuring the thermal diffusion effect on the Earth.

Chapter 4

Calculations for Binary Mixtures

The available expressions for the thermal diffusion factor have been compared with different sets of experimental data for binary systems. Diversity of the experimental data requires implementation of different equations of state suitable to determine the thermodynamic properties needed for the calculations. In this chapter we compare sets of experimental systems found in the literature with the different models presented in Chapter 2. The results are presented in the two sections: the first one, where for four binary mixtures several EoS are used, and the second section, where we compare different models by analyzing the errors of calculation.

4.1 Sets of experimental data

There is a large amount of experimental data for thermal diffusion coefficients. Among them, we analyzed only the data presented by numbers, not by plots. Experimental data for several isotopic mixtures have been reported in the literature, but we do not include them in our analysis. The binary mixtures selected for comparison with the models are presented in Table 4.1, where setup used for measurement is also specified.

Table 4.1: List of binary mixtures, experimental setup and references found in the literature for the thermal diffusion effect.

	Substance 1	Substance 2	Setup	Reference
1	Methane	n-Butane	Diaph-cell	[101]
2	Benzene	Carbon Tetrachloride	Diaph-cell ThFFF	[121] [66]
3	Benzene	n-Hexane	2Chamber P-TGC	[62] [8]
4	Benzene	i-Heptane	C-TGC	[125]
5	Benzene	n-Heptane	2Chamber P-TGC C-TGC	[62] [8] [125]
6	Benzene	n-Octane	2Chamber	[62]
7	Benzene	n-Decane	C-TGC	[125]
9	Benzene	n-Tetradecane	2Chamber C-TGC	[62] [125]
10	Benzene	n-Hexadecane	C-TGC	[125]
11	Benzene	n-Octadecane	C-TGC	[125]
12	Benzene	Cyclohexane	Diaph-cell	[121]
13	Benzene	Nitrobenzene	P-TGC	[93]
14	Benzene	Chloro Benzene	P-TGC	[93]
15	Carbon Disulfide	Carbon Tetrachloride	P-Diaph-cell	[98]
16	Carbon Disulfide	Benzene	P-Diaph-cell	[98]
17	Carbon Disulfide	2 Methylpentane	DiapH-cell P-Diaph-cell	[28] [100]
18	Carbon Disulfide	2,2 Dimethyl Butane	Diaphr-cell P-Diaph-cell	[28] [100]
19	Carbon Disulfide	2,3 Dimethyl Butane	Diaph-cell P-Diaph-cell	[28] [100]
20	Carbon Disulfide	3 Methyl Pentane	Diaph-cell P-Diaph-cell	[28] [100]
21	Carbon Disulfide	n-Hexane	Diaph-cell P-Diaph-cell	[28] [99, 100]
22	Carbon Disulfide	n-Heptane	P-Diaph-cell	[99]
23	Carbon Disulfide	n-Octane	P-Diaph-cell	[99]
24	Carbon Disulfide	m-Xylene	Diaph-cell	[28]
25	Carbon Disulfide	o-Xylene	Diaph-cell	[28]
26	Carbon Disulfide	p-Xylene	Diaph-cell	[28]
27	Carbon Disulfide	Isobutyl Chloride	Diaph-cell	[27]
28	Carbon Disulfide	Ethyl Benzene	Diaph-cell	[28]
29	Carbon Disulfide	Chloro Benzene	P-Diaph-cell	[98]
30	Carbon Disulfide	Bromo Benzene	P-Diaph-cell	[98]
31	Carbon Disulfide	Ethyl Iodine	P-Diaph-cell	[98]
32	Carbon Disulfide	1,1 Dichloro Ethane	Diaph-cell	[28]

	Substance 1	Substance 2	Setup	Reference
33	Carbon Disulfide	1,2 Dichloro Ethane	Diaph-cell	[28]
34	Carbon Disulfide	cis-Dichloro Ethylene	Diaph-cell	[28]
35	Carbon Disulfide	trans-Dichloro Ethylene	Diaph-cell	[28]
36	Carbon Disulfide	n-Butyl Bromide	P-Diaph-cell	[98]
37	Carbon Disulfide	n-Butyl Chloride	Diaph-cell P-Diaph-cell	[27] [98]
38	Carbon Disulfide	n-Butyl Iodide	P-Diaph-cell	[98]
39	Carbon Disulfide	sec-Butyl Chloride	Diaph-cell	[28]
40	Carbon Disulfide	t-Butyl Chloride	Diaph-cell	[28]
41	Carbon Tetrachloride	Carbon Tetrabromide	Diaph-cell	[27, 108]
42	Carbon Tetrachloride	1,1,2,2tetrachloro Ethane	Diaph-cell	[108]
43	Carbon Tetrachloride	1,1,2,2tetrabromo Ethane	Diaph-cell	[108]
44	Cyclohexane	Carbon Tetrachloride	Diaph-cell ThFFF	[121] [65]
45	Cyclohexane	n-Hexane	P-TGC	[93]
46	n-Pentane	n-Decane	TDFRS	[84]
47	n-Hexane	Carbon Tetrachloride	P-TGC	[8, 93]
48	n-Heptane	Carbon Tetrachloride	P-TGC	[8]
49	n-Hexane	Nitrobenzene	P-TGC ThFFF	[31] [120]
50	n-Hexane	Toluene	P-TGC	[8]
51	n-Hexane	1,1,2,2tetrachloro Ethane	Diaphr-cell	[109]
52	Toluene	n-Heptane	P-TGC	[8]
53	n-Heptane	1,1,2,2tetrachloro Ethane	Diaph-cell	[109]
54	n-Heptane	n-Dodecane	C-TGC	[125]
55	n-Heptane	n-Tetradecane	C-TGC	[125]
56	n-Heptane	n-Pentadecane	C-TGC	[125]
57	n-Heptane	n-Hexadecane	Diaphr-cell	[115]

58	n-Heptane	n-Octadecane	C-TGC	[125]
59	i-Heptane	n-Dodecane	C-TGC	[125]
60	i-Heptane	n-Hexadecane	C-TGC	[125]
61	o-Xylene	m-Xylene	P-TGC	[93]
62	1,2 Dichloro Ethane	1,2 Dibromo Ethane	Diaphr-cell	[108]
63	n-Octane	1,1,2,2tetrachloro Ethane	Diaphr-cell	[109]
64	n-Nonane	1,1,2,2tetrachloro Ethane	Diaph-cell	[109]
65	1,1,2,2tetrachloro Ethane	n-Tetradecane	Diaph-cell	[109]
66	1,1,2,2tetrachloro Ethane	n-Octadecane	Diaph-cell	[109]
67	1,1,2,2tetrachloro Ethane	1,1,2,2tetrabromo Ethane	Diaph-cell ThFF	[108] [64]
68	1,1,2,2tetrachloro Ethane	Carbon Tetrabromide	Diaph-cell P-TGC	[108] [64]
69	1,2,3,4tetrahydronaphtalene	n-Dodecane	LDV Pk-TGC P-TGC TDFRS TDFRS	[86] [19] [9] [69] [130]
70	1,2,3,4tetrahydronaphtalene	isobutylbenzene	LDV Pk-TGC P-TGC TDFRS TDFRS	[86] [19] [9] [69] [130]
71	Isobutyl Benzene	n-Dodecane	LDV Pk-TGC P-TGC TDFRS TDFRS	[86] [19] [9] [69] [130]

80	Methanol	Benzene	Diaph-cell P-TGC ThFFF	[121] [94] [68]
81	Methanol	Carbon Tetrachloride	2Chambers Diaph-cell	[6] [121]
82	Ethanol	Cyclohexane	P-TGC	[94]
83	Ethanol	Triethylamine	Diaph-cell	[121]
84	Water	Methanol	Diaph-cell ThFFF	[80, 121] [65]
85	Water	Ethanol	Diaph-cell LDV Pk-cell ThFFF	[80, 121] [30] [20] [65]
86	Water	Diethylamine	Diaph-cell	[121]
87	Water	2 Propanol	Diaph-cell	[20]
88	Ethanol	Diethylamine	Diaph-cell	[121]
92	n-Butyl Alcohol	Carbon Disulfide	Diaph-cell	[28, 121]

The input data are presented in Appendix A, where the sources are also listed.

In order to calculate the thermodynamic properties of the mixtures, we used the SRK (Soave-Redlich-Kwong) and the PR (Peng-Robinson) equations of state [75]. These EoS show good performance for hydrocarbon mixtures. However, these equations are imprecise when used for prediction of the molar volumes. Therefore, in our first calculations we implemented two different methods for evaluation of the partial molar volumes: the Peneloux correction [83] and a method based on the principle of corresponding states [75].

In the second set of calculations we used only the SRK and the PR equations of state for mixture 1 to mixture 71 and the CPA (Cubic plus association) EoS [59] for mixture 80 to mixture 92. These last mixtures contain at least one alcohol component. Even though it has been shown that the EoS has a large influence on the estimation of the thermal diffusion factor [42, 53], we restricted ourselves with

these three EoS. Ohterwise, the amount of computation could be too large, without bringing really new results.

4.2 Results

Here we present the calculations performed for four binary mixtures. We compare the impact of different equations of state on the calculation of the thermal diffusion factor. In the next section we compare ten different models, using only the SRK, PR and CPA EoS, according to explanations mentioned in the previous section.

The notation used in the plots is specified in Table 4.3.

Table 4.3: The models tested in the calculations

Notation		Equation	Reference
α_{EXP}	Experimental thermal diffusion factor	-	
α_{RD54A}	Rutherford - Drickamer 1954 A	2.36	[98]
α_{RD54A}	Rutherford - Drickamer 1954 B	2.37	[98]
α_{DD55A}	Dougherty - Drickamer 1955 A	2.40	[27]
α_{DD55B}	Dougherty - Drickamer 1955 B	2.47	[28]
α_{TIC56}	Tichacek - Dougherty - Drickamer 1956	2.44	[121]
α_{SHI69}	Shieh 1969	2.45	[115]
α_{HAA69}	Haase 1969	2.49	[44]
α_{KEM89}	Kempers 1989	2.51	[52]
α_{SHF98}	Shukla - Firoozabadi 1998	2.50	[116]
α_{KEM02}	Kempers 2002	2.52	[53]

4.2.1 Evaluation of the Thermal diffusion factor with different equations of state

Seven thermodynamic models for the thermal diffusion factor were tested: the Rutherford and Drickamer (A), α_{RD54A}; the Dougherty and Drickamer α_{DD55A}; the Dougherty and Drickamer α_{DD55B}; the Haase α_{HAA69}; the Shukla and Firoozabadi α_{SHF98}; the Kempers α_{KEM89}; and, finally the Kempers α_{KEM02}. See table 4.3 for details.

Four sets of experimental data were choosen for this analysis: n-Pentane + n-Decane [84], Benzene + Cyclohexane [27], Methane + Propane [45], Methane + n-Butane [101].

4.2.1.1 n-Pentane + n-Decane

Figure 4.1 shows the results obtained for three different compositions of this mixture at 300.15 K and atmospheric pressure. Thermodynamic properties are calculated by the SRK EoS (plots (a), (c) and (e)), and the PR EoS ((b), (d) and (f)). The Peneloux correction was used in plots (c) and (d). Plots (e) and (f) are produced with application of the principle of corresponding states.

The models predicting the correct sign are those of Rutherford and Drickamer (2.36) and Haase (2.49). Equation (2.36) overestimates the thermal diffusion ratio, while the Haase model, equation (2.49), gives the best approximation, with an average deviation of 19.85 per cent. The Kempers equations (2.51) and (2.52) behave differently, depending on an EoS used. When the SRK EoS is applied, both Kempers models give the wrong sign for the thermal diffusion ratio. When the PR EoS is applied, both Kempers models give the correct sign, but underestimate the thermal diffusion factor. As regards to the thermodynamic models, the PR EoS provides generally better results than the SRK EoS. The volume corrections are not always useful. For example, there was a negative effect when the Peneloux correction was applied together with the SRK EoS. The Kempers thermal diffusion factor noticeably decreased, moving out from the measured values. The volume correction based on the method of corresponding states slightly improved the results for some of the models, while it had a negative effect on some other ones. In the case of the Haase model, no change is observed when the volume corrections are applied.

4.2.1.2 Benzene + Cyclohexane

Measurements of the thermal diffusion factor for this mixture were carried out by Dougherty and Drickamer [27] at 313K and atmospheric pressure, at three different

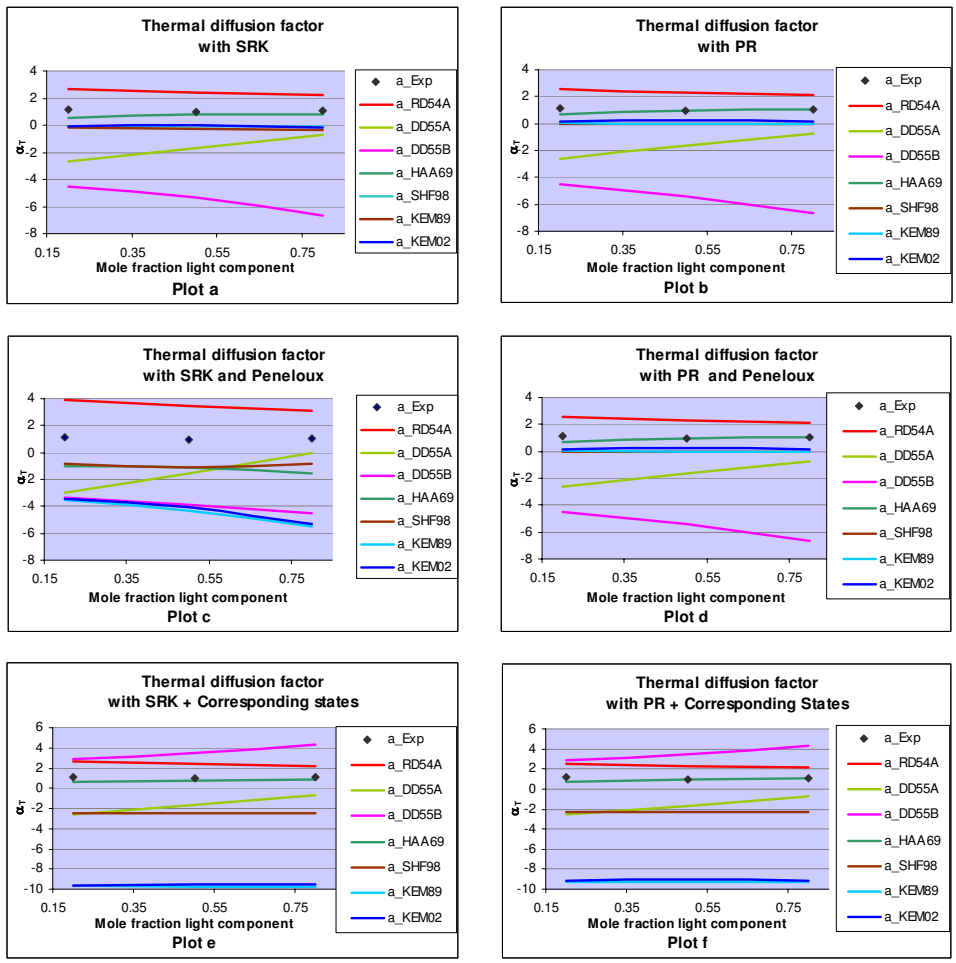

Figure 4.1: Comparison between experiments and calculations for the thermal diffusion factor for n-Pentane - n-Decane mixture at 300.15K and atmospheric pressure using different equations of state. The measured values are denoted by a_EXP; the Rutherford and Drickamer model is represented by a_RD54a; the Dougherty and Drickamer first model by a_DD55a; the Dougherty and Drickamer second model by a_DD55b; the Haase model by a_HAA69; the Shukla and Firoozabadi by a_SHF98; the Kempers from 1989 by a_KEM89; and finally the Kempers from 2002 by a_KEM02.

concentrations. The results of comparison of the measured points with our simulation are shown in Figure 4.2, which is organized in the same way as Figure 4.1.

For this mixture, the models of Rutherford and Drickamer (2.36) and of Dougherty and Drickamer (2.47) are not able to predict correct sign of the thermal diffusion factor. Among the models predicting the right sign, the models of Shukla and Firoozabadi (2.50) and of Haase (2.49), are the most precise. The average deviation for the best model (2.50) is around 6.84 %. As in the previous case, application of the PR EoS is more advantageous than that of the SRK EoS. The Peneloux corrections do not affect accuracy of the results when used with the PR EoS. However, when they are used with the SRK EoS, the calculated values move away from the experimental data. The method of corresponding states presents some improvements when applied to some of the models, as for example, to both of Kempers models. However, for the model of Shukla and Firoozabadi, the results are moving away from the experimental values.

4.2.1.3 Methane + Propane

The measurements were carried out under near-critical conditions, at 346.08K and 5.6 MPa at seven different mole fractions of methane. The experimental data were obtained by Haase et al. [45]. Comparison of the measured points with our simulations is shown in Figure 4.3, which is organized in the same way as Figures 4.1 and 4.2.

For this mixture the models of Rutherford and Drickamer (2.36), and both models of Dougherty and Drickamer (2.40) and (2.47), are not able to predict the correct sign of the thermal diffusion factor. As far as the rest of the models are concerned, those of Haase (2.49) and Shukla and Firoozabadi (2.50) are the closest to experimental data. The average deviation for the best model (2.50) is around 43.93 %, which is still high. This may be explained by the fact that the classical equations of state, which are used in this study, do not perform well close to critical points. Some models perform very well for the low mole fractions of methane, as for example the Kempers models (2.51) and (2.52). However, for higher mole fractions of methane

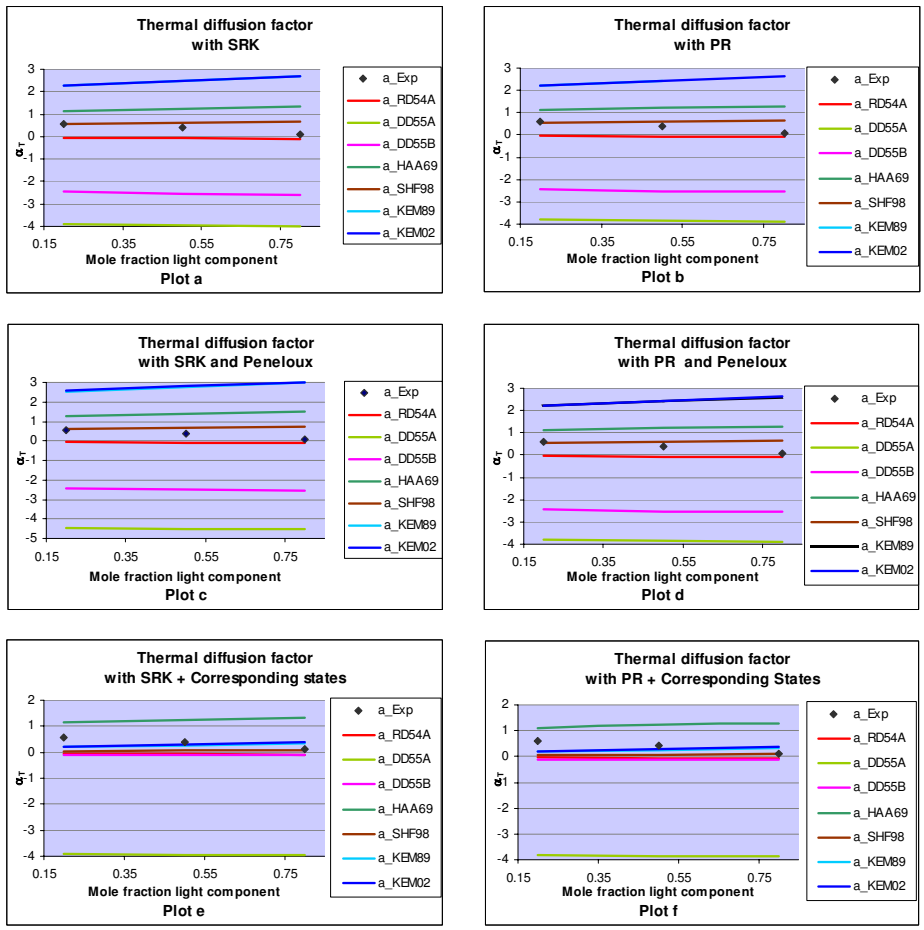

Figure 4.2: Comparison between experiments and calculations for the thermal diffusion factor for Benzene - Cyclohexane mixture at 313K and atmospheric pressure using different equations of state. The measured values are denoted by a_EXP; the Rutherford and Drickamer model is represented by a_RD54a; the Dougherty and Drickamer first model by a_DD55a; the Dougherty and Drickamer second model by a_DD55b; the Haase model by a_HAA69; the Shukla and Firoozabadi by a_SHF98; the Kempers from 1989 by a_KEM89; and finally the Kempers from 2002 by a_KEM02.

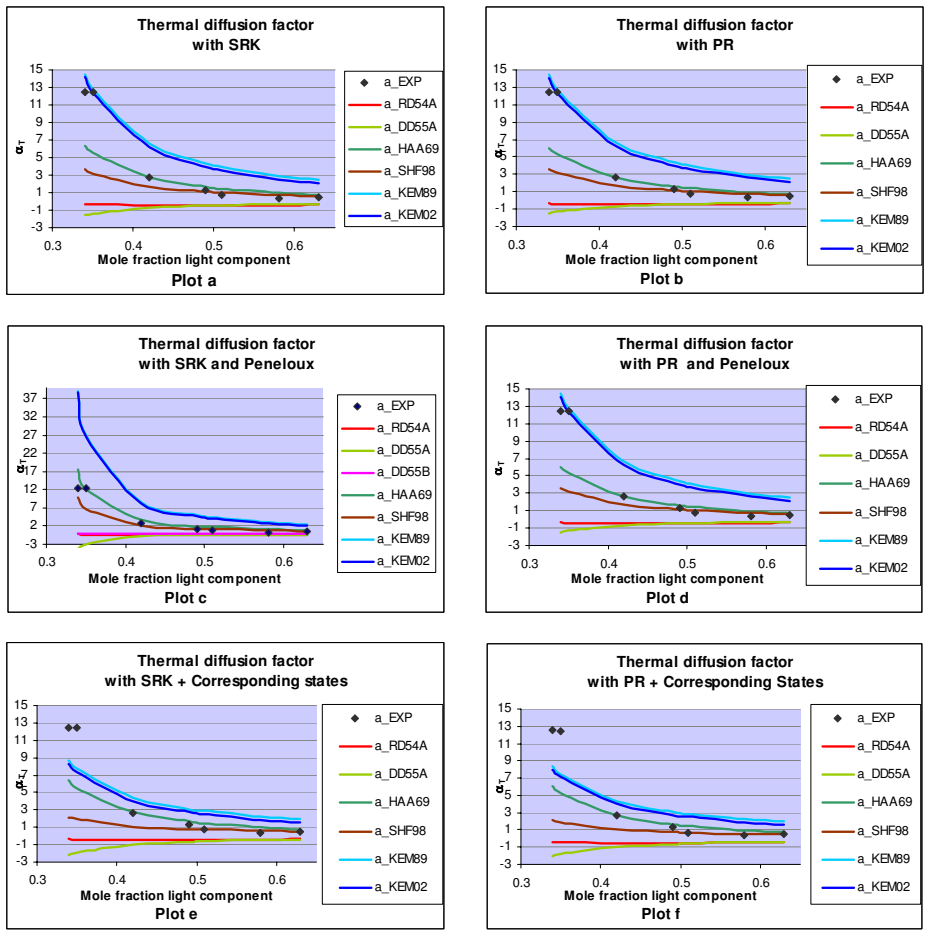

Figure 4.3: Comparison between experiments and calculations for the thermal diffusion factor for Methane - Propane mixture at 346.08 K and 5.6 MPa using different equations of state. The measured values are denoted by a_EXP; the Rutherford and Drickamer model is represented by a_RD54a; the Dougherty and Drickamer first model by a_DD55a; the Dougherty and Drickamer second model by a_DD55b; the Haase model by a_HAA69; the Shukla and Firoozabadi by a_SHF98; the Kempers from 1989 by a_KEM89; and finally the Kempers from 2002 by a_KEM02.

these models move away from the experimental values. The Shukla and Firoozabadi and the Haase models provide very good approximation for high mole fractions, but are not that close for low mole fractions. Concerning the equations of state, some models perform better when the SRK EoS is used and some others when the PR EoS is applied. The Peneloux correction does not improve the results when applied with the PR EoS, however, for the SRK EoS, a major improvement is observed for one of the best models (2.50). On the other hand, the Peneloux correction has a negative effect on the Haase correlation (2.49). The volume correction based on the method of corresponding states improves the results when applied with the SRK EoS. However, its effect for the model (2.50) is not as good as the effect of the Peneloux correction. The Dougherty-Drickamer model (2.47) is not shown on the plot since the results are completely out of range.

4.2.1.4 Methane + n-Butane

The measurements were carried out by Rutherford and Roots [101] for a single composition (40 molar percent of methane), but different pressures and temperatures. Comparison of experimental and calculated thermal diffusion factors for different thermodynamic conditions (29 data points) is shown in Tables 4.4 to 4.9.

The models of Haase (2.49), Shukla and Firoozabadi (2.50), and both Kempers models (2.51) and (2.52) predict correctly the sign of the thermal diffusion factor, while the Rutherford and Drickamer (2.36) and both Dougherty and Drickamer

Table 4.4: Comparison of the calculated and experimental thermal diffusion factors for the mixture of Methane (0.4) and n-Butane (0.6) for different temperatures and pressures using the SRK equation of state

	T (K)	P (atm)	a_Exp	SRK						
				a_RD54a	a_DD55a	a_DD55b	a_HAA69	a_SHF98	a_KEM89	a_KEM02
1	319.4	6.41	-3.56	*2.124*	*1.444*	*7.424*	**-3.031**	-2.719	-10.87	-10.50
2	319.2	6.85	-3.06	*2.087*	*1.369*	*6.648*	**-2.833**	**-2.578**	-10.314	-9.943
3	394.1	6.88	-16.33	*0.987*	*2.757*	*77.39*	-8.307	-5.359	-21.43	-20.92
4	344.5	6.96	-5.7	*1.916*	*1.771*	*13.00*	-4.199	-3.330	-13.32	-12.91
5	377.8	7.22	-12.19	*1.290*	*2.392*	*34.98*	-6.613	-4.563	-18.25	-17.78
6	344.7	7.29	-4.96	*1.945*	*1.674*	*11.73*	-3.925	-3.145	-12.58	-12.18
7	394.3	7.37	-13.11	*1.055*	*2.397*	*49.90*	-7.039	-4.629	-18.52	-18.04
8	377.9	7.67	-9.43	*1.342*	*2.117*	*26.84*	-5.734	-4.025	-16.10	-15.65
9	319.4	7.68	-2.92	*2.029*	*1.258*	*5.580*	**-2.549**	**-2.372**	-9.487	-9.124
10	344.8	8.15	-3.98	*2.043*	*1.476*	*9.247*	**-3.367**	-2.769	-11.08	-10.69
11	377.5	8.19	-7.26	*1.401*	*1.877*	*20.72*	-4.964	-3.556	-14.22	-13.80
12	394.2	8.22	-9.45	*1.157*	*1.955*	*29.46*	-5.511	-3.743	-14.97	-14.53
13	377.7	8.43	-7.07	*1.419*	*1.793*	*18.90*	-4.701	-3.392	-13.57	-13.15
14	319.1	8.59	-2.47	*1.979*	*1.157*	*4.588*	**-2.289**	**-2.184**	-8.736	-8.380
15	377.8	9.27	-5.78	*1.487*	*1.551*	*14.06*	-3.946	-2.924	-11.69	-11.30
16	394.5	9.29	-6.62	*1.252*	*1.605*	*18.75*	-4.335	-3.047	-12.19	-11.78
17	344.5	9.31	-3.38	*1.924*	*1.284*	*6.982*	**-2.831**	-2.408	-9.631	-9.262
18	377.9	10.26	-2.76	*1.393*	*1.885*	*21.03*	-4.997	-3.572	-14.29	-13.86
19	318.9	10.27	-2.24	*1.907*	*1.019*	*3.209*	**-1.939**	**-1.927**	-7.71	-7.360
20	344.6	10.43	-2.82	*1.842*	*1.153*	*5.505*	**-2.469**	-2.160	-8.639	-8.280
21	394.5	11.08	-4.45	*1.373*	*1.267*	*11.09*	-3.222	-2.381	-9.526	-9.150
22	378.0	11.58	-3.67	*1.634*	*1.175*	*7.846*	-2.792	-2.198	-8.792	-8.426
23	378.0	11.58	-4.49	*1.553*	*1.356*	*10.66*	**-3.342**	-2.546	-10.18	-9.804
24	344.7	11.84	-2.60	*1.770*	*1.030*	*4.160*	**-2.138**	-1.929	-7.717	-7.367
25	319.5	11.99	-2.24	*1.848*	*0.919*	*2.209*	-1.696	-1.740	-6.962	-6.622
26	377.6	12.92	-2.76	*1.668*	*1.045*	*5.953*	**-2.397**	-1.947	-7.789	-7.434
27	344.9	13.22	-2.30	*1.716*	*0.940*	*3.188*	**-1.899**	-1.760	-7.041	-6.698
28	394.6	13.30	-3.12	*1.486*	*1.031*	*6.913*	-2.473	-1.922	-7.687	-7.331
29	319.7	13.54	-2.06	*1.806*	*0.847*	*1.467*	-1.522	-1.607	-6.426	-6.092

Table 4.5: Comparison of the calculated and experimental thermal diffusion factors for the mixture of Methane (0.4) and n-Butane (0.6) for different temperatures and pressures using the SRK equation of state and the Peneloux correction.

	T	P		SRK + Peneloux						
	(K)	(atm)	a_Exp	a_RD54a	a_DD55a	a_DD55b	a_HAA69	a_SHF98	a_KEM89	a_KEM02
1	319.4	6.41	-3.56	*2.367*	*1.659*	*7.141*	**-3.498**	**-3.106**	-12.42	-12.03
2	319.2	6.85	-3.06	*2.340*	*1.595*	*6.551*	**-3.340**	**-2.988**	-11.95	-11.56
3	394.1	6.88	-16.33	*1.142*	*4.735*	*160.6*	**-13.98**	-9.085	-36.34	-35.66
4	344.5	6.96	-5.7	*2.238*	*2.033*	*12.25*	**-4.740**	-3.793	-15.17	-14.75
5	377.8	7.22	-12.19	*1.523*	*3.114*	*38.34*	-8.389	-5.874	-23.50	-22.97
6	344.7	7.29	-4.96	*2.265*	*1.947*	*11.93*	**-4.511**	-3.632	-14.53	-14.11
7	394.3	7.37	-13.11	*1.218*	*3.771*	*80.91*	**-10.89**	-7.201	-28.80	-28.21
8	377.9	7.67	-9.43	*1.569*	*2.749*	*29.92*	-7.296	-5.174	-20.70	-20.20
9	319.4	7.68	-2.92	*2.296*	*1.499*	*5.720*	**-3.105**	**-2.809**	-11.24	-10.85
10	344.8	8.15	-3.98	*2.326*	*1.762*	*9.415*	**-4.019**	**-3.286**	-13.14	-12.74
11	377.5	8.19	-7.26	*1.625*	*2.428*	*23.36*	**-6.331**	-4.559	-18.23	-17.77
12	394.2	8.22	-9.45	*1.328*	*2.837*	*40.90*	**-7.920**	-5.381	-21.53	-21.02
13	377.7	8.43	-7.07	*1.640*	*2.321*	*21.46*	**-6.017**	-4.354	-17.42	-16.96
14	319.1	8.59	-2.47	*2.256*	*1.406*	*4.893*	**-2.878**	**-2.637**	-10.547	-10.171
15	377.8	9.27	-5.78	*1.702*	*2.009*	*16.25*	**-5.098**	-3.760	-15.04	-14.61
16	394.5	9.29	-6.62	*1.425*	*2.231*	*24.51*	**-6.021**	-4.206	-16.82	-16.37
17	344.5	9.31	-3.38	*2.197*	*1.572*	*7.489*	**-3.515**	-2.930	-11.72	-11.33
18	377.9	10.26	-2.76	*1.616*	*2.444*	*23.79*	-6.387	-4.590	-18.36	-17.89
19	318.9	10.27	-2.24	*2.196*	*1.272*	*3.674*	**-2.558**	**-2.389**	-9.56	-9.19
20	344.6	10.43	-2.82	*2.123*	*1.436*	*6.155*	**-3.159**	**-2.676**	-10.70	-10.32
21	394.5	11.08	-4.45	*1.546*	*1.709*	*14.10*	**-4.405**	-3.198	-12.79	-12.38
22	378.0	11.58	-3.67	*1.832*	*1.530*	*9.451*	**-3.705**	-2.848	-11.39	-11.00
23	378.0	11.58	-4.49	*1.762*	*1.760*	*12.54*	**-4.369**	**-3.284**	-13.14	-12.73
24	344.7	11.84	-2.60	*2.055*	*1.305*	*4.884*	**-2.822**	**-2.431**	-9.724	-9.352
25	319.5	11.99	-2.24	*2.143*	*1.171*	*2.751*	**-2.326**	**-2.202**	-8.809	-8.449
26	377.6	12.92	-2.76	*1.914*	*1.364*	*7.345*	**-3.227**	**-2.533**	-10.13	-9.750
27	344.9	13.22	-2.30	*2.002*	*1.206*	*3.938*	**-2.572**	**-2.247**	-8.987	-8.622
28	394.6	13.30	-3.12	*1.652*	*1.374*	*8.868*	**-3.396**	**-2.555**	-10.22	-9.837
29	319.7	13.54	-2.06	*2.105*	*1.096*	*2.044*	**-2.154**	**-2.063**	-8.251	-7.896

Table 4.6: Comparison of the calculated and experimental thermal diffusion factors for the mixture of Methane (0.4) and n-Butane (0.6) for different temperatures and pressures using the SRK equation of state with the corresponding states volume correction.

	T (K)	P (atm)	a_Exp	SRK + CS						
				a_RD54a	a_DD55a	a_DD55b	a_HAA69	a_SHF98	a_KEM89	a_KEM02
1	319.4	6.41	-3.56	*2.124*	*1.468*	*5.972*	**-3.031**	-2.536	-10.14	-9.767
2	319.2	6.85	-3.06	*2.087*	*1.386*	*5.776*	**-2.833**	**-2.467**	-9.868	-9.497
3	394.1	6.88	-16.33	*0.983*	*3.236*	*7.577*	-8.366	-3.444	**-13.78**	**-13.26**
4	344.5	6.96	-5.7	*1.916*	*1.865*	*6.095*	-4.199	-2.673	-10.69	-10.29
5	377.8	7.22	-12.19	*1.290*	*2.678*	*6.807*	-6.613	-3.108	**-12.43**	**-11.96**
6	344.7	7.29	-4.96	*1.945*	*1.758*	*5.929*	-3.925	-2.580	-10.32	-9.923
7	394.3	7.37	-13.11	*1.055*	*2.770*	*6.929*	-7.039	-3.055	**-12.22**	**-11.74**
8	377.9	7.67	-9.43	*1.342*	*2.356*	*6.381*	-5.734	-2.835	-11.34	**-10.89**
9	319.4	7.68	-2.92	*2.029*	*1.265*	*5.505*	**-2.549**	-2.270	-9.079	-8.723
10	344.8	8.15	-3.98	*2.043*	*1.537*	*5.572*	**-3.367**	-2.392	-9.569	-9.185
11	377.5	8.19	-7.26	*1.401*	*2.073*	*5.999*	-4.964	-2.601	-10.41	-9.981
12	394.2	8.22	-9.45	*1.157*	*2.228*	*6.165*	-5.511	-2.610	**-10.44**	**-10.00**
13	377.7	8.43	-7.07	*1.419*	*1.975*	*5.861*	-4.701	-2.518	-10.07	-9.655
14	319.1	8.59	-2.47	*1.979*	*1.152*	*5.236*	**-2.289**	**-2.270**	-9.079	-8.723
15	377.8	9.27	-5.78	*1.487*	*1.690*	*5.451*	-3.946	-2.286	-9.142	-8.746
16	394.5	9.29	-6.62	*1.252*	*1.800*	*5.544*	-4.335	-2.264	-9.055	-8.649
17	344.5	9.31	-3.38	*1.924*	*1.321*	*5.190*	**-2.831**	-2.214	-8.856	-8.488
18	377.9	10.26	-2.76	*1.393*	*2.084*	*6.012*	-4.997	**-2.607**	-10.43	-10.00
19	318.9	10.27	-2.24	*1.907*	*0.993*	*4.800*	**-1.939**	**-2.142**	-8.566	-8.220
20	344.6	10.43	-2.82	*1.842*	*1.170*	*4.891*	**-2.469**	-2.091	-8.365	-8.006
21	394.5	11.08	-4.45	*1.373*	*1.383*	*4.899*	-3.222	-1.941	-7.762	-7.386
22	378.0	11.58	-3.67	*1.634*	*1.241*	*4.736*	-2.792	-1.930	-7.720	-7.355
23	378.0	11.58	-4.49	*1.553*	*1.458*	*5.096*	**-3.342**	-2.100	-8.399	-8.019
24	344.7	11.84	-2.60	*1.770*	*1.025*	*4.578*	**-2.138**	-1.977	-7.908	-7.559
25	319.5	11.99	-2.24	*1.848*	*0.873*	*4.431*	-1.696	**-2.042**	-8.168	-7.828
26	377.6	12.92	-2.76	*1.668*	*1.080*	*4.451*	**-2.397**	-1.811	-7.244	-6.889
27	344.9	13.22	-2.30	*1.716*	*0.915*	*4.323*	**-1.899**	**-1.892**	-7.568	-7.225
28	394.6	13.30	-3.12	*1.486*	*1.086*	*4.394*	-2.473	-1.720	-6.882	-6.526
29	319.7	13.54	-2.06	*1.806*	*0.783*	*4.154*	-1.522	**-1.972**	-7.888	-7.553

Table 4.7: Comparison of the calculated and experimental thermal diffusion factors for the mixture of Methane (0.4) and n-Butane (0.6) for different temperatures and pressures using the PR equation of state.

	T (K)	P (atm)	a_Exp	PR						
				a_RD54a	a_DD55a	a_DD55b	a_HAA69	a_SHF98	a_KEM89	a_KEM02
1	319.4	6.41	-3.56	*2.091*	*1.416*	*8.071*	**-2.912**	-2.764	-11.06	-10.68
2	319.2	6.85	-3.06	*2.054*	*1.341*	*7.241*	**-2.715**	**-2.619**	-10.48	-10.11
3	394.1	6.88	-16.33	*0.996*	*2.697*	*99.65*	-8.099	-5.497	-21.99	-21.48
4	344.5	6.96	-5.7	*1.920*	*1.778*	*14.81*	-4.177	-3.479	-13.92	-13.51
5	377.8	7.22	-12.19	*1.293*	*2.419*	*43.21*	-6.671	-4.831	-19.32	-18.85
6	344.7	7.29	-4.96	*1.952*	*1.677*	*13.32*	-3.893	-3.281	-13.12	-12.72
7	394.3	7.37	-13.11	*1.064*	*2.362*	*61.45*	-6.912	-4.787	-19.15	-18.67
8	377.9	7.67	-9.43	*1.346*	*2.137*	*32.39*	-5.767	-4.254	-17.01	-16.57
9	319.4	7.68	-2.92	*1.997*	*1.231*	*6.107*	**-2.431**	**-2.406**	-9.626	-9.263
10	344.8	8.15	-3.98	*2.062*	*1.472*	*10.46*	**-3.316**	-2.878	-11.51	-11.13
11	377.5	8.19	-7.26	*1.399*	*1.898*	*24.97*	-5.009	-3.768	-15.07	-14.64
12	394.2	8.22	-9.45	*1.407*	*1.890*	*24.58*	-4.977	-3.751	-15.00	-14.58
13	377.7	8.43	-7.07	*1.167*	*1.940*	*35.05*	-5.441	-3.898	-15.59	-15.15
14	319.1	8.59	-2.47	*1.426*	*1.803*	*22.30*	-4.705	-3.574	-14.30	-13.88
15	377.8	9.27	-5.78	*1.946*	*1.130*	*5.054*	**-2.169**	**-2.212**	-8.848	-8.493
16	394.5	9.29	-6.62	*1.497*	*1.555*	*16.37*	-3.927	-3.071	-12.29	-11.89
17	344.5	9.31	-3.38	*1.264*	*1.595*	*21.88*	-4.279	-3.181	-12.72	-12.32
18	377.9	10.26	-2.76	*1.902*	*1.275*	*7.892*	**-2.764**	-2.490	-9.962	-9.592
19	318.9	10.27	-2.24	*1.567*	*1.354*	*12.32*	-3.305	-2.666	-10.66	-10.28
20	344.6	10.43	-2.82	*1.875*	*0.991*	*3.602*	**-1.817**	**-1.946**	-7.784	-7.438
21	394.5	11.08	-4.45	*1.821*	*1.140*	*6.246*	**-2.391**	-2.226	-8.905	-8.545
22	378.0	11.58	-3.67	*1.391*	*1.256*	*12.79*	-3.164	-2.484	-9.937	-9.560
23	378.0	11.58	-4.49	*1.658*	*1.169*	*9.047*	-2.738	-2.292	-9.169	-8.803
24	344.7	11.84	-2.60	*1.748*	*1.014*	*4.768*	-2.049	-1.981	-7.925	-7.575
25	319.5	11.99	-2.24	*1.816*	*0.891*	*2.560*	-1.573	-1.754	-7.017	-6.678
26	377.6	12.92	-2.76	*1.644*	*1.034*	*6.886*	**-2.331**	-2.024	-8.094	-7.739
27	344.9	13.22	-2.30	*1.694*	*0.922*	*3.712*	-1.804	-1.802	-7.208	-6.865
28	394.6	13.30	-3.12	*1.518*	*1.018*	*7.982*	-2.403	-1.998	-7.992	-7.636
29	319.7	13.54	-2.06	*1.775*	*0.819*	*1.788*	-1.396	-1.616	-6.464	-6.130

Table 4.8: Comparison of the calculated and experimental thermal diffusion factors for the mixture of Methane (0.4) and n-Butane (0.6) for different temperatures and pressures using the PR equation of state and the Peneloux correction.

	T (K)	P (atm)	a_Exp	PR + Peneloux							
				a_RD54a	a_DD55a	a_DD55b	a_HAA69	a_SHF98	a_KEM89	a_KEM02
1	319.4	6.41	-3.56	*2.091*	*1.416*	*8.071*	**-2.912**	-2.764	-11.06	-10.68
2	319.2	6.85	-3.06	*2.054*	*1.341*	*7.241*	**-2.715**	**-2.619**	-10.48	-10.11
3	394.1	6.88	-16.33	*0.996*	*2.697*	*99.65*	-8.099	-5.497	-21.99	-21.48
4	344.5	6.96	-5.7	*1.920*	*1.778*	*14.81*	-4.177	-3.479	-13.92	-13.51
5	377.8	7.22	-12.19	*1.293*	*2.419*	*43.21*	-6.671	-4.831	-19.32	-18.85
6	344.7	7.29	-4.96	*1.952*	*1.677*	*13.32*	-3.893	-3.281	-13.12	-12.72
7	394.3	7.37	-13.11	*1.064*	*2.362*	*61.45*	-6.912	-4.787	-19.15	-18.67
8	377.9	7.67	-9.43	*1.346*	*2.137*	*32.39*	-5.767	-4.254	-17.01	-16.57
9	319.4	7.68	-2.92	*1.997*	*1.231*	*6.107*	**-2.431**	**-2.406**	-9.626	-9.263
10	344.8	8.15	-3.98	*2.062*	*1.472*	*10.46*	**-3.316**	-2.878	-11.51	-11.13
11	377.5	8.19	-7.26	*1.399*	*1.898*	*24.97*	-5.009	-3.768	-15.07	-14.64
12	394.2	8.22	-9.45	*1.407*	*1.890*	*24.58*	-4.977	-3.751	-15.00	-14.58
13	377.7	8.43	-7.07	*1.167*	*1.940*	*35.05*	-5.441	-3.898	-15.59	-15.15
14	319.1	8.59	-2.47	*1.426*	*1.803*	*22.30*	-4.705	-3.574	-14.30	-13.88
15	377.8	9.27	-5.78	*1.946*	*1.130*	*5.054*	**-2.169**	**-2.212**	-8.848	-8.493
16	394.5	9.29	-6.62	*1.497*	*1.555*	*16.37*	-3.927	-3.071	-12.29	-11.89
17	344.5	9.31	-3.38	*1.264*	*1.595*	*21.88*	-4.279	-3.181	-12.72	-12.32
18	377.9	10.26	-2.76	*1.902*	*1.275*	*7.892*	**-2.764**	-2.490	-9.962	-9.592
19	318.9	10.27	-2.24	*1.567*	*1.354*	*12.32*	-3.305	-2.666	-10.66	-10.28
20	344.6	10.43	-2.82	*1.875*	*0.991*	*3.602*	**-1.817**	**-1.946**	-7.784	-7.438
21	394.5	11.08	-4.45	*1.821*	*1.140*	*6.246*	**-2.391**	-2.226	-8.905	-8.545
22	378.0	11.58	-3.67	*1.391*	*1.256*	*12.79*	-3.164	-2.484	-9.937	-9.560
23	378.0	11.58	-4.49	*1.658*	*1.169*	*9.047*	-2.738	-2.292	-9.169	-8.803
24	344.7	11.84	-2.60	*1.748*	*1.014*	*4.768*	-2.049	-1.981	-7.925	-7.575
25	319.5	11.99	-2.24	*1.816*	*0.891*	*2.560*	-1.573	-1.754	-7.017	-6.678
26	377.6	12.92	-2.76	*1.644*	*1.034*	*6.886*	**-2.331**	-2.024	-8.094	-7.739
27	344.9	13.22	-2.30	*1.694*	*0.922*	*3.712*	-1.804	-1.802	-7.208	-6.865
28	394.6	13.30	-3.12	*1.518*	*1.018*	*7.982*	-2.403	-1.998	-7.992	-7.636
29	319.7	13.54	-2.06	*1.775*	*0.819*	*1.788*	-1.396	-1.616	-6.464	-6.130

Table 4.9: Comparison of the calculated and experimental thermal diffusion factors for the mixture of Methane (0.4) and n-Butane (0.6) for different temperatures and pressures using the PR equation of state and the corresponding states volume correction.

	T (K)	P (atm)	a_Exp	PR + CS							
				a_RD54a	a_DD55a	a_DD55b	a_HAA69	a_SHF98	a_KEM89	a_KEM02
1	319.4	6.41	-3.56	*2.091*	*1.428*	*5.967*	**-2.912**	-2.501	-10.00	-9.627
2	319.2	6.85	-3.06	*2.054*	*1.346*	*5.770*	**-2.715**	-2.432	-9.728	-9.357
3	394.1	6.88	-16.33	*0.993*	*3.162*	*7.534*	-8.153	-3.386	**-13.55**	-13.03
4	344.5	6.96	-5.7	*1.920*	*1.860*	*6.128*	-4.177	-2.677	-10.71	-10.30
5	377.8	7.22	-12.19	*1.293*	*2.702*	*6.870*	-6.671	-3.138	**-12.55**	**-12.08**
6	344.7	7.29	-4.96	*1.952*	*1.749*	*5.958*	-3.893	-2.581	-10.32	-9.923
7	394.3	7.37	-13.11	*1.064*	*2.727*	*6.918*	-6.912	-3.025	**-12.10**	**-11.62**
8	377.9	7.67	-9.43	*1.346*	*2.371*	*6.432*	-5.767	-2.857	-11.43	**-10.98**
9	319.4	7.68	-2.92	*1.997*	*1.225*	*5.499*	**-2.431**	-2.328	-9.311	-8.948
10	344.8	8.15	-3.98	*2.062*	*1.522*	*5.592*	**-3.316**	-2.386	-9.545	-9.160
11	377.5	8.19	-7.26	*1.399*	*2.091*	*6.053*	-5.009	-2.623	-10.49	-10.06
12	394.2	8.22	-9.45	*1.407*	*2.080*	*6.041*	-4.977	-2.617	-10.47	-10.04
13	377.7	8.43	-7.07	*1.167*	*2.205*	*6.174*	-5.441	-2.599	**-10.39**	**-9.956**
14	319.1	8.59	-2.47	*1.426*	*1.979*	*5.898*	-4.705	-2.531	-10.13	-9.706
15	377.8	9.27	-5.78	*1.946*	*1.112*	*5.229*	**-2.169**	**-2.235**	-8.941	-8.585
16	394.5	9.29	-6.62	*1.497*	*1.686*	*5.479*	-3.927	-2.292	-9.169	-8.770
17	344.5	9.31	-3.38	*1.964*	*1.782*	*5.555*	-4.279	-2.258	-9.033	-8.626
18	377.9	10.26	-2.76	*1.902*	*1.300*	*5.202*	**-2.764**	-2.203	-8.811	-8.441
19	318.9	10.27	-2.24	*1.567*	*1.448*	*5.115*	-3.305	-2.101	-8.404	-8.023
20	344.6	10.43	-2.82	*1.875*	*0.951*	*4.792*	**-1.817**	**-2.107**	-8.428	-8.082
21	394.5	11.08	-4.45	*1.821*	*1.144*	*4.898*	**-2.391**	-2.077	-8.307	-7.947
22	378.0	11.58	-3.67	*1.391*	*1.364*	*4.908*	-3.164	-1.936	-7.743	-7.366
23	378.0	11.58	-4.49	*1.658*	*1.224*	*4.749*	-2.738	-1.927	-7.708	-7.341
24	344.7	11.84	-2.60	*1.748*	*0.996*	*4.581*	-2.049	-1.960	-7.840	-7.490
25	319.5	11.99	-2.24	*1.816*	*0.831*	*4.423*	-1.573	**-2.008**	-8.032	-7.693
26	377.6	12.92	-2.76	*1.644*	*1.058*	*4.459*	**-2.331**	-1.805	-7.219	-6.864
27	344.9	13.22	-2.30	*1.694*	*0.884*	*4.323*	-1.804	**-1.873**	-7.493	-7.150
28	394.6	13.30	-3.12	*1.518*	*1.063*	*4.399*	-2.403	-1.714	-6.856	-6.499
29	319.7	13.54	-2.06	*1.775*	*0.740*	*4.146*	-1.396	**-1.938**	-7.754	-7.420

models (2.40), (2.47) do not predict the right sign. For this system the Haase model with the SRK EoS and Peneloux corrections performs better than other models, with an average deviation of around 10.62%. The best-fitted experimental points, with the deviations within 20%, are marked bold in Tables 4.4 to 4.9. The cells marked with italic font correspond to the values that do not predict the correct sign for the thermal diffusion factor. Comparing the equations of state, we observed that the SRK EoS provides better results. The Peneloux correction, again, gives no significant improvement when used with the PR EoS. However when this correction is used with the SRK EoS, the results obtained with the Haase model (2.49) and Shukla and Firoozabadi (2.50) are significantly improved. The volume correction based on the corresponding states model slightly improves the results for the models of Shukla and Firoozabadi (2.50) and both Kempers approaches (2.51) and (2.52); however it is not as good as the Peneloux correction.

4.2.2 Other sets of binary mixtures

We extended the calculations described above to additional sets of binary mixtures. The results are diveded into two parts: the first part where the components are not alcohols (mixture 1 to the mixture 71), and the second part, where at least one of the substances is an alcohol (mixture 80 to mixture 92). We implemented three EoS to determine the thermodynamic properties, as described above. The results were analysed in terms of correct sign of the thermal diffusion factor and of the average deviation. For the mixture of Benzene + n-Heptane (mixture 5) we report comparison between the models and the three sets of experimental values presented in the literature. In the second part we present different results obtained for the mixture of Methanol + Benzene (mixture 80).

Appendix B contains all the results obtained for each mixture of Table 4.1 using the models specified in table 4.3.

4.2.2.1 Mixtures without alcohol components

First we analysed, which of the models was capable of correctly determining the sign for the thermal diffusion factor. We found that the Haase model, equation

(2.49), was able to predict the correct sign for 50 mixtures out 71 mixtures. The Rutherford and Drickamer models, equation (2.36) and equation (2.37), did so for 49 mixtures followed by Dougherty and Drickamer first model, equation (2.40), with 38 mixtures. Both of Kempers approaches, equation (2.51) and equation (2.52) and the Shukla and Firoozabadi model, equation (2.50) estimated the correct sign for 36 mixtures. The second approach of Dougherty and Drickamer model, equation (2.47), and the Tichacek model, equation (2.44), estimated the correct sign for 35 mixtures and, at last, the Shieh model, (2.45), did so only for 34 mixtures. For most of the mixtures, when the models of Dougherty and Drickamer, Tichacek et al. and Shieh estimated the correct sign, both models of Kempers and Shukla and Firoozabadi did not, and vice versa. On the other hand, the Rutherford and Drickamer and the Haase equations do not seem to follow any particular behavior with respect to other models. Furthermore, both approaches of Rutheford and Drickamer exhibit change of sign for some mixtures. In some cases the changes are expected, in comparison with the experimental data, and in some other cases are not.

We analysed which of the models gave the smallest standard deviation error. The results obtained show that in most of the cases Rutherford and Drickamer model, equation (2.36), had the smallest error for 21 mixtures out of 71, while their second model, expression (2.36), presented the smallest error for 9 mixtures. The Shukla and Firoozabadi model (2.50) and the Haase model (2.49) gave the smallest deviations for 13 and 11 mixtures, correspondingly. The model of Dougherty and Drickamer, equation (2.40), gave the smallest error for 13 mixtures. For the case where this model gave the best approximation, generally the models of Haase, Shukla and Firoozabadi, and Kempers failed. It has to be remarked that for some mixtures even the smallest error remains very large, of the order of 10^5 percent.

Some very good approximations were obtained for the mixture of Toluene + n-Heptane (mixture 52) for which the model of Shukla and Firoozabadi gave a standard deviation of 5.6% with the SRK EOS. The Rutherford and Drickamer model gave standard deviations of 4.19% (with the SRK EoS) and 3.91% (with the PR EoS) for the mixtures of Isobutyl-benzene + n-Dodecane (mixture 71). The model of Haase, equation (2.49), gave a standard deviation of 0.89% for the mixture of n-

Table 4.10: Experimental thermal diffusion factor reported for the mixture of Benzene + n-Heptane (mixture 5) by three different sources, Trevoy and Drickamer [124], Korsching [62] and Bou-Ali et al. [8].

Trevoy and Drickamer [124]			Korsching [62]			Bou-Ali et al. [8]		
$z_{Benzene}$	T	α^T_{Exp}	$z_{Benzene}$	T	α^T_{Exp}	$z_{Benzene}$	T	α^T_{Exp}
0.5	296.10	-1.19	0.1	308.70	0.69	0.1	298.00	0.92
0.5	306.20	-1.20	0.2	308.70	0.75			
0.5	321.35	-1.06	0.3	308.70	0.84	0.3	298.00	1.03
0.5	337.10	-1.14	0.4	308.70	1.00			
0.5	306.35	-1.24	0.5	308.70	1.21	0.5	298.00	1.48
0.5	306.55	-1.28	0.6	308.70	1.41			
			0.7	308.70	1.56	0.75	298.00	2.06
			0.8	308.70	1.83	0.8	298.00	2.19
			0.9	308.70	2.02	0.9	298.00	2.47

Heptane + n-Octadecane (mixture 58) with the PR EoS. The models of Kempers, equation (2.51) and eqution (2.52), gave standard errors of 3.76% and 3.75% for the system Benzene + Carbon Tetrachloride (mixture 02) with the SRK EoS. For the system n-Heptane + n-Pentadecane (mixture 56) the smallest errors were also obatined with the first and second model of Kempers models with 10.78% and 10.58% correspondingly, with the SRK EoS in both cases. Finally, we found that the model of Shukla and Firoozabadi, equation (2.50), gave an error of 5.6% for the mixture Toluene + n-Heptane (mixture 52) with the SRK EoS. The system of Tetrahydronaphtaline + n-Dodecane presented good approximation both with the Haase model (3.84%) and for the Shukla and Firoozabadi model (5.96%) with the SRK EoS.

Some data for the same mixtures were measured using different experimental techniques. We noticed in some cases inconsistencies between the experimental values. In particular, we found that for the mixture of Benzene + n-Heptane (mixture 5) the measurements performed by Trevoy and Drickamer [125] present an opposite sign from those reported by Korsching [62] and Bou-Ali et al. [8]. The results obtained by the three different research groups are reported in Table 4.10.

We have compared each of the three experimental sets presented in Table 4.10 with different models. Figure 4.4 shows the obtained results. The notation used

in the plots follows the specifications given in Table 4.3. Plots (a) and (b) present the results in comparison with the experimental data of Trevoy and Drickamer. The results are plotted as functions of the temperature. Plots (c) and (d) show comparison with the experimental data of Korsching. The results are presented as functions of the mole fraction. Finally, plots (e) and (f) shows the results for the conditions given by Bou-Ali et al. They are also plotted as functions of the mole fraction.

The models of Rutherford and Drickamer (2.36) and (2.36), Haase (2.49), Shukla and Firoozabadi (2.50) and both of Kempers models (2.51) and (2.52) predict positive thermal diffusion factor for this mixture. On the contrary, both models of Dougherty and Drickamer (2.40) and (2.47), Tichacek et al. (2.44) and Shieh (2.45) predict negative thermal diffusion factor. The models of Shukla and Firoozabadi (2.50) and Rutherford and Drickamer (2.36) provide the best approximation in comparison with Korsching and Bou-Ali et al. data. On the other hand, the model of Dougherty and Drickamer (2.40) provides the best approximation in comparison with Trevoy and Drickamer data [125]. We believe that the last reported values by Korsching [62] and Bou-Ali et al. [8] are more reliable than those reported by Trevoy and Drickamer [125]. One would expect for all the mixtures containing Benzene + n-Alcane, where the n-Alcane is of higher density than Benzene, to have a positive thermal diffusion factor. The results presented by Trevoy and Drickamer [125] show exactly the opposite (mixtures 05, 07, 08, 09, 10 and 11).

The thermal diffusion factor for 26 mixtures containing carbon disulfide have been reported [28, 98, 99]. Comparing the experimental values with those calculated by different models, we see that the best model is the one of Rutherford and Drickamer, which can predict the correct sign for 21 mixtures and has the lowest standard error. However, this model presents an unexpected change of sign for some systems, as for example the mixtures with Benzene (mixture 16), Bromo-Benzene (mixture 30), n-Butyl Bromide (mixture 36) and n-Butyl Chloride (mixture 37). The model of Haase predicts the correct sign for 17 mixtures and the Shukla and Firoozabadi model and both of Kempers approaches can predict the correct sign for 15 mixtures. The Shukla and Firoozabadi model, equation (2.50), is the best between these four

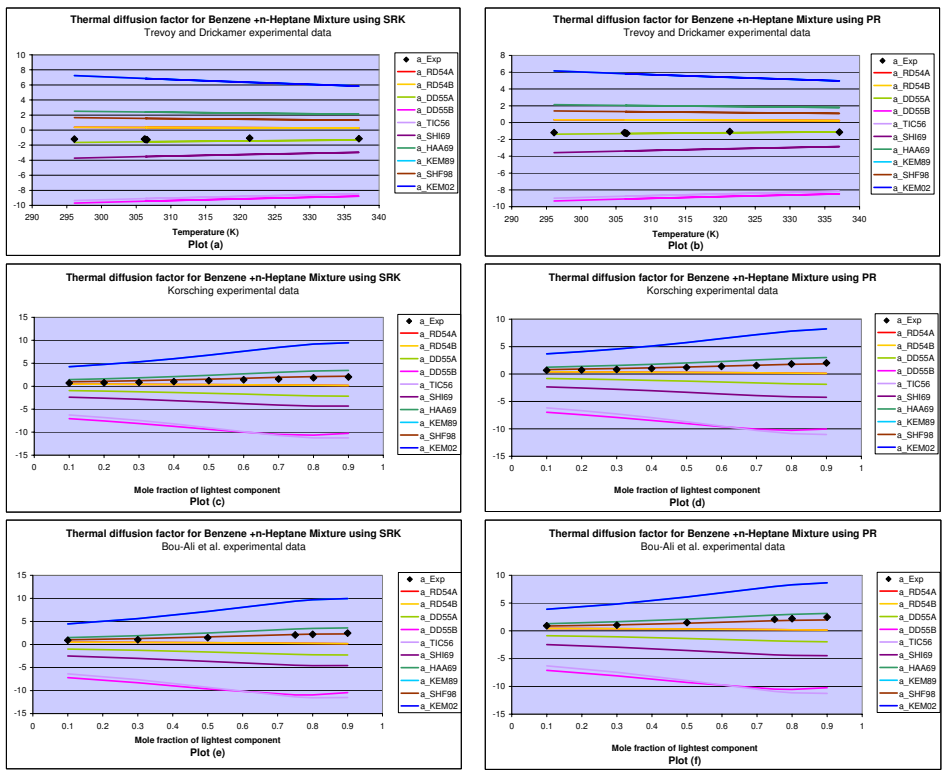

Figure 4.4: Comparison between experiments and calculations for the thermal diffusion factor for Benzene - nHeptane mixture reported by three different sources. The measured values are denoted by a_EXP; the Rutherford and Drickamer model is represented by a_RD54a; their second model by a_RD54b; the Dougherty and Drickamer first model by a_DD55a; the Dougherty and Drickamer second model by a_DD55b; the Tichacek et al. model by a_TIC56; the Shieh model by a_SHI69; the Haase model by a_HAA69; the Shukla and Firoozabadi by a_SHF98; the Kempers from 1989 by a_KEM89; and finally the Kempers from 2002 by a_KEM02.

Table 4.11: Results obtained from different models for the mixtures where one of the components is alcohol.

Model	Components	Mixtures	Error
Rutherford and Drickamer	Water + 2-Propanol	87	28.98 %
	Ethanol + Diethylamine	88	51.94 %
	Ethanol + Triethylamine	83	80.84 %
	Water + Ethanol	85	181.7 %
	Water + Methanol	84	203.8 %
	Methanol + Benzene	80	597.6 %
Shukla and Firoozabadi	Methanol + Carbon Tetrachloride	81	66.70 %
	Ethanol + Cyclohexane	82	98.40 %
	Water + Diethylamine	86	373.1 %
Douherty and Drickamer	2-Butanol + Carbon Disulfide	92	65.70 %

expressions, followed by the Haase model. The rest of the models, both of Dougherty and Drickamer, Tichacek et al. and Shieh, can only predict the correct sign for 13 mixtures. The model of Dougherty and Drickamer, equation (2.40), gives the best approximation among these last expressions.

4.2.2.2 Mixtures with alcohol

Thermodiffusion factors of ten mixtures containing an alcohol compound were compared with experimental values. As mentioned before, only the CPA EoS was used to determine the thermodynamic properties. The results obtained for these mixtures are more difficult to analyze. It was noticed that the experimental values change sign depending on the concentration (mixtures 82 and 84). For mixture 86 the models present change of sign, contrary to the experimental data. We have evaluated the models in terms of the lowest error. However, the errors still remain very large. Table 4.11 details the results for each of the models.

The Ethanol + Cyclohexane mixture (mixture 82) exhibits a change of sign in the experiments and this can not be predicted by any of the models. The Water + Methanol mixture (mixture 84) exhibits a change of sign both in the experimental and in the calculated values. However, these changes of sign do not correspond to each other.

Legros et al. [68] compared different sets of experimental data found in the literature for the mixture Methanol + Benzene (mixture 80). Figure 4.5 presents in plot (a) the experimental values reported by Legros et al. Plot (b) shows the results obtained with different models. Large disagreement can be noticed between the experimental data from different sources, as well as between the models.

Some of the data exhibits change of sign for high concentrations of Methanol. None of the models is capable of predicting this effect. The tendency is not reproduced, either. In particular, the values obtained by Thomaes are much smaller than other experimental values. No sign agreement for this mixture can be establised. Therefore, the only conclusion with regards to this mixture is complete indefiniteness of the information available.

4.3 Conclusions

The analysis leads to the conclusion that, although if none of the models correctly describes the thermal diffusion factor for all the mixtures, we can use the Haase expression, equation (2.49), as a first estimation. One can see that the Haase model is the best for the systems of n-Pentane + n-Decane and Methane + n-Butane. For the systems of Benzene + Cyclohexane and Methane + n-Propane the best approach is that of Shukla and Firoozabadi (2.50). However, for the last two systems the Haase model gives good approximation as well. The Kempers model is capable to correctly predict the sign of the thermal diffusion factor; however, it overestimates its value with respect to the experimental data. One may conclude that the Haase model provides generally reasonable and stable results. The Shukla and Firoozabadi and the Kempers models may be better for some systems or experimental values, however, they may give large errors for other systems. Both models of Dougherty and Drickamer do not provide good results for the investigated mixtures, even for the mixtures of similar molecules, for which they were originally designed. The second series of calculations, confirms good performance of the Haase model. Surprisingly good approximations were obtained with the model of Rutherford and Drickamer, which in the first series of calculations did not give good results. It is important to

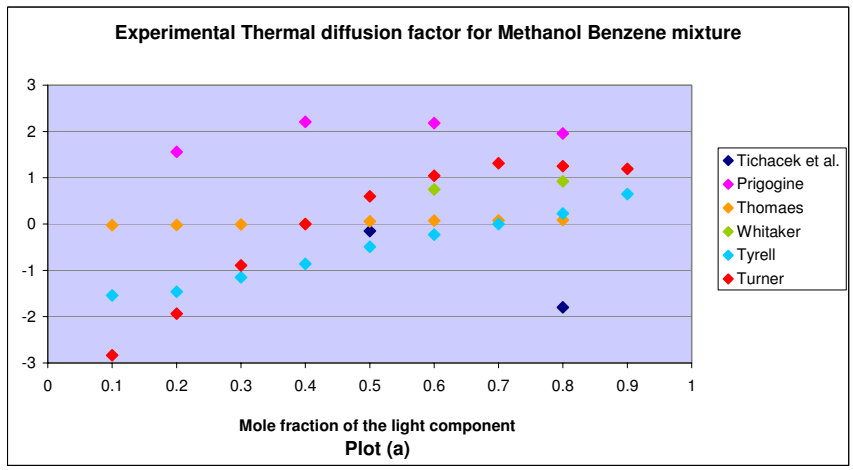

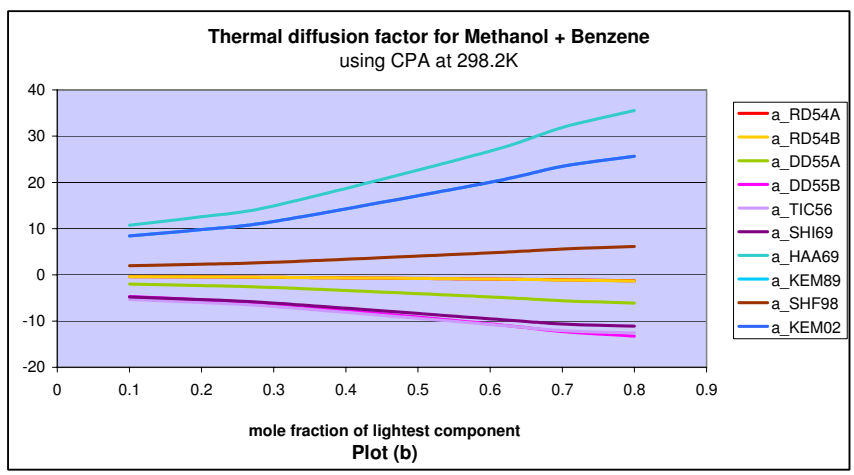

Figure 4.5: Experimental thermal diffusion factor reported in the litterature for the mixture Methanol + Benzene by six different research groups are shown in plot (a). Plot (b) shows the models resutls where the Rutherford and Drickamer model is represented by a_RD54a; their second model by a_RD54b; the Dougherty and Drickamer first model by a_DD55a; the Dougherty and Drickamer second model by a_DD55b; the Tichacek et al. model by a_TIC56; the Shieh model by a_SHI69; the Haase model by a_HAA69; the Shukla and Firoozabadi by a_SHF98; the Kempers from 1989 by a_KEM89; and finally the Kempers from 2002 by a_KEM02.

point out that the standard errors are in general very large, with only few exceptions.

We can confirm an observation made by Kempers [53] that the thermal diffusion factors are very sensitive to the values of partial molar properties. Therefore, they are sensitive to the EoS chosen as well as to a method applied for calculation of the partial molar volume. It is even more difficult to correctly calculate the thermodynamic properties for the mixtures with associating compounds. As mentioned in the work of Kempers [53], there is a need for improving the existing equations of state in such a way that they are not only able to predict the phase equilibria, but also the partial molar properties with a high degree of accuracy. This is the well-known limitation for the presently available equations of state. The fact that the Peneloux corrections do not improve the results in the most cases (while they improve prediction of the partial molar properties) may be interpreted as insufficiency and roughness of the existing models for the thermal diffusion factors.

Our work was complicated by the fact that the experimental data on thermal diffusion coefficients were not very reliable, as indicated by disagreement between the different sources. For the same systems, the experimental values reported could present large disagreement.

Chapter 5

A new model for estimation of the thermal diffusion coefficients

Several thermodynamic models for the thermodiffusion coefficients have been proposed along the years. However, the analysis performed in Chapter 4, where the different models were tested by comparison with experimental data, indicated that there has been no single model, which would uniformly be good for all the data sets. Prediction of the thermal diffusion factors within an order of magnitude and prediction of the right sign seems to be a maximum possible achievement of a model. It should be noted that all the models are based on different more or less rough assumptions, which imprecision is difficult to evaluate. For the only case of ideal gas mixtures, where the rigorous theory exists (based on the Boltzmann gas kinetic theory [47]), it provides a good approximation to the thermodiffusion coefficients, at least, for the binary mixtures as it is shown in Chapter 6.

In order to overcome this problem, a general and rigorous theory of the transport properties was developed on the basis of the statistical mechanics and the non-equilibrium theory of fluctuations [113, 114]. Particular implementation of the theory was successfully tested by evaluation of the diffusion coefficients in binary mixtures [74]. In this chapter we present general results of this new theory for description of thermodiffusion in binary mixtures. An expression for the thermal diffusion coefficient in a general non-ideal binary mixture is presented, based on the standard thermodynamic quantities and on the new variables, the penetration

lengths. The properties of the thermal diffusion coefficient are discussed based on the derived expression.

As was mentioned in the literature [111], one of the problems in modeling the thermodiffusion coefficients lies in the fact that the fundamental thermodynamic quantities, energy and entropy, are determined within a constant. If these quantities, or other partial molar quantities, enter a modeling expression for a transport coefficient, it is reasonable to require that the result is invariant with regard to the constants determining the values of entropy and energy at the reference state. This requirement is not satisfied for most of the models for thermodiffusion coefficients discussed in Chapter 2.

Another, somehow more delicate question, is dependence of the transport properties on formation energies and formation entropies (often reported as formation enthalpies and formation Gibbs energies, [96]). The chemical potentials and many other partial molar values depend on these quantities. Together with the partial molar values, the energies and the entropies of formation enter modeling expressions for the thermodiffusion coefficients. However, there is no physical grounds why the thermodiffusion coefficients should depend on these values.

We demonstrate invariance of the thermal diffusion coefficient, derived within our model, with regard to the reference state, as well as with regard to the energies and entropies of formation. This provides a good theoretical validation for the proposed model, although further validation and testing of the theory is required.

5.1 Diffusion and thermodiffusion coefficients in a binary mixture

The general theory of transport coefficients in multicomponent mixtures was formulated in [113] and afterwards extended onto non-isothermal mixtures in [114]. The approach consisted in considering the fluctuations around an equilibrium state in a two-vessel system. The equilibrium distribution of the thermodynamic values in the vessels may be found from the basic formalism of the statistical mechanics, while dynamics of the fluctuations may be described in the framework of the theory of

random processes. The theoretical deduction is rather complicated and we will only bring the final results.

We calculate the $n \times n$ matrix $\mathbf{L}$ of diffusion and heat transfer coefficients for the n-component mixture. This matrix is determined as a proportionality matrix between the $n-1$ diffusion fluxes $\dot{\mathbf{d}}_i$, the nth heat flux $\dot{\mathbf{d}}_n$, and the corresponding n thermodynamic forces $\mathbf{X}_i$:

$$\dot{\mathbf{d}}_i = \sum_{j=1}^{n-1} L_{ij}\mathbf{X}_j \tag{5.1}$$

The fluxes and the forces are chosen according to the principles of the non-equilibrium thermodynamics, so that the sum $\dot{\mathbf{d}}_i\mathbf{X}_i$ is equal to the entropy production. In the convective-diffusive system of thermodynamic variables [23], the first $(n-1)$ fluxes are diffusion fluxes, while the nth flux is the non-convective heat transfer:

$$\dot{\mathbf{d}}_i = M_i\dot{\mathbf{n}}_i - c_i\mathbf{x}_c,\ \mathbf{x}_c = \sum_{j=1}^{n} M_i\dot{\mathbf{n}}_i\ (i = 1, \ldots, n-1);\ \dot{\mathbf{d}}_n = \dot{\mathbf{u}} - \frac{h}{M}\mathbf{x}_c; \tag{5.2}$$

$$\mathbf{X}_i = \nabla\left(\frac{\mu^n}{M_nT} - \frac{\mu^i}{M_iT}\right) \quad (i = 1, \ldots, n-1);\ \mathbf{X}_n = \nabla\left(\frac{1}{T}\right) \tag{5.3}$$

Here $\dot{\mathbf{n}}_i$ are the molar fluxes of the components, M_i their molecular masses, c_i the mass fractions, $\mathbf{x}_c$ the mass convective flux, $\dot{\mathbf{u}}$ the flux of internal energy, h the molar enthalpy, μ^i the chemical potentials, and T the temperature. The average molar mass M is equal to $\sum M_iz_i$, or $\sum M_iN_i/N$, where N_i are partial molar densities, $N = \sum N_i$ the overall molar density, and z_i the molar fractions.

Such a defined matrix $\mathbf{L}$ has been found to be expressed in terms of the symmetrized transfer matrix $\overline{\mathbf{L}}_{Tr}$, responsible for the fluctuation-induced transfer of $\dot{\mathbf{n}}_j,\ \dot{\mathbf{u}}$:

$$\mathbf{L} = \mathbf{G}\overline{\mathbf{L}}_{Tr}\mathbf{G}^T, \quad \overline{\mathbf{L}}_{Tr} = \frac{1}{2}(\mathbf{L}_{Tr} + \mathbf{L}_{Tr}^T) \tag{5.4}$$

Here $\mathbf{G}$ is the transformation matrix to the convective-diffusive system of ther-

modynamic variables, expressed as follows:

$$\mathbf{G} = \begin{pmatrix} (1-c_1)M_1 & -c_1M_2 & \cdots & \cdots & -c_1M_n & 0 \\ -c_2M_1 & (1-c_2)M_2 & \cdots & \cdots & -c_2M_n & 0 \\ \vdots & \vdots & \ddots & \vdots & \vdots & \vdots \\ -c_{n-1}M_1 & -c_{n-1}M_2 & \cdots & (1-c_{n-1})M_{n-1} & -c_{n-1}M_n & 0 \\ \frac{-M_1h}{M} & \frac{-M_2h}{M} & \cdots & \frac{-M_{n-1}h}{M} & \frac{-M_nh}{M} & 1 \end{pmatrix} \tag{5.5}$$

The $(n+1)\times(n+1)$ matrix $\mathbf{L}_{Tr}$ possesses a block structure, consisting of the $n\times n$ molecular transfer matrix $\mathbf{L}_N$, the $1\times n$ block of convective energy transfer $\mathbf{L}_{NU}$, the $n\times 1$ block of the thermally induced mass transfer $\mathbf{L}_{UN}$, and the 1×1 block (single coefficient) for the energy transfer:

$$\mathbf{L}_{Tr} = \begin{pmatrix} \mathbf{L}_N & \mathbf{L}_{UN} \\ \mathbf{L}_{NU} & L_{UU} \end{pmatrix} \tag{5.6}$$

The coefficients of the corresponding matrices may be found as:

$$L_{N,ij} = \frac{C_i}{4}\left[-Z_i f_{ij} + N_i \sum_k \frac{\partial Z_i}{\partial N_k} f_{kj} + N_i \frac{\partial Z_i}{\partial U} f_{n+1,j}\right] \quad (i,j=1,...,n); \tag{5.7}$$

$$L_{NU,i} =$$

$$\frac{C_i}{4}\left[-Z_i f_{i,n+1} + N_i \sum_k \frac{\partial Z_i}{\partial N_k} f_{k,n+1} + N_i \frac{\partial Z_i}{\partial U} f_{n+1,n+1} + N_i Z_i \frac{T}{2}\right]; \tag{5.8}$$

The expressions for the components of the vector column $\mathbf{L}_{UN}$ and for the element L_{UU} are expressed in terms of the previously determined coefficients:

$$L_{UN,i} = \sum_j \left(u_j + \frac{RT}{2}\right) L_{N,ji} + \frac{1}{4}\sum_j C_j N_j \left(Z_j - 2Z_U\right)\chi_{ij}; \tag{5.9}$$

$$L_{UU} = \sum_j \left(u_j + \frac{RT}{2}\right) L_{NU,j} + \frac{1}{4}\sum_j C_j N_j \left(Z_j - 2Z_U\right)\left(\chi_{n+1,j} - \frac{RT^2}{8}\right) \tag{5.10}$$

In expressions (5.7) to (5.10) the partial molar energies u_j are involved. The values of $C_i = (8RT/\pi M_i)^{1/2}$ are average molecular velocities of the ith component.

The thermodynamic coefficients f_{ij} are determined as follows. First, the entropy

of a unit volume S is expressed in terms of its proper variables: molar densities N_i and the internal energy density U. Then the $(n+1) \times (n+1)$ matrix of second derivatives is found:

$$F_{ij} = \frac{\partial^2 S}{\partial N_i \partial N_j}; \quad F_{i,n+1} = F_{n+1,i} = \frac{\partial^2 S}{\partial N_i \partial U}; \quad F_{n+1,n+1} = \frac{\partial^2 S}{\partial U^2} \tag{5.11}$$

$$(i, j = 1, \ldots, n)$$

Finally, the matrix $\mathbf{f}$ consisting of the coefficients f_{ij} $(i, j = 1, \ldots, n+1)$ is determined as inverse to the matrix $\mathbf{F}$:

$$\mathbf{f} = \mathbf{F}^{-1} \tag{5.12}$$

The thermodynamic parameters χ_{ij} are determined by the formula

$$\chi_{ij} = \sum_l f_{il} \frac{\partial u_j}{\partial N_l} + f_{i,n+1} \frac{\partial u_j}{\partial U} \; (i = 1, \ldots, n+1; \; j = 1, \ldots, n) \tag{5.13}$$

The values of u_j are the partial molar energies $(\partial U(\mathbf{N}, V, T)/\partial N_j)$ taken as functions of the variables N_i, U. These dependencies are rather non-trivial. The way of their expressing in terms of more "standard" thermodynamic values is shown in [114].

Apart from the thermodynamic quantities, the expressions (5.7) to (5.10) involve other type of values, *the penetration lengths*, Z_i and Z_U. These lengths were determined and thoroughly discussed in [113, 114] (see also [74]), being the key values for our approach. However, we summarized the concept behind this variables in the following section.

The penetration lengths

Here we describe in further detail the newly introduced variables, the molecular penetration lengths Z_i and the energy penetration length Z_U. These penetration lengths are the key parameters for the new model.

Let us consider the ideal imaginary setup of the two vessels **A** and **B** of the same volume V connected with each other by a conductor of the length h and cross section

σ, which volume is much smaller than the volume of the vessels and large enough to contain macroscopic amounts of molecules. The energy of the system is conserved, since there is no loss of energy exist between the molecules and the walls. The system is supposed to be in equilibrium. The vectors $\mathbf{y}_A = (N_{A,1}, N_{A,2}, ..., N_{A,n}, U_A)$ and $\mathbf{y}_B = (N_{B,1}, N_{B,2}, ..., N_{B,n}, U_B)$ denote the composition of the mixture in each vessel. $y = (\dot{N}_1, N_2^{\cdot}, ..., \dot{N}_n, \dot{U})$ are the fluxes inside the conductor.

When a molecule of *ith* component in vessel **A** enters the conductor, it has intial characteristics γ_0, including initial velocity v_0. The molecule can either reach the vessel **B** with a probavility: $\lambda_i(\gamma_0, \mathbf{y}'')$ or return to vessel **A** with the probability $1 - \lambda_i(\gamma_0, \mathbf{y}'')$. The value of $\lambda_i(\gamma_0, \mathbf{y}'')$ is the *penetration probability*. The *average penetration probability* is: $\Lambda_i(\mathbf{y}'') = E(\lambda_i v_0 \mid \mathbf{y}'')/E(v_0 \mid \mathbf{y}'')$. The expression $a(\mathbf{y}'')$ refers to variable a in the environment $''$, where environmet $'$ referes to the vessel **A** and environmetn $''$ referes to the rest of the system. The penetration probability depends on the length of the conductor, however it was shown in [113] that the value of the *penetration length* $\zeta_i = h\lambda_i$ and the average penetration length $Z_i = h\Lambda_i$ are invariant. The value of ζ_i can be determined as an average traveling distance, after which the molecule "forgets" its initial velocity and starts participating in the random walks along with other molecules.

The energy transfer from vessel **A** to vessel **B** may be described similarly to the molecular transfer, with the difference that in this case two types of the energy transfer are possible: the convective and the non-convective. The first type represents the energy transported by the molecules that reach the outlet of the conductor and can be estimated as $u_i'' \lambda_i$ where u_i'' is the partial molar energy corresponding to the thermodynamic conditions in the conductor. Taking into account the statistics of the molecules leaving the vessel, it is possible to estimate the total convective energy transfer $\dot{U}_c$.

The non-convective energy transfer $\dot{U}_{nc}$ can be physically interpreted in terms of the "energy particles", if the energy is considered to be split into quanta (only for explanation sake). The non-convective energy transfer is the random walk of the "particles" of energy between different molecules, passing them to each other. When a molecule in vessel **A** appears in the entrance of the conductor, it transfers

some energy to the molecules in the tube without necessarily entering it. Some part of this energy has the possibility of reaching the end of the conductor via molecular interactions. Due to the analogy between the random walks of the molecules leading to diffusion and the random walks of the energetic "particles" leading to the non-convective enregy transfer, the concept of energy penetration probability λ_U and the energy penetration length ζ_U is introduced. Averaging them similarly to the molecular penetration lengths, we obtain the average values Λ_U and Z_U, correspondingly.

The portion of energy emitted by the molecule at the entrance of the conductor is likely to be split into many parts. Each part can move independently of the others and they are also independent of the initial molecule. Therefore, the energy penetration probability and the energy penetration length can be considered to be independent of the initial parameters of the molecule γ_0 and of the portion of energy initially emitted. Under these conditions $\lambda_U = \Lambda_U$ and $Z_U = \zeta_U$.

A more rigorous theoretical explanation of the concepts of penetration probability and penetration length may be found in [113, 114]. An expression for estimating the molecular penetration lengths was proposed [74]. Regarding the energy penetration length only the first fitting has been made, no expression has been deduced yet.

The diffusion and the thermal diffusion coefficients

Let us present the formulae for the diffusion and the thermodiffusion coefficients in binary mixtures, which follow from the multicomponent formulation presented above. These formulae may be obtained after cumbersome, although rather trivial transformations. For the case of the binary mixture, there is only one diffusional flux $\dot{\mathbf{d}} = \dot{\mathbf{d}}_1$, and a heat flux $\dot{\mathbf{d}}_2$ determined by equation (5.2). Correspondingly, matrix $\mathbf{L}$ from equation (5.1) is a 2×2 matrix. The coefficient L_{11} is responsible for "pure" diffusion and will further be denoted by L_D. The coefficient $L_{12} = L_{21}$ are responsible for thermodiffusion and diffusional heat conduction (Soret and Dufour effects) and will be referred to as L_{DT}. The coefficient L_{22}, responsible for heat conductivity, will not be considered in the present work.

Matrix $\mathbf{L}_N$ is a 2×2 matrix consisting of the coefficients

$$L_{N,11} = \frac{C_1}{4}\left[-Z_1 f_{11} + N_1\left(\frac{\partial Z_1}{\partial N_1} f_{11} + \frac{\partial Z_1}{\partial N_2} f_{21} + \frac{\partial Z_1}{\partial U} f_{31}\right)\right];$$

$$L_{N,12} = \frac{C_1}{4}\left[-Z_1 f_{12} + N_1\left(\frac{\partial Z_1}{\partial N_1} f_{12} + \frac{\partial Z_1}{\partial N_2} f_{22} + \frac{\partial Z_1}{\partial U} f_{32}\right)\right];$$

$$L_{N,21} = \frac{C_2}{4}\left[-Z_2 f_{21} + N_2\left(\frac{\partial Z_2}{\partial N_1} f_{11} + \frac{\partial Z_2}{\partial N_2} f_{21} + \frac{\partial Z_2}{\partial U} f_{31}\right)\right];$$

$$L_{N,22} = \frac{C_2}{4}\left[-Z_2 f_{22} + N_2\left(\frac{\partial Z_2}{\partial N_1} f_{12} + \frac{\partial Z_2}{\partial N_2} f_{22} + \frac{\partial Z_2}{\partial U} f_{32}\right)\right]$$

The diffusional coefficient L_D may be expressed in terms of $L_{N,ij}$:

$$L_D = \frac{M_1^2 M_2^2}{M^2}\left(z_2^2 L_{N,11} - z_1 z_2 (L_{N,12} + L_{N,21}) + z_1^2 L_{N,22}\right) \tag{5.14}$$

The expression for the thermal diffusion coefficient requires more effort. First, we determine coefficients $L_{NU,i}$ $(i = 1, 2)$ as follows:

$$L_{NU,1} = \frac{C_1}{4}\left[-Z_1 f_{13} + N_1\left(\frac{\partial Z_1}{\partial N_1} f_{13} + \frac{\partial Z_1}{\partial N_2} f_{23} + \frac{\partial Z_1}{\partial U} f_{33}\right)\right] + \frac{C_1}{4} N_1 Z_1 \frac{T}{2}$$

$$L_{NU,2} = \frac{C_2}{4}\left[-Z_2 f_{23} + N_2\left(\frac{\partial Z_2}{\partial N_1} f_{13} + \frac{\partial Z_2}{\partial N_2} f_{23} + \frac{\partial Z_2}{\partial U} f_{33}\right)\right] + \frac{C_2}{4} N_2 Z_2 \frac{T}{2}$$

The coefficients $L_{UN,i}$ are convenient to represent in the form of

$$L_{UN,i} = A_i - B_i Z_U \ (i = 1, 2),$$

where

$$A_1 = \left(u_1 + \frac{RT}{2}\right) L_{N,11} + \left(u_2 + \frac{RT}{2}\right) L_{N,21} + \frac{C_1}{4} N_1 Z_1 \chi_{11} + \frac{C_2}{4} N_2 Z_2 \chi_{12};$$

$$A_2 = \left(u_1 + \frac{RT}{2}\right) L_{N,12} + \left(u_2 + \frac{RT}{2}\right) L_{N,22} + \frac{C_1}{4} N_1 Z_1 \chi_{21} + \frac{C_2}{4} N_2 Z_2 \chi_{22};$$

$$B_1 = \frac{C_1}{2} N_1 \chi_{11} + \frac{C_2}{2} N_2 \chi_{12};\ B_2 = \frac{C_1}{2} N_1 \chi_{21} + \frac{C_2}{2} N_2 \chi_{22}$$

In terms of the introduced quantities, the Onsager thermodiffusion coefficient

L_{DT} is determined as

$$L_{DT} = A + BZ_U$$

$$A = M_1 c_2 \left(\frac{1}{2} A_1 + \frac{1}{2} L_{NU,1} - \frac{1}{M} h M_1 L_{N,11} - \frac{1}{M} h M_2 \left(\frac{1}{2} L_{N,12} + \frac{1}{2} L_{N,21} \right) \right)$$

$$- M_2 c_1 \left(\frac{1}{2} A_2 + \frac{1}{2} L_{NU,2} - \frac{1}{M} h M_2 L_{N,22} - \frac{1}{M} h M_1 \left(\frac{1}{2} L_{N,12} + \frac{1}{2} L_{N,21} \right) \right)$$

$$B = \frac{1}{2} \left(-M_1 c_2 B_1 + M_2 c_1 B_2 \right)$$

The diffusion flux $\dot{\mathbf{d}} = \dot{\mathbf{d}}_1$ is expressed as (see equations (5.1), (5.2)):

$$\dot{\mathbf{d}} = L_D \nabla \left(\frac{\mu^2}{M_2 T} - \frac{\mu^1}{M_1 T} \right) + L_{DT} \nabla \frac{1}{T}$$

On the other hand, the standard definition of the diffusion and thermal diffusion coefficients in a binary mixture exceeds from an equation [23]:

$$\dot{\mathbf{d}} = -D \rho \nabla c_1 - D_T \rho c_1 c_2 \nabla T$$

Comparison of the two equations results in the following connection between D, D_T and L_D, L_{DT}, correspondingly. After standard transformations involving the Gibbs-Duhem equality, it may be obtained that

$$D = \frac{1}{\rho} L_D \frac{M^3}{T M_1^2 M_2^2 z_2} \frac{\partial \mu^1}{\partial z_1}; \tag{5.15}$$

$$D_T = \frac{1}{\rho c_1 c_2} \left[\frac{L_{DT}}{T^2} + L_D \frac{\partial}{\partial T} \left(\frac{\mu^1}{M_1 T} - \frac{\mu^2}{M_2 T} \right) \right] \tag{5.16}$$

Equations (5.14), (5.15) for the diffusion coefficient are relatively straightforward. In particular, the last equation shows how the so-called "thermodynamic correction" $\partial \mu^1 / \partial z_1$ enters the diffusion coefficient. The expression for the thermal diffusion coefficient is much more cumbersome and much more difficult to analyze. Some necessary analysis is provided below.

5.2 The problem of reference state and of formation energies

In the present section we discuss dependence of the thermodynamic quantities on the reference states chosen in definitions of the energy and entropy. These fundamental thermodynamic quantities are determined within a constant. If entropies s, s_* and energies u, u_* are related to the two different reference states for the same body, then

$$u - u_* = u_0, \quad s - s_* = s_0 \tag{5.17}$$

In statistical mechanics, constant s_0 is, in principle, fixed by the Third Law of thermodynamics postulating that it is equal to zero at zero Kelvin. However, more detailed analysis of this law indicates that zero may be substituted by an arbitrary constant without violation of all the consequences. To the best of our knowledge, direct calculation of the constant s_0 from the Third Law of thermodynamics for any body under "normal" conditions has not been carried out with a reasonable accuracy.

The constants u_0, s_0 are extensive: if the body increases homogeneously a times, the constants should also increase:

$$u_0 = aU_0; \quad s_0 = aS_0 \tag{5.18}$$

The scaling parameter a may be associated with any extensive value: molar amount n, mass m, volume v etc. The constants U_0, S_0 are reference constants per unit of the corresponding extensive quantity. For a single-component fluid, all the choices of this extensive quantity a are equivalent. However, for a multicomponent mixture, these choices lead to different answers for intensive parameters, like chemical potentials, partial molar enthalpies etc.

Indeed, since, for example, chemical potentials μ^i are determined as derivatives of the Gibbs energy, $\partial g/\partial n_i|_{T,P,n_j}$, and $g = u - Ts + Pv$ (and, correspondingly, $g_* = u_* - Ts_* + Pv$), then it follows from equations (5.17), (5.18) that

$$\mu^i - \mu^i_* = (U_0 - TS_0) \left.\frac{\partial a}{\partial n_i}\right|_{T,P,n_j} \tag{5.19}$$

Similarly, for partial molar energies and partial molar enthalpies it may be obtained that

$$u^i - u^i_* = h^i - h^i_* = U_0 \left.\frac{\partial a}{\partial n_i}\right|_{T,P,n_j}$$

Appearance of arbitrary constants is not a problem for the equilibrium thermodynamics, since these constants disappear from most of the thermodynamic relations determining actual physical conditions. For example, the gas-liquid phase equilibria are described in terms of equalities of phase chemical potentials, $\mu^i_g = \mu^i_l$, and arbitrary constants disappear from the both parts of the equality. However, in the non-equilibrium thermodynamics the dependence on the arbitrary constants becomes more strict.

It has been proven [41] that the Onsager reciprocal relations and the Onsager phenomenological coefficients are independent of the reference state if the value of a is (proportional to) the mass:

$$a = m = \sum M_i n_i$$

The mass plays an exceptional rule in the non-equilibrium thermodynamics, unlike the equilibrium thermodynamics, where, for example, mass and molar amount are interchangeable. The reason is that main conservation laws are formulated in terms of mass, but not molar or other amounts. This especially relates to the momentum law.

From now on, we consider $a = m$, and equation (5.19) assumes the form of

$$\mu^i = (U_0 - TS_0)M_i + ...;\ u^i = U_0 M_i + ...;\ h^i = U_0 M^i + ... \tag{5.20}$$

Here ... denote the terms independent of the reference states.

Let us now consider existing models for the thermodiffusion coefficients proposed by different authors. As stated in Chapter 2, the thermodiffusion factor α_T in most of such models may be represented in a single form

$$\alpha_T = \frac{a_1 Q^*_2 - a_2 Q^*_1}{a z_1 \partial\mu^1/\partial z_1} \tag{5.21}$$

Here Q_i^* are the so-called heats of transport [25], and a_i are partial molar volumes v_i or molar masses M_i, depending whether the center of volumes or the center of masses is selected as a reference. For the values of Q_i^*, different expressions are proposed. From equation (5.21) the Haase model [44], the Kempers models [52, 53], the model of Shukla and Firoozabadi [116], and other models may be obtained. As can be seen from equation (5.20), of these models, only the model of Haase is invariant with regard to the choice of the reference state.

One of the ways to get rid of the problem of the reference states is to modify the model to the form of

$$\alpha_T = \frac{a_1(Q^2 - Q_0^2) - a_2(Q^1 - Q_0^1)}{a z_1 \partial\mu^1/\partial z_1} + \frac{\alpha_{T0} RT}{z_1 \partial\mu^1/\partial z_1} \tag{5.22}$$

Here Q_i^{*0} and α^{T0} are the heats of transport and the thermodiffusion factor in a reference state. Normally such a state is taken to be the ideal gas state, so that the value of α^{T0} may be computed by formulae of the Boltzmann gas kinetic theory [47].

Let us now consider another problem, dependence of the thermodiffusion coefficients of the formation constants. These formation constants Δh_f^i and Δs_f^i describe the amount of enthalpy and entropy for producing a given substance from elements at standard reference temperature $T_0 = 298.2$ K. They should be included into the expressions for the internal energy, for chemical potentials and other quantities. In fact, the complete expressions for the chemical potentials, taking into account equation (5.20), are:

$$\mu^k = RT \ln \phi^k + RT \ln(z^k P/P_0) + h_0^k(T) - T s_0^k(T), \tag{5.23}$$

where

$$s_0^k(T) = M_k S_0 + \Delta s_f^k + \int_{T_0}^{T} \frac{C_p^k(T)}{T}\, dT$$

$$h_0^k(T) = M_k U_0 + \Delta h_f^k + \int_{T_0}^{T} C_p^k(T)\, dT$$

Here ϕ^k are the fugacity coefficients, P_0 reference pressure (normally equal to 1 atm), C_p^k are the molar heat capacities at constant pressure P_0. Correspondingly, it

may be shown that full expressions for the internal energy and entropy are:

$$U = \sum N_i \left(\int_{T_0}^{T} C_p^k(T)\, dT - RT^2 \frac{\partial \ln \phi_i}{\partial T} \right) - P + \sum N_i \left(M_i U_0 + \Delta h_f^i \right) \tag{5.24}$$

$$S = -\sum N_i \left(R \ln \phi_i z_i (P/P_0) + RT \frac{\partial \ln \phi_i}{\partial T} - \int_{T_0}^{T} \frac{C_p^k(T)}{T}\, dT \right) + \sum N_i \left(M_i S_0 + \Delta s_f^i \right) \tag{5.25}$$

That is, variation of the reference and formation constants leads to variation of energy and entropy, which is linear with regard to the molar amounts. With regard to the partial molar energies and enthalpies, equation (5.20) is extended to

$$u^i = U_0 M_i + \Delta h_f^k + ...;\ h^i = U_0 M^i + \Delta h_f^k + ... \tag{5.26}$$

Should the thermodiffusion coefficient be independent of Δh_f^i and Δs_f^i? Formally, this is not required. While invariance with regard to U_0, S_0 should be fulfilled, since these constants are essentially arbitrary, the constants Δh_f^i and Δs_f^i are fixed and tabulated for different compounds (see, f.ex., [96]). However, on the other hand, it is not clear why separation of the components under the action of the thermal gradient should be dependent on the energies spent on their formation in chemical reactions. It should also be noted that the constants Δh_f^i, Δs_f^i do not influence the conditions of phase equilibria, since they disappear from the equalities of the chemical potentials for different phases.

All the models referred above, which may be represented in the form of equation (5.21), depend on the reference constants Δh_f^i and/or Δs_f^i. Moreover, since these constants are rather large, under certain conditions they may provide a major contribution to the thermal diffusion factors. The models, which may be represented in the form (5.22), may or may not depend on the reference constants, depending, what model for Q_i^* is chosen, and whether the reference state is chosen under temperature T_0 or under temperature T.

It was shown in [41] that the thermal diffusion coefficient computed as described in section 5.1 is independent of the reference states, as well as the enthalpies and the entropies of formation.

5.3 Comparison with experimental data

The applicability of the model was checked in the following way. The expression for the thermal diffusion coefficient may be represented in the following general form:

$$D_T = \alpha(\text{Thermodynamics}, Z_i) + \beta(\text{Thermodynamics}, Z_i) Z_U$$

Let us consider a mixture, for which the data on both diffusion and thermal diffusion coefficients are available, and thermodynamics is also known (may be described by a proper thermodynamic model). The molecular penetration lengths Z_i may be found by fitting the data on diffusion coefficients, as in [74], since the diffusion coefficients are independent of Z_U. Then the energy penetration lengths may be found from the experimental data for the thermal diffusion coefficients. Since this operation is rather formal, the resulting values of the penetration lengths Z_U may a priori behave in any possible way, do not owing even to be positive. The fact that they are positive, have a right order of magnitude, and behave in a reasonable way, might indicate that the model is acceptable.

For testing, we used three mixtures of hydrocarbons and hydrocarbon-like components: Heptane–Carbon Tetrachloride, Hexane–Carbon Tetrachloride and Heptane–Benzene. Selection of the mixtures was rather restrictive, since they should have obeyed the following criteria: (i) Existence on reliable data on thermodiffusion; (ii) Existence of reliable data on diffusion coefficients *at multiple temperatures* (otherwise fitting of the diffusion penetration lengths seems to be rather unreliable); (iii) Existence of a simple and reliable thermodynamic model, allowing for computation of the necessary properties of the mixture.

As regards to the last criterion, all the selected mixtures may well be modelled by simple Soave-Redlich-Kwong (SRK) equation of state, with the Peneloux volume shift [75]. Diffusion data at different temperatures were modelled with application of the same temperature-independent (and energy independent) dependencies for Z_i:

$$Z_i = A\sqrt{\frac{M_i}{M_{12}}}(1 - B_1 N_1 - B_2 N_2 - B_{12}\frac{N_1 N_2}{N_1 + N_2})$$

Thus, we had four constant parameters for each mixture. These parameters were sufficient for fitting the diffusion coefficients on the basis of equations (5.14), (5.15) with great accuracy, as shown in Figure 5.1.

The experimental data for the thermal diffusion coefficient s_T for these mixtures are shown in Figure 5.2. In spite the fact that the data are rather uniform, and the thermodiffusion coefficients do not vary very much, the energy penetration lengths show a non-monotonous behavior with maximum in the middle, as shown in Figure 5.3. All the penetration lengths are positive and have a right order of magnitude, generally, of around 10^{-9}m, which is comparable to the intermolecular distances. On the other hand, they exhibit a nontrivial behavior, showing a sharp maximum in the middle. This nontrivial behavior may probably be explained by behavior of the partial molar properties and their derivatives found from an equation of state. The SRK EoS, as all the modern equations of state, has been designed and fitted to the data on phase equilibria, not on the partial molar properties and, especially, to their derivatives. Non-trivial behavior of such derivatives may be an artifact related to particular shape of an EoS.

5.4 Conclusions

The study described above has proven principal applicability of the theory developed in [113, 114] to evaluation of the diffusion and thermal diffusion coefficients in binary mixtures. While diffusion coefficients are reasonably described, further modeling work is required in order to provide realistic predictable evaluation of the thermodiffusion coefficients. The theory should further be tested with regard to the agreement with the basic observations and empirical laws, which have been reported for the thermal diffusion coefficients. The main direction of modeling should be associated with development of the thermodynamic equations of state providing reliable and stable evaluation of the partial molar properties and their derivatives. More experimental data is required for the mixtures where diffusion coefficients are available, in order to better test the theory and to provide reliable predictable expressions for the energy penetration lengths.

Figure 5.1: Diffusion coefficients for the mixtures n-Hexane + Carbon Tetra Chloride at 298.15K and n-Heptane + Carbon Tetra Chloride at 303.15K and n-Heptane + Benzene at three different temperatures presented by [74].

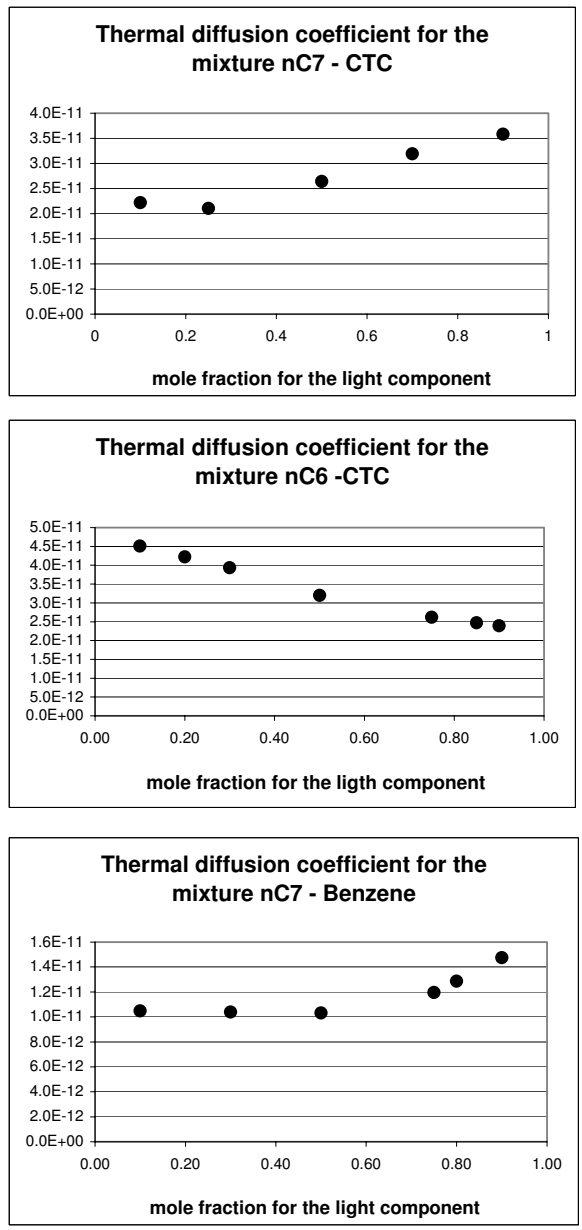

Figure 5.2: Experimental thermal diffusion coefficients data in [8] for nHexane + Carbon Tetra Chloride, n-Heptane + Carbon Tetra Chloride and n-Heptane + Benzene at 298.2 K and atmospheric pressure

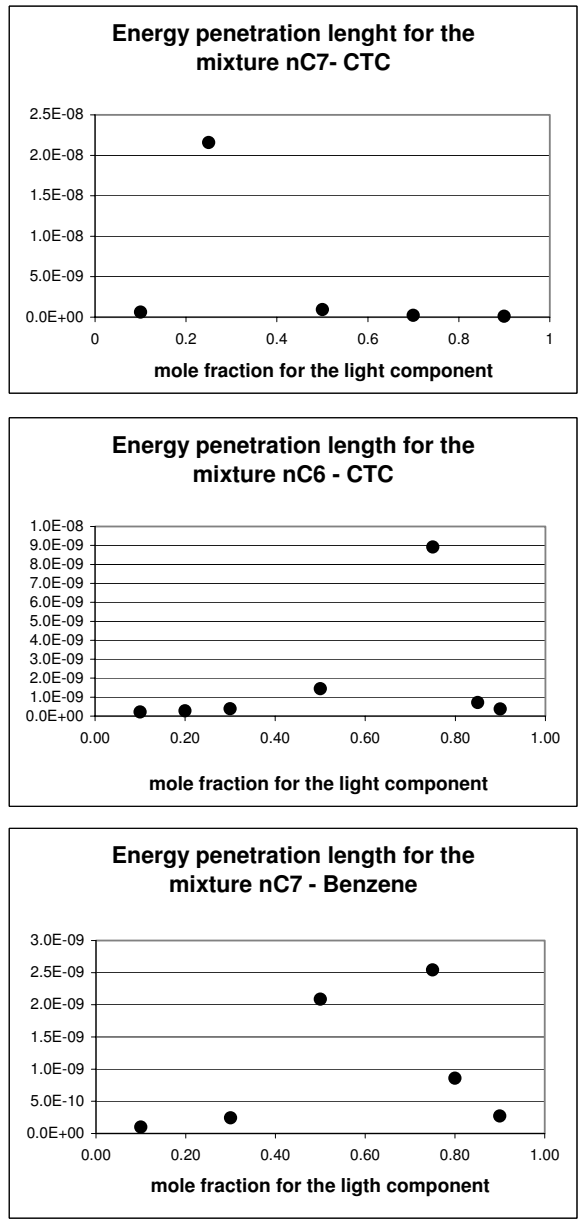

Figure 5.3: Energy penetration lengths for the mixtures n-Hexane + Carbon Tetra Chloride, n-Heptane + Carbon Tetra Chloride and n-Heptane + Benzene fitted to the experimental data.

Chapter 6

Thermal diffusion in ideal gas mixtures

The goal of this chapter is to present the evaluation of the thermal diffusion effect for multicomponent mixtures of ideal gases. In Chapter 7 we extend the calculations to non-ideal multicomponent mixtures.

Hirschfelder et al. [47] rigorously described the transport phenomena based on the gas kinetic theory. The system under study is described by means of the Boltzmann distribution function from which general transport equations are derived. By expansion of the system, a set of integral equations for the transport coefficients is obtained, which are then solved by the perturbation technique proposed by Enskog.

The expressions are obtained for different transport coefficients: diffusion, thermal diffusion, heat conductivity and viscosity. These coefficients are expressed in terms of standard integrals of the Sonine polynomials, which depend, in turn, on the molecular interaction parameters. It was observed that it is sufficient to consider the first order approximation to get a good estimation for the diffusion coefficients. In order to determine the thermal diffusion factor, it is necessary to take, at least, second order approximation in the Sonine expansion, since the first order form vanishes.

Expressions for the thermal diffusion coefficients based on the kinetic theory of gases were extended onto diatomic gases or denser systems [54, 56, 129]. Yamakawa et al. [129] based their theory on the approach of Hirschfelder et al., but considered

diatomic molecules. They split the thermal diffusion factor into the two contributions: transitional and internal ones. Comparison between this model and the original formula is presented in [129] only for a binary mixture. The model is in good agreement with the original model of Hirschfelder et al., unless high temperatures are considered.

Another study was carried out by Kincaid et al. [54, 55, 72, 73]. They presented a detailed analysis of further approximations of the Enskog theory for hard-sphere systems of multicomponent mixtures, giving explicit expressions for transport coefficients as functions of the masses, Lennard-Jones parameters, and concentrations of the components in a mixture. Two approaches were considered: the standard theory (SET) and the revised theory (RET). It is worth pointing out that the RET is consistent with the irreversible thermodynamics theory [92], while SET leads to conflict with that theory when describing the mutual diffusion by higher order approximations. The fourth of this series of papers [54] presents a detailed study of the dependency of the thermal diffusion factor on different properties. Of the multicomponent systems, only ternary mixtures of isotopic components are considered. This theory was successfully tested for diluted alloys of tin [128]. For concentrated solutions, it was concluded that, in order to achieve a uniform accuracy of 1%, the seventh-order approximation is needed. The third or fourth order approximation are reasonably good except when the masses of the components are rather different.

In this chapter we analyzed three expressions for the thermal diffusion ratio for binary mixtures given in Hirschfelder et al. [47]: the second approximation, k^T_{2ACS}, the third approximation, k^T_{3ACS} and the Kihara approximation, k^T_{Kihara}. In [47], there is only one explicit formula for the thermal diffusion coefficient D^T_{2A} for multicomponent systems, but it is possible to deduce the third order approximation for the thermal diffusion coefficient, D^T_{3A}, by means of the tables given by Chapman and Cowling [14].

The binary formulae are applied for these multicomponent systems by an alternative approach based on the corresponding states law, where a ternary system is considered as a binary system of one substance and of a pseudo component. This pseudo component is formed from the two other components of the mixture by

means of the corresponding states law. This is the so-called pseudo-binary formulation. We have found a similar study of the properties of multicomponent mixtures of monatomic gases (Helium, Neon, Argon, Krypton and Xenon) [46]. The authors [46] analyzed different properties for the ternary system of Neon-Argon-Krypton applying the corresponding states law. However, their study for the thermal diffusion coefficients was incomplete since no comparison was made between the binary and the multicomponent formulations.

The transport coefficients in diluted gas mixtures are estimated on the basis of the kinetic gas theory. Further, we compare different models for estimating the thermal diffusion ratio for ideal gas systems. Due to lack of the experimental data on ternary mixtures of noble gases, we compare theoretical results in the limiting case of binary systems. Experimental data for the thermal diffusion factor in such systems are available in the literature [122].

6.1 Theoretical background

The basis of the gas kinetic theory [47], from where the expressions for the transport coefficients are derived, is briefly described in the first subsection. The second subsection presents different formulas for the thermal diffusion ratios in ideal gas mixtures.

6.1.1 The kinetic theory of dilute gases

The gas kinetic theory describes non-equilibrium properties by means of statistical methods. Complete description of the transport properties of a dilute gas may be obtained on the basis of the Boltzmann equation for a distribution function $f(\mathbf{r}, \mathbf{v}, t)$. Hirschfelder et al. [47] presented two derivations for the Boltzmann equation: one giving a physical interpretation of various terms and a second derivation, more mathematically rigorous. Both derivations arrive to the same Boltzmann equation:

$$\begin{aligned} &\frac{\partial f_i^{(1)}}{\partial t} + \frac{1}{m_i}\left(\mathbf{p}_i \bullet \frac{\partial f_i^{(1)}}{\partial \mathbf{r}}\right) + \mathbf{X}_i \bullet \frac{\partial f_i^{(1)}}{\partial \mathbf{p}_i} \\ &= \sum \int\int\int \left(f_i^{(1)'} f_j^{(1)'} - f_i^{(1)} f_j^{(1)}\right) g_{ij} b \, db \, d\epsilon \, d\mathbf{p}_j \end{aligned} \tag{6.1}$$

This equation describes variation of the functions $f_i^{(1)}$ with time. Here $\mathbf{X}_i$ are the external forces acting on the molecules, $(\mathbf{r}, \mathbf{p}_i)$ are the coordinates $\mathbf{r}$ and the momentum $\mathbf{p}_i$ of a molecule, m_i is the mass of the ith component and $f_i^{(1)} = f_i^{(1)}(\mathbf{r}, \mathbf{p}_i, t)$, $f_j^{(1)} = f_j^{(1)}(\mathbf{r}, \mathbf{p}_j, t)$, $f_i^{(1)'} = f_i^{(1)}(\mathbf{r}, \mathbf{p'}_i, t)$ and $f_j^{(1)'} = f_j^{(1)}(\mathbf{r}, \mathbf{p'}_j, t)$, where $\mathbf{p}_i$ is the momentun before collision and $\mathbf{p'}_j$ is the momentun after collision.

It is possible to write the Boltzmann equation in terms of the velocities instead of momenta:

$$\begin{aligned} &\tfrac{\partial f_i}{\partial t} + \mathbf{v}_i \bullet \tfrac{\partial f_i}{\partial \mathbf{r}} + \tfrac{1}{m_i}\left(\mathbf{X}_i \bullet \tfrac{\partial f_i^{(1)}}{\partial \mathbf{v}_i}\right) \\ &\quad = \sum \int\int\int \left(f_i' f_j' - f_i f_j\right) g_{ij} b \, db \, d\epsilon \, d\mathbf{v}_j \end{aligned} \tag{6.2}$$

Multiplying equation (6.2) by some molecular property ψ_i associated with the ith component, and integrating over $\mathbf{v}_i$ we obtain the equation of change for property ψ_i:

$$\begin{aligned} &\tfrac{\partial n_i \overline{\psi_i}}{\partial t} + \left(\tfrac{\partial}{\partial \mathbf{r}} \bullet n_i \overline{\psi_i \mathbf{v}_i}\right) - n_i\left(\overline{\tfrac{\partial \psi_i}{\partial t}} + \overline{\left(\mathbf{v}_i \bullet \tfrac{\partial \psi_i}{\partial \mathbf{r}}\right)} + \tfrac{\mathbf{X}_i}{m_i} \bullet \overline{\tfrac{\partial \psi_i}{\partial \mathbf{v}_i}}\right) \\ &\quad = \sum \int\int\int\int\int \psi_i \left(f_i' f_j' - f_i f_j\right) g_{ij} b \, db \, d\epsilon \, d\mathbf{v}_j d\mathbf{v}_i \end{aligned}$$

The "over line" represents average values of the corresponding variable. Summation over all the components gives the value of the property ψ for the entire gas.

It can be proven that equation (6.2) has an equilibrium solution:

$$f_i^0 = n_i \left(\frac{m_i}{2\pi k T}\right)^{3/2} \exp\left[-\frac{m_i(\mathbf{v}_i - \mathbf{v}_0)^2}{2kT}\right]$$

where $n_i = n_i(\mathbf{r}, t)$, $v_0 = v_0(\mathbf{r}, t)$ and $T = T(\mathbf{r}, t)$ are functions of space and time. In order for this function to represent the local values of the physical quantities; molar density, mass velocity and temperature, it should be postulated that

$$\int f_i d\mathbf{v}_i = n_i;$$

$$\sum m_i \int \mathbf{v}_i f_i d\mathbf{v}_i = \rho \mathbf{v}_0;$$

$$\frac{1}{2} \sum m_i \int (\mathbf{v}_i - \mathbf{v}_0)^2 f_i d\mathbf{v}_i = \frac{3}{2} nkT$$

Chapman and Cowling [14] represent function $f_i = f_i^0 \phi_i$, where ϕ_i is the perturbation function. Expansion of the Boltzmann equation with application of the conservation laws gives the integral equation for ϕ_i:

$$\begin{aligned} f_i^0 \left[\tfrac{n}{n_i} (\mathbf{V}_i \bullet \mathbf{d}_i) + \left(\mathbf{b}_i : \tfrac{\partial}{\partial \mathbf{r}} \mathbf{v}_0 \right) - \left(\tfrac{5}{2} - \mathbf{W}_i^2 \right) \left(\mathbf{V}_i \bullet \tfrac{\partial \ln T}{\partial \mathbf{r}} \right) \right] \\ = \textstyle\sum_j \int\int\int f_i^0 f_j^0 (\phi_i' + \phi_j' - \phi_i - \phi_j) g_{ij}\, b\, db\, d\epsilon\, d\mathbf{v}_j \end{aligned} \tag{6.3}$$

where

$$\mathbf{d}_i = \frac{\partial}{\partial \mathbf{r}} \left(\frac{n_i}{n} \right) + \left(\frac{n_i}{n} - \frac{n_i m_i}{\rho} \right) \frac{\partial \ln p}{\partial \mathbf{r}} - \left(\frac{n_i m_i}{\rho p} \right) \left(\frac{\rho}{m_i} \mathbf{X}_i - \sum_j n_j \mathbf{X}_j \right) \tag{6.4}$$

$$\mathbf{b}_i = 2 \left[\mathbf{W}_i \mathbf{W}_j - \frac{1}{3} W_i^2 \mathsf{U} \right] \tag{6.5}$$

$\mathbf{W}_i = \mathbf{V}_i \sqrt{\frac{m_i}{2kT}}$ is the dimensionless velocity. The variables $\mathbf{d}_i$ satisfy the condition $\sum_i \mathbf{d}_i = 0$. The perturbation function is a function of space and time, by means of the variables n_i, $\mathbf{v}_0$ and T. It can be represented as:

$$\phi_i = -\left(\mathbf{A}_i \bullet \frac{\partial \ln T}{\partial \mathbf{r}} \right) - \left(\mathbf{B}_i : \frac{\partial}{\partial \mathbf{r}} \mathbf{v}_0 \right) + n \sum_j \left(\mathbf{C}_i^{(j)} \bullet \mathbf{d}_i \right) \tag{6.6}$$

where $\mathbf{A}_i$, $\mathbf{B}_i$ and $\mathbf{C}_i$ are functions of the dimensionless velocity, $\mathbf{W}_i$, the local position and the local temperature:

$$\mathbf{A}_i = \mathbf{W}_i A_i(W_i); \tag{6.7}$$

$$\mathbf{B}_i^{(j)} = \left\{ \mathbf{W}_i \mathbf{W}_i - \frac{1}{3} W_i^2 \mathsf{U} \right\} B_i(W_i); \tag{6.8}$$

$$\mathbf{C}_i^{(j)} = \mathbf{W}_i C_i^{(j)}(W_i) \tag{6.9}$$

A general solution was obtained by Chapman and Cowling [14] by infinite expansion by the Sonine polynomials. It is necessary to consider a finite number of terms to be able to determine the transport coefficients. The system of equations for the expansion coefficients $t_{jm'}^{(h,k)}$ has the form of:

$$\sum_j \sum_{m'=0}^{\xi-1} \tilde{Q}_{ij}^{mm'} t_{jm'}^{(h,k)}(\xi) = -R_{im}^{(h,k)} \tag{6.10}$$

where ξ is the degree of approximation used, $t_{jm'}^{(h,k)}$ is the the unknown coefficient to be found, being either $c_{i0}^{(j,i)}$ or a_{i0}, depending wether we want to estimate the diffusion coefficients or the thermal diffusion coefficients correspondingly. The coefficients $\tilde{Q}_{ij}^{mm}$ are defined as

$$\tilde{Q}_{ij}^{mm} = Q_{ij}^{mm'} - \frac{n_j\sqrt{m_j}}{n_i\sqrt{m_i}} Q_{ii}^{mm'} \delta_{m0}\delta_{m'0}$$

where

$$Q_{ij}^{mm'} = \sum_l n_i n_l \left[\begin{array}{l} \delta_{ij}\left[\mathsf{W}_i S_n^{(m)}(W_i^2); \mathsf{W}_i S_n^{(m')}(W_i^2)\right]_{il} \\ +\delta_{jl}\left[\mathsf{W}_i S_n^{(m)}(W_i^2); \mathsf{W}_l S_n^{(m')}(W_l^2)\right]_{il} \end{array} \right] \tag{6.11}$$

$$R_{im}^{(h,k)} = \int \left(\mathsf{R}_i^{(h,k)} : \mathsf{W}_i\right) S_n^{(m)}(W_i^2) d\mathbf{V}_i \tag{6.12}$$

Here W_i and W_i are reduced velocity vector and its magnitude correspondingly; $\mathsf{R}_i^{(h,k)} = \frac{1}{n_i} f_i^{(0)}(\delta_{ih} - \delta_{ik})\mathbf{V}_i$ for calculation of the isothermal diffusion coefficients and $= f_i^{(0)}(\frac{5}{2} - W_i^2)\mathbf{V}_i$ for calculation of the thermal diffusion coefficients. $S_n^{(m)}(W_i^2)$ represents the Sonine polynomial as a function of W_i^2:

$$S_n^{(m)}(x) = \sum_j \frac{(-1)^j (m+n)!}{(n+j)!(m-j)!j!} x^j$$

In a system under non-equilibrium conditions several macroscopic gradients exist. They create different types of fluxes: mass flux, energy and momentum fluxes. In particular, for evaluation of the diffusion and the thermal diffusion coefficients, it is necessary to consider the mass flux, which can be written as

$$V_i = \frac{n^2}{n_i \rho} \sum_j m_j D_{ij} \mathbf{d}_i - \frac{1}{n_i m_i} D_i^T \frac{\partial \ln T}{\partial \mathbf{r}}$$

where $\mathbf{d}_i$ were defined in equation (6.4), D_{ij} are the multicomponent diffusion coefficients, and D_i^T are the multicomponent thermal diffusion coefficients:

$$D_{ij} = \frac{\rho}{3nm_j}\sqrt{\frac{2kT}{m_i}}\int C_i^{(j)}(W_i)W_i^2 f_i^0 d\mathbf{V}_i \tag{6.13}$$

$$D_i^T = \frac{m_i}{3}\sqrt{\frac{2kT}{m_i}}\int A_i(W_i)W_i^2 f_i^0 d\mathbf{V}_i \tag{6.14}$$

In terms of the Sonine polynomial expansions the diffusion and the thermal diffusion coefficients become:

$$D_{ij}(\xi) = \frac{\rho}{3nm_j}\sqrt{\frac{2kT}{m_i}}\sum_{m=0}^{\xi-1} c_{im}^{(j,i)}(\xi)\int V_i^2 S_{3/2}^{(m)}(W_i^2) f_i^0 d\mathbf{V}_i \tag{6.15}$$

$$D_i^T(\xi) = \frac{m_i}{3}\sqrt{\frac{2kT}{m_i}}\sum_{m=0}^{\xi-1} a_{im}(\xi)\int A_i(W_i)W_i^2 f_i^0 d\mathbf{V}_i \tag{6.16}$$

Due to the properties of the integrals of the Sonine polynomials:
$\int_0^\infty x^n e^{-x} S_n^{(m)}(x)\, S_n^{(m')}(x)\, dx = \frac{(n+m)!}{m!}\delta_{mm'}$, equations (6.15) and (6.16) are simplified to:

$$D_{ij}(\xi) = \frac{\rho n_i}{3nm_j}\sqrt{\frac{2kT}{m_i}}c_{i0}^{(j,i)}(\xi) \tag{6.17}$$

$$D_i^T(\xi) = \frac{n_i m_i}{2}\sqrt{\frac{2kT}{m_i}}a_{i0}(\xi) \tag{6.18}$$

The argument ξ of $D_{ij}(\xi)$ and $D_i^T(\xi)$ represents the number of terms used in the expansion. The diffusion coefficient and the thermal diffusion coefficient are expressed in terms of the zeroth approximation only: $c_{i0}^{(i,j)}$ and a_{i0}. No matter how many terms are used in the expansion, it is only the zeroth coefficient, which remains after the integration. However, the values of the coefficients $c_{i0}^{(j,i)}$ and a_{i0} are determined from the system of equation (6.10), which depends upon the number of expansion terms ξ.

Solution of this equation is carried out as a standard lineal system of equations.

The coefficients $Q_{ij}^{mm'}$ in the system (6.10) are expressed in terms of the standard integral functions Ω, which are tabulated as functions of the reduced temperature. It is possible to obtain up to the third approximation ($\xi = 3$) for the thermal diffusion

coefficient from the tables presented in [47].

For the diffusion coefficient D_{ij}, it has been observed that for $\xi = 1$ rather good approximation is obtained. When the order of approximation is increased to 2, small corrections are introduced [47]. However, for the thermal diffusion coefficient a first order approximation ($\xi = 1$) vanishes. Therefore, it is necessary to consider, at least, the second order approximation ($\xi = 2$). Kincaid et al. [54, 55, 72, 73] showed that the seventh order approximation is necessary to achieve a uniform accuracy of 1%.

6.1.2 Evaluation of the thermal diffusion coefficient

Here we present the correlations for estimating the thermal diffusion ratio in terms of parameters of the Lennard-Jones potentials, the molecular weights, reduced temperature and standard integral functions. In the book of Hirschfelder et al. [47], different values for these parameters may be found. First, the thermal diffusion ratio for binary mixtures in the second order approximation is presented. The two other expressions are the general third approximation and the Kihara approximation. Finally, the second order expression for the thermal diffusion coefficient in multicomponent mixtures is presented. We have extended this expression up to the third order approximation. Details of each of the expressions are given below.

The second-order expansion for the thermal diffusion ratio is expressed in terms of the intermolecular forces, molecular weights and the integral omega-functions Ω. The second order approximation for the thermal diffusion factor in a binary mixture is:

$$k_{2ACS}^{T} = \frac{z_1 z_2}{[\lambda_{12}]_1} \frac{\left(S^{(1)} z_1 - S^{(2)} z_2\right)\left(C_{12}^{*} - \frac{5}{6}\right)}{\frac{z_1(1+U^{(1)})}{[\lambda_1]_1} + \frac{z_1 z_2 (1+U^{(Y)})}{[\lambda_{12}]_1} + \frac{z_2(1+U^{(2)})}{[\lambda_2]_1}} \tag{6.19}$$

$$S^{(1)} = \frac{M_1 + M_2}{2M_2} \frac{[\lambda_{12}]_1}{[\lambda_1]_1} - \frac{15}{4A_{12}^{*}} \left(\frac{M_2 - M_1}{2M_1}\right) - 1 \tag{6.20}$$

$$S^{(2)} = \frac{M_1 + M_2}{2M_1} \frac{[\lambda_{12}]_1}{[\lambda_2]_1} - \frac{15}{4A_{12}^{*}} \left(\frac{M_1 - M_2}{2M_2}\right) - 1 \tag{6.21}$$

$$U^{(1)} = \frac{4A_{12}^*}{15} - \left(\frac{B_{12}^*}{5} + \frac{1}{12}\right)\frac{M_1}{M_2} + \frac{(M_1 - M_2)^2}{2M_1M_2} \tag{6.22}$$

$$U^{(2)} = \frac{4A_{12}^*}{15} - \left(\frac{B_{12}^*}{5} + \frac{1}{12}\right)\frac{M_2}{M_1} + \frac{(M_2 - M_1)^2}{2M_1M_2} \tag{6.23}$$

$$U^{(Y)} = \frac{4A_{12}^*}{15}\frac{(M_1 + M_2)^2}{4M_1M_2}\frac{[\lambda_{12}]_1^2}{[\lambda_1]_1[\lambda_2]_2} - \left(\frac{B_{12}^*}{5} + \frac{1}{12}\right) - \frac{(12B_{12}^* - 25)}{32A_{12}^*}\frac{(M_1 - M_2)^2}{M_1M_2} \tag{6.24}$$

where A_{12}^*, B_{12}^* and C_{12}^* are ratios of the integral functions Ω and are tabulated in [47]. The quantities $[\lambda_1]_1$ and $[\lambda_2]_1$ are the first approximations for the thermal conductivities of the pure components, and $[\lambda_{12}]_1$ is the mixture thermal conductivity. These values are expressed as

$$[\lambda_i]_1 = 1.9891e^{-4}\frac{\sqrt{T/M_i}}{\sigma^2\Omega_{12}^{(2,2)*}(T_r)}$$

$$[\lambda_{12}]_1 = 1.9891e^{-4}\frac{\sqrt{T(M_1 + M_2)/2M_1M_2}}{\sigma_{12}^2\Omega_{12}^{(2,2)*}(T_r)}$$

where T is the temperature in Kelvin (K), $T_r = Tk_B/\varepsilon$ the reduced temperature, M_1 and M_2 the molecular weights in kg/mol, and σ, ε/k_B are the potential functions in Å and K, respectively. $[\lambda]$ has the unit of calories/cm/sec/K.

The third approximation for the thermal diffusion factor was also tested. This approximation is expressed in terms of the determinants of the three matrices, which are functions of the molecular weights and of the integrals above:

$$k_{3ACS}^T = \frac{5\left(z_1\sqrt{\frac{M_1+M_2}{2M_1}}\,|S_{01}| + z_2\sqrt{\frac{M_1+M_2}{2M_2}}\,|S_{0-1}|\right)}{2\,|S_{00}|} \tag{6.25}$$

The determinants $|S_{00}|$, $|S_{01}|$ and $|S_{0-1}|$ are shown in Appendix C.

The Kihara approximation was also tested. The characteristic feature of this model is that it is expressed in terms of the third approximation by the Sonine polynomial expansion. However, its structure is rather simple, since Kihara observed that the main contribution to the estimation of the thermal diffusion coefficient is

given by the diagonal elements of the matrix. The Kihara expression for the thermal diffusion coefficient is

$$k_{Kihara} = \frac{5\left(6C_{12}^{*} - 5\right)\left(z_1 S^{(1)} - z_2 S^{(2)}\right)}{z_1 Q^1 - z_1 z_2 Q^{12} + z_2 Q^2} \tag{6.26}$$

When considering multicomponent formulae we tested the second approximation for the thermal diffusion coefficient presented by Hirschfelder et al. This formula is much more complex in comparison with the previous equation. It has the form

$$D_{2A}^{T}(i) = \frac{8M_i}{5R} \frac{\begin{vmatrix} \mathbf{L}^{00} & \mathbf{L}^{01} & 0 \\ \mathbf{L}^{10} & \mathbf{L}^{11} & \mathbf{Z} \\ \delta_{\mathbf{i}} & 0 & 0 \end{vmatrix}}{\begin{vmatrix} \mathbf{L}^{00} & \mathbf{L}^{01} \\ \mathbf{L}^{10} & \mathbf{L}^{11} \end{vmatrix}} \tag{6.27}$$

where R is the gas constant and $\mathbf{L}^{00}$, $\mathbf{L}^{01}$, $\mathbf{L}^{10}$ and $\mathbf{L}^{11}$ are matrices, which are shown explicitly in Appendix D. $\mathbf{Z} = (z_1, z_2, ..., z_n)$ is the transposed vector of mole fractions and $\delta_{\mathbf{i}} = (\delta_{i1}, \delta_{i2}, ..., \delta_{in})$ the vector of the Kronecker delta fohgr component i.

Finally, since it has been proven [54] that a higher order of expansion by the Sonine polynomials significantly improves estimations of the thermal diffusion coefficients, we implemented the third order expansion by Sonine polynomials. This approximation has the form of

$$D_{3A}^{T}(i) = z_i \sqrt{\frac{m_i k_B T}{2}} \frac{\begin{vmatrix} \mathbf{Q}^{00} & \mathbf{Q}^{01} & \mathbf{Q}^{02} & 0 \\ \mathbf{Q}^{10} & \mathbf{Q}^{11} & \mathbf{Q}^{12} & \mathbf{R} \\ \mathbf{Q}^{20} & \mathbf{Q}^{21} & \mathbf{Q}^{22} & 0 \\ \delta_{\mathbf{i}} & 0 & 0 & 0 \end{vmatrix}}{\begin{vmatrix} \mathbf{Q}^{00} & \mathbf{Q}^{01} & \mathbf{Q}^{02} \\ \mathbf{Q}^{10} & \mathbf{Q}^{11} & \mathbf{Q}^{12} \\ \mathbf{Q}^{20} & \mathbf{Q}^{21} & \mathbf{Q}^{22} \end{vmatrix}} \tag{6.28}$$

where m_i is the mass of component i, k_B and the Boltzmann constant. The

matrices, which determinants enter the fraction, are composed of submatrices $\mathbf{Q}^{00}$, $\mathbf{Q}^{01}$, $\mathbf{Q}^{02}$, $\mathbf{Q}^{10}$, $\mathbf{Q}^{20}$, $\mathbf{Q}^{11}$, $\mathbf{Q}^{12}$, $\mathbf{Q}^{21}$, $\mathbf{Q}^{22}$ and $\mathbf{R}$. The coefficients entering these matrices are explicitly presented in Appendix C.

It is important to link the thermal diffusion coefficient and the thermal diffusion ratio, in order to be able to compare equation (6.19), (6.25) and (6.26) with the multicomponent formulae for D^T (6.27) and (6.28). Hirschfelder et al. do not present this relation directly for multicomponent mixtures, but only for binary systems. The diffusion equation may be expressed in a general way in terms of the relative motion of particles as:

$$\sum \frac{z_i z_j}{D_{ij}}(\overline{\mathbf{V}}_j - \overline{\mathbf{V}}_i) = \mathbf{d}_i - \frac{\partial \ln T}{\partial \mathbf{r}} \sum_j \frac{z_i z_j}{D_{ij}} \left(\frac{D_j^T}{n_j M_j} - \frac{D_i^T}{n_i M_i} \right)$$

There are many possible ways to determined the thermal diffusion ratio from this equation (see also next chapter) we propose the following way:

$$k_i^T = \sum \frac{z_i z_j}{D_{ij}} \left(\frac{D_j^T}{n_j M_j} - \frac{D_i^T}{n_i M_i} \right) \tag{6.29}$$

where D_{ij} is the binary diffusion coefficient for components i in j. In case of a binary system, $k_1^T = -k_2^T$, this relation is simplified to

$$k^T = \frac{\rho}{N^2 M_1 M_2} \frac{D^T}{D_{12}} \tag{6.30}$$

where N is the total molar density, ρ the density of the mixture and D_{12} is the binary diffusion coefficient.

We tested the formulae above for simple mixtures of noble gases, comparing them to experimental data found in the literature. The components chosen for the calculations, their molecular masses and the Lennard-Jones potential parameters are presented in Table 6.1.

6.2 Results for binary mixtures

First, we compare the results obtained by application of different formulations presented in the previous section with seven sets of experimental data for binary mix-

Table 6.1: Parameters used in the calculations of the thermal diffusion ratios for ideal gas mixtures [96]

Substance	Mr Weight (kg/mol)	σ (Å)	$\varepsilon/k_B(K)$
Helium	4.0026	2.567	10.22
Neon	20.183	2.82	32.8
Argon	39.948	3.542	93.3
Krypton	83.8	3.655	178.9
Xenon	131.1	4.055	331.0

tures of ideal gases measured at atmospheric pressure and 300K. The experiments were carried out by Trengove et al. in 1959 [122] for Helium-Neon, Helium-Argon, Helium-Krypton, Helium-Xenon, Neon-Argon, Neon-Krypton and Neon-Xenon mixtures.

In the plots, the following notation is used: k^T_{Exp} represents the experimental data; k^T_{2ACS} represents the results obtained with the second approximation for binary mixtures, equation (6.19); k^T_{3ACS} represents the results obtained with the third approximation, equation (6.25); k^T_{Kihara} corresponds to the results obtained with the binary Kihara approximation, equation (6.26). The coefficients obtained on the basis of the multicomponent approximations are: the second approximation of the thermal diffusion coefficient k^T_{2A} deduced from equations (6.27) and (6.29); the third approximation k^T_{3A} (equation (6.28) transformed according to (6.29) or (6.30)).

Figure 6.1 shows the results obtained for all the binary mixtures for different compositions at 300 K and atmospheric pressure. Plots (a), (c), (e), (g) and (i) present the results obtained for the mixtures where Helium is the light component (the other element being respectively Ne, Ar, Kr and Xe). Plots (b), (d), (f), (h) and (j) present the results for the mixtures with Neon as light component (with respectively Ar, Kr and Xe). Plots (a) and (b) show the results obtained for the binary second order approximation, plots (c) and (d) for the binary third order approximation and plots (e) and (f) for Kihara approximation. Similarly, plots (g), (h), (i) and (j) show the results obtained for multicomponent formulation with the second and third approximation correspondingly.

It may clearly be seen that the results obtained by different formulations disagree.

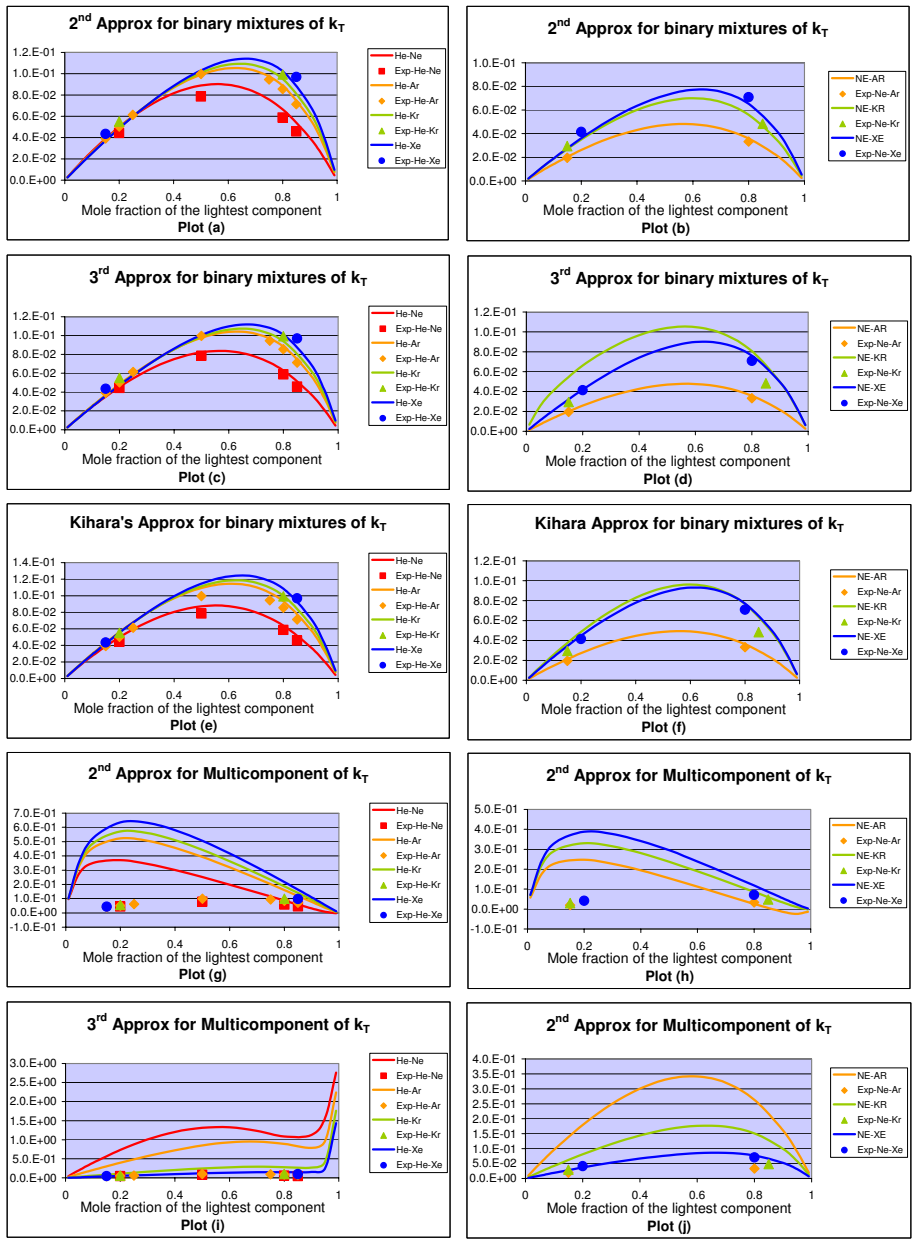

Figure 6.1: Plots (a), (c), (e), (g) and (i): Thermal diffusion ratios for binary mixture with Helium. Plots (b), (d), (f), (h) and (j): Thermal diffusion ratios for binary mixtures with Neon. The second approximation for binary mixture is exhibited in plots (a) and (b), the third approximation for binary mixture is exhibited in plot (c) and (d), the Kihara approximation is shown in plots (e) and (f). The results for multicomponent equations are shown in plots (g) and (h) for the second approximation and plots (i) and (j) for the third approximation.

Excellent agreement is obtained between the binary formulations for k^T (equation (6.19), equation (6.25) and equation (6.26)) and the experimental values. On the contrary, for the four mixtures containing Helium the thermal diffusion ratio determined from the third approximation (shown in Figure 6.1 plot (i)) does not tend to zero for high concentrations of He. The thermal diffusion factors obtained with the second multicomponent approximation (Figure 6.1 plot (g)) are much higher than the experimental results.

The compositions maximizing the thermal diffusion factor are significantly different in binary and in multicomponent formulations. For heavy molecules, the second multicomponent approximation exhibits change of sign at high concentrations of the lightest component.

In the third multicomponent approximation, the thermal diffusion ratio decreases with increase of the particle size of the heavy component, being always larger than predicted by the binary formulation and by experimental observations. Only for Neon-Xenon results of the multicomponent formulation are comparable to the binary formulation.

It may generally be concluded that the multicomponent formulation predicts too large thermodiffusion factors for binary systems, while the binary formulation gives very good approximations, independently of the order of expansion.

6.3 The Corresponding States Law for thermal diffusion

Since no experimental data exists for ternary systems, and due to large discrepancies between the binary and the multicomponent formulations, we suggest an alternative approach to estimate the thermal diffusion ratios in ternary systems. We define pseudo-binary systems by means of the corresponding state approach. This approach has been successfully used to determine other properties as viscosity [96], and it has been shown for molecular dynamics simulations [37] that the thermal diffusion ratios determined in this way, gives very similar results as the ratios obtained when cosidering the components individually.

The ternary system is represented by a pseudo-binary one, in which two components define a synthetic single component mixed with the third component. The synthetic component may be defined by one of the two existing approaches [96]: the classical or macroscopic approach, as presented by van der Waals, and the molecular, or microscopic approach. We implemented the second approach, estimating the pseudo parameters as:

$$(1 - z_k)\sigma_k^3 = \sum_{i \neq k} \sum_{j \neq k} z_i z_j \sigma_{ij}^3 \tag{6.31}$$

$$(1 - z_k)\varepsilon_k \sigma_k^3 = \sum_{i \neq k} \sum_{j \neq k} z_i z_j \varepsilon_{ij} \sigma_{ij}^3 \tag{6.32}$$

$$(1 - z_k)M_k = \sum_{i \neq k} z_i M_i \tag{6.33}$$

The thermal diffusion ratio, k^T, was calculated from the binary formulations (equations (6.19), (6.25) and (6.26)), on the basis of the properties of the selected component and of the pseudo component. The microscopic interaction parameters of the pseudo binary approach were defined by

$$\sigma_{12} = \frac{(\sigma_k + \sigma_{pseudo})}{2} \tag{6.34}$$

$$\varepsilon_{12} = \sqrt{\varepsilon_k \varepsilon_{pseudo}} \tag{6.35}$$

The thermal diffusion ratio for multicomponent mixture can now be calculated from the binary formulae, equation (6.19) equation (6.25) and equation (6.26), by implementing the corresponding states law.

6.4 Ternary Mixtures

The ternary systems considered are combinations of the noble gases excluding Radon. Since, to the best of our knowledge, no experimental data is available for them, comparison was carried out between different formulations mentioned above: the pseudo

binary formulation and the multicomponent formulation of Hirschfelder et al. Different ternary compositions were considered in order to cover the whole concentration range. The simulations were carried out at 300K and atmospheric pressure.

We have selected three most representative ternary systems: Helium-Neon-Krypton, Neon-Argon-Krypton and Neon-Krypton-Xenon. The results are shown in Figures 6.2, 6.3 and 6.4 correspondingly. Each figure contains 15 plots. The first column of plots shows the thermal diffusion factor for the lightest component in the mixture, the last column for the heaviest and the middle column shows the results for the thermal diffusion factor for the intermediate component. The first row of plots shows the values obtained with the second approximation (k^T_{2ACS}) for the thermal diffusion ratio in binary systems with the corresponding states law. The second and the third rows show the values for k^T obtained by the third (k^T_{3ACS}) and the Kihara approximation (k^T_{Kihara}). The two last rows show the values of the thermal diffusion ratios obtained by application of the multicomponent approach for D^T, with the second (k^T_{2A}) and third approximation (k^T_{3A}), correspondingly.

Nine curves for the thermal diffusion ratio corresponding to nine different concentrations of the heaviest component are shown in each plot. The horizontal axis is the molar fraction of lightest component. In all cases, as might be expected, the light component tends towards the hot region (negative k^T) and the heavy component towards the cold region (positive k^T). The intermediate component exhibits alternating behavior, tending to the cold or to the hot side depending on the composition of the system. It can also be observed that this component exhibits almost inert behavior for intermediate concentrations, with a very small thermal diffusion coefficient.

As for the comparison of different formulations, the discrepancies concern mainly the intermediate component. For pseudo-binary formulation, k^T_{2ACS} tends to change the sign according to the component concentration. If the intermediate component is relatively light and similar to the lighter component, its thermal diffusion factor is mainly negative over all the composition range, while it is mainly positive when the intermediate component is closer to the heavy component.

It may also be observed that the thermal diffusion coefficient increases in the

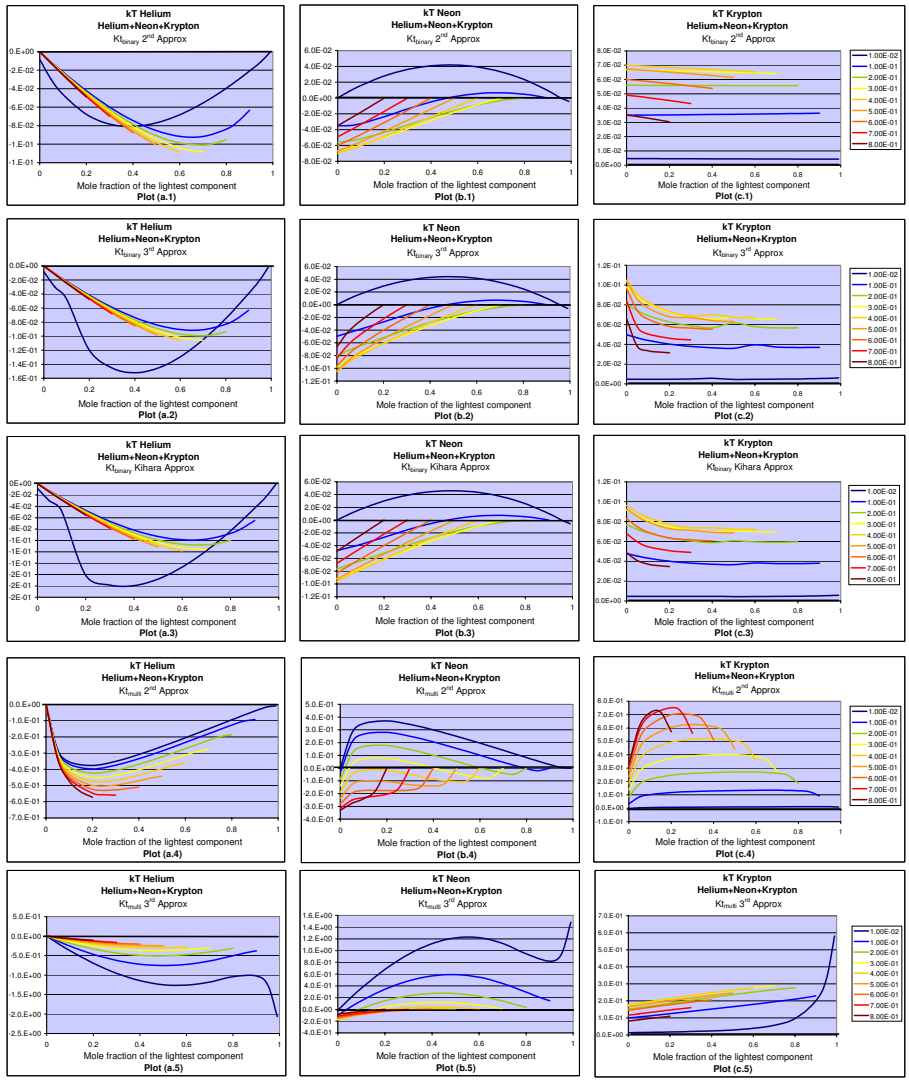

Figure 6.2: Plots (a.1), (a.2), (a.3), (a.4) and (a.5): thermal diffusion ratios for the Helium. Plots (b.1), (b.2), (b.3), (b.4) and (b.5): thermal diffusion ratios for Neon and Plots (c.1), (c.2), (c.3), (c.4) and (c.5): thermal diffusion ratio for Krypton. Plots (a.1), (b.1), (c.1): obtained by the binary second order approximation; Plots (a.2), (b.2) and (c.2): third-order binary approximation; Plots (a.3), (b.3) and (c.3): obtained with the Kihara approximation; Plots (a.4), (b.4) and (c.4): obtained with the second-order multicomponent approximation and plots (a.5), (b.5) and (c.5): obtained with the third-order multicomponent approximation.

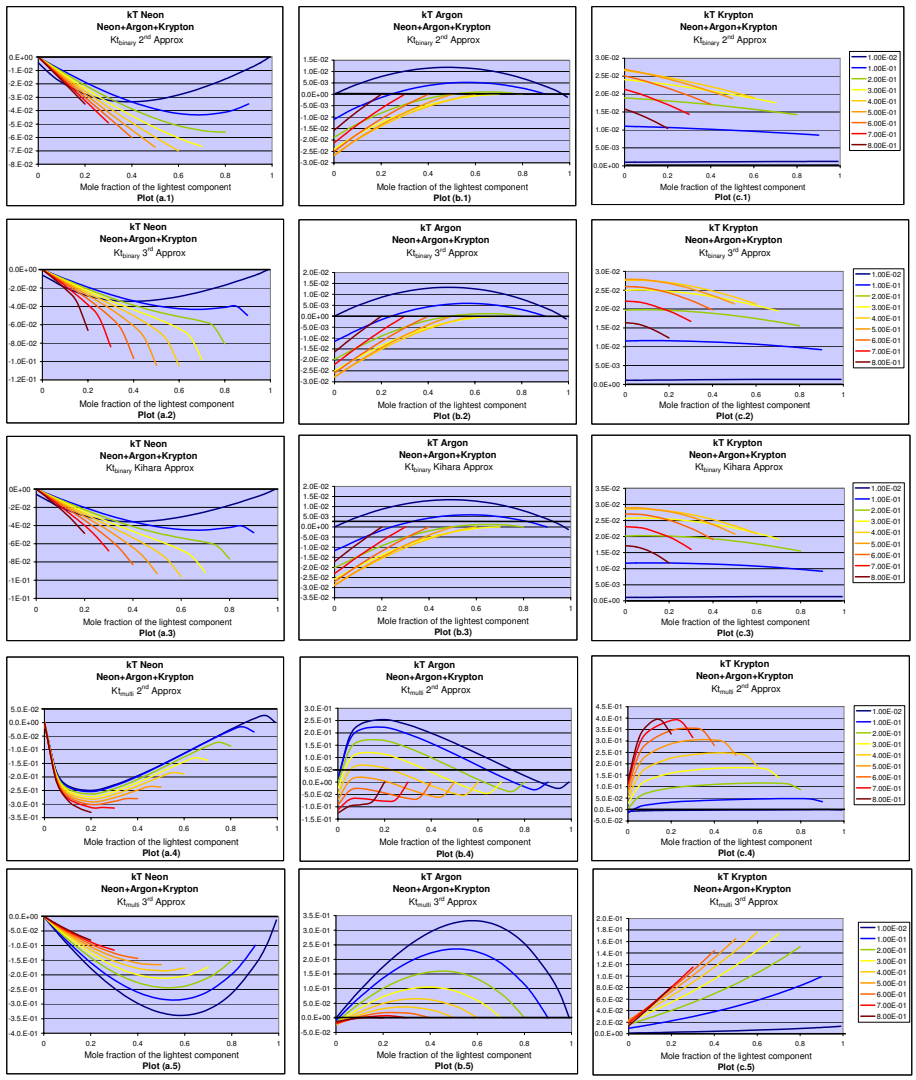

Figure 6.3: Plots (a.1), (a.2), (a.3), (a.4) and (a.5): thermal diffusion ratios for the Neon. Plots (b.1), (b.2), (b.3), (b.4) and (b.5): thermal diffusion ratios for Argon and Plots (c.1), (c.2), (c.3), (c.4) and (c.5): thermal diffusion ratio for Krypton. Plots (a.1), (b.1), (c.1): obtained by the binary second order approximation; Plots (a.2), (b.2) and (c.2): third-order binary approximation; Plots (a.3), (b.3) and (c.3): obtained with the Kihara approximation; Plots (a.4), (b.4) and (c.4): obtained with the second-order multicomponent approximation and plots (a.5), (b.5) and (c.5): obtained with the third-order multicomponent approximation.

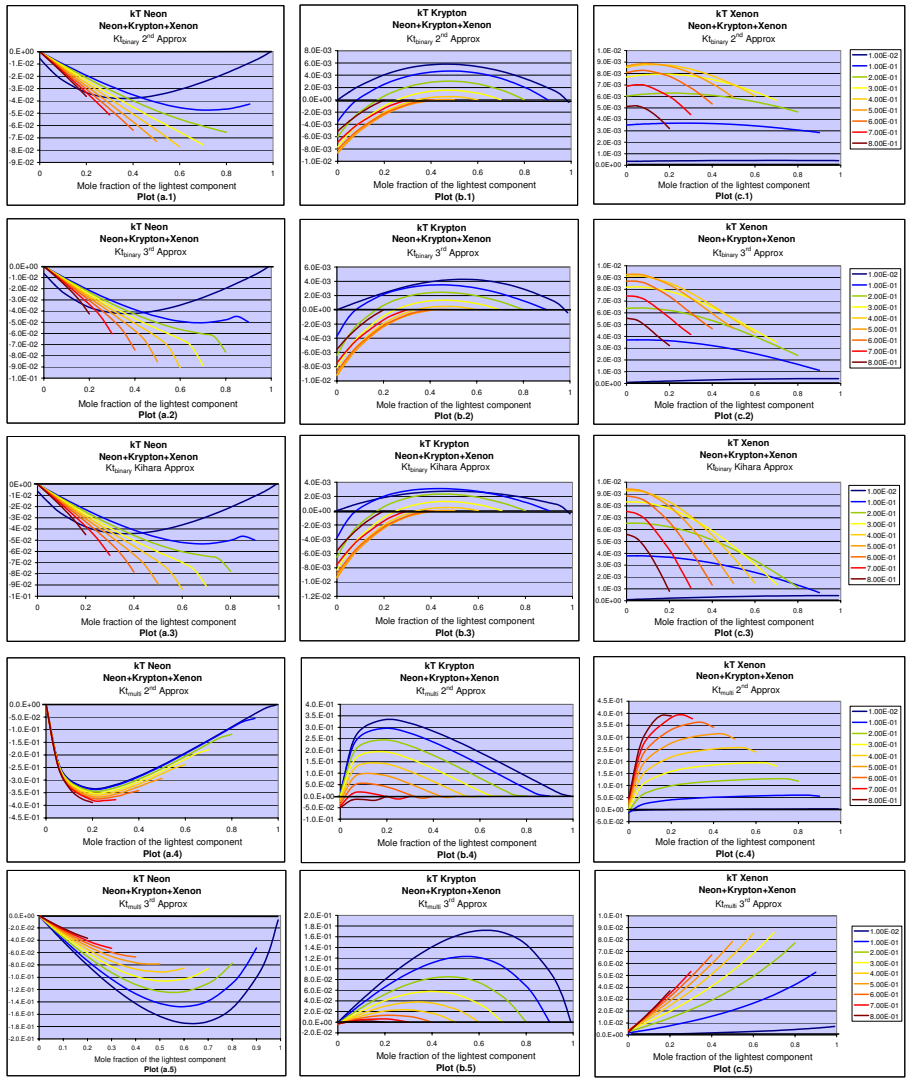

Figure 6.4: Plots (a.1), (a.2), (a.3), (a.4) and (a.5): thermal diffusion ratios for the Neon. Plots (b.1), (b.2), (b.3), (b.4) and (b.5): thermal diffusion ratios for Krypton and Plots (c.1), (c.2), (c.3), (c.4) and (c.5): thermal diffusion ratio for Xenon. Plots (a.1), (b.1), (c.1): obtained by the binary second order approximation; Plots (a.2), (b.2) and (c.2): third-order binary approximation; Plots (a.3), (b.3) and (c.3): obtained with the Kihara approximation; Plots (a.4), (b.4) and (c.4): obtained with the second-order multicomponent approximation and plots (a.5), (b.5) and (c.5): obtained with the third-order multicomponent approximation.

second, but decreases in the third approximation with increasing the amount of the third component. For the binary formulation the behavior is indefinite. The last remark can be made about the second approximation for multicomponent mixtures, where for some concentrations we observed unrealistic behavior consisting in several changes of sign for the thermal diffusion ratio of the intermediate component.

A fundamental difficulty seems to be risen; when one component of a ternary mixture tends toward zero, the thermal diffusion ratio should approximate the corresponding binary thermal diffusion ratio. The theory should reflect this. However the formulae for multicomponent mixtures, the thermodiffusion ratio do not seem to obey this consistency requirement.

6.5 Conclusions

Several conclusions can be drawn from this study. First, excellent estimation of the thermal diffusion factor obtained by the binary approach is confirmed (equation (6.19), (6.25) and (6.26)).

Second, the second-order approximation to the thermal diffusion coefficient for multicomponent systems (equation (6.27)), has been truly tested, to our knowledge, for the first time. We also evaluated the third order approximation. It was observed that these two approaches do not agree with the binary experimental data for k^T. It may be concluded that the formulae shown in Hirschfelder et al. for estimating the thermal diffusion coefficient in multicomponent systems does not verify the consitency check. Therefore, we strongly recommend careful application of the multicomponent formulae.

Chapter 7

The thermal diffusion effect in multicomponent mixtures

As it was presented in Chapter 2, most of the theoretical developments dealing with the description of the thermal diffusion effect are related to binary systems. In this chapter we present an analysis of the thermal diffusion effect in multicomponent systems. Several existing models are applicable to this type of mixtures. We evaluated these models and compared them to molecular dynamics simulations, since the only experimental data found in the literature for ternary systems deal with polymer solutions and associating fluids [13, 22, 63].

The properties needed for estimation of the thermal diffusion factor were calculated using the SRK equation of state. In binary systems, it is irrelevant whether to define the thermal diffusion factor with respect to the mole fraction or to the mass fraction. However, for multicomponent systems this is not valid. We compared both definitions.

7.1 The thermal diffusion parameters

7.1.1 From binary to multicomponent mixtures

The thermal diffusion factor is defined by Kempers [53] from the relation:

$$\Delta z_i = -z_i(1-z_i)\alpha_i^T \frac{\Delta T}{T} \qquad (i = 1, ..., n) \tag{7.1}$$

which for binary mixtures becomes:

$$\Delta z_1 = -z_1(1-z_1)\alpha_1^T \frac{\Delta T}{T} \tag{7.2}$$

On the other hand, de Groot [23] presents the same relation in terms of the mass fractionS instead of the mole fractions:

$$\Delta c_1 = -c_1(1-c_1)\alpha_1^T \frac{\Delta T}{T} \tag{7.3}$$

It can be shown that these two expressions are equivalent for binary systems. Let us now assume that this last expression can directly be extended to multicomponent systems as:

$$\Delta c_i = -c_i(1-c_i)\alpha_i^T \frac{\Delta T}{T} \qquad (i = 1, ..., n) \tag{7.4}$$

Since $\Delta c_i = \sum(\partial c_i/\partial z_j)\Delta z_j$ equation (7.4) becomes:

$$\sum \frac{\partial c_i}{\partial z_j}\Delta z_j = -c_i(1-c_i)\alpha_i^T \frac{\Delta T}{T} \qquad (i = 1, ..., n) \tag{7.5}$$

This expression can be transformed into:

$$\Delta z_j = -\sum_i \frac{\partial z_j}{\partial c_i} c_i(1-c_i)\alpha_i^T \frac{\Delta T}{T} \qquad (i = 1, ..., n) \tag{7.6}$$

Since $z_i = \frac{c_i/M_i}{\sum c_k(1/M_k - 1/M_n)+1/M_n}$, then it can be deduced that its derivative with respect to the mole fraction under independent variables $(c_1, c_2, ..., c_{n-1})$ is:

$$\frac{\partial z_j}{\partial c_i} = \frac{\frac{\delta_{ij}}{M_i}\sum_k c_k\left(\frac{1}{M_k}-\frac{1}{M_n}\right)+\frac{1}{M_n}-\frac{c_i}{M_i}\left(\frac{1}{M_j}-\frac{1}{M_n}\right)}{\left(\sum_k c_k\left(\frac{1}{M_k}-\frac{1}{M_n}\right)+\frac{1}{M_n}\right)^2}$$

Substituting $\partial z_j/\partial c_i$ in equation (7.6), we obtain:

$$\Delta z_j = \sum_i \frac{\frac{\delta_{ij}}{M_i}\sum_k c_k\left(\frac{1}{M_k}-\frac{1}{M_n}\right)+\frac{1}{M_n}-\frac{c_i}{M_i}\left(\frac{1}{M_j}-\frac{1}{M_n}\right)}{\left(\sum_k c_k\left(\frac{1}{M_k}-\frac{1}{M_n}\right)+\frac{1}{M_n}\right)^2} c_i(1-c_i)\alpha_i^T \frac{\Delta T}{T} \tag{7.7}$$

Substituting $c_i = \frac{z_i M_i}{\sum z_l (M_l - M_n) + M_n}$ in this last equation and rearranging we get:

$$\Delta z_j = -\sum_i \left(\delta_{ij} \frac{M_i}{M_j} - z_j \left(1 - \frac{M_i}{M_n} \right) \right) z_i \left(1 - \frac{z_i M_i}{\sum z_k (M_k - M_n) + M_n} \right) \alpha_i^T \frac{\Delta T}{T} \tag{7.8}$$

In the case of binary mixtures equations (7.8) simplifies to:

$$\Delta z_1 = -z_1 z_2 \alpha_1^T \frac{\Delta T}{T} \tag{7.9}$$

which is equal to the original definition given by Kempers, equation (7.2). Thus, it is equivalent, for binary mixtures, to define the thermal diffusion factor in terms of the mass fraction or in terms of the mole fraction. However, for multicomponent mixtures this is not valid.

Hence, the definitions for the thermal diffusion factor as a function of the mass fraction and as a function of the mole fraction are not equivalent in multicomponent systems. To overcome this problem, we can define two different thermal diffusion factors according to the definition employed. When working with multicomponent systems we will use α_i^{mT} as the mass thermal diffusion factor and α_i^T for the molar thermal diffusion factor. In binary systems $\alpha_1^{mT} = \alpha_1^T = -\alpha_2^{mT} = -\alpha_2^T$.

7.1.2 Definitions of different thermal diffusion parameters

In multicomponent systems, one should be careful when applying the definitions for the thermal diffusion coefficient, factor and ratio. These values have been defined only for binary systems. The definitions for the thermal diffusion coefficient D^T, the Soret coefficient S^T, the thermal diffusion factor α^T, and the thermal diffusion ratio k^T were introduced in Chapter 2 as

$$D^T = L_{11} \frac{(Q_1^* - h_1 + h_2)}{T \rho c_1 (1 - c_1)},$$

$$S^T = \frac{D^T}{D_{12}},$$

$$\alpha^T = T\frac{D^T}{D_{12}},$$

$$k^T = Tc_1c_2\frac{D^T}{D_{12}}$$

These definitions cannot be directly applicable to multicomponent mixtures. In [35, 39] the thermal diffusion coefficient, factor and ratio were defined in terms of a reference fluid. Considering component n as a reference substance, one obtains:

$$\Delta z_i = -z_i z_n \alpha_i^T \frac{\Delta T}{T} \qquad (i = 1, ..., n-1) \tag{7.10}$$

Correspondingly, the thermal diffusion coefficient and the thermal diffusion ratio are expressed as:

$$D_i^T = \frac{M_i M_n}{M} D_{in} \frac{k_i^T}{T}$$

$$k_i^T = \frac{M_i z_i M_n z_n}{MRTL_{ii}} \sum_{j=1}^{n-1} L_{ij} \left(\frac{Q_j^*}{M_j} - \frac{Q_n^*}{M_n} \right),$$

where $D_{in} = \frac{M^2 R L_{ii}}{c M_i^2 M_n^2 z_i z_n}$ is the diffusion coefficient for the reference component n, L_{ij} are the phenomenological coefficients and Q_i^* the net heats of transport. The authors [35, 39] proposed an expression in terms of the partial internal energy to estimate these heats of transport. This theory seems to be able to define the thermal diffusion effect in multicomponent mixtures. However, the problem is that the definition is not symmetric and requires one reference substance n. In case of dilute solutions this may be convenient, since the solutes interact mostly with solvent n, but not with each other. However, in case of concentrated solutions this definition seems to be is artificial. Here we propose a different approach for defining the thermal diffusion coefficient in multicomponent systems. In order to do so, we should go back to the expression for the flux, defined by equation (2.21):

$$\mathbf{J}_i = \sum_{k=1}^{n-1} L_{ik} \begin{pmatrix} \mathbf{F}_k - \mathbf{F}_n - (v_k - v_n)\nabla P \\ -\sum_{j=1}^{n-1} \frac{\partial(\mu_k - \mu_n)}{\partial z_j} \nabla z_j - (Q_k^* - h_k + h_n) \frac{\nabla T}{T} \end{pmatrix} \tag{7.11}$$

This equation was obtained by expressing the flux of component n as a function of the other fluxes, since $\sum J_i = 0$. Instead, we can use flux of component i as a reference. In this way, the expression for the flux obtains the form:

$$\mathbf{J}_i = \sum_{\substack{j=1 \\ j \neq i}}^{n} L_{ik} \begin{pmatrix} \mathbf{F}_j - \mathbf{F}_i - (v_j - v_i)\nabla P \\ -\sum_{k=1}^{n} \frac{\partial(\mu_j - \mu_i)}{\partial z_k} \nabla z_k - (Q_i^* - h_j + h_i) \frac{\nabla T}{T} \end{pmatrix} \tag{7.12}$$

Rearranging we get

$$\mathbf{J}_i = \sum_{\substack{j=1 \\ j \neq i}}^{n} L_{ij} (\mathbf{F}_j - \mathbf{F}_i) - \sum_{\substack{j=1 \\ j \neq i}}^{n} L_{ik}(v_j - v_i)\nabla P - \left(\sum_{\substack{k=1 \\ k \neq i}}^{n} \left(\sum_{\substack{j=1 \\ j \neq i}}^{n} L_{ij} \frac{\partial(\mu_j - \mu_i)}{\partial z_k} \right) \nabla z_k \right) - \sum_{\substack{j=1 \\ j \neq i}}^{n} L_{ij} (Q_i^* - h_j + h_i) \frac{\nabla T}{T} \tag{7.13}$$

In this way we can derive the definitions for the diffusion coefficient, and the thermal diffusion coefficient as:

$$\rho D_{ik} = \sum_{\substack{j=1 \\ j \neq i}}^{n} L_{ij} \frac{\partial (\mu_j - \mu_i)}{\partial z_k} \tag{7.14}$$

$$\rho z_i (1 - z_i) D_i^T = \sum_{\substack{j=1 \\ j \neq i}}^{n} L_{ij} (Q_i^* - h_j + h_i) \frac{1}{T} \tag{7.15}$$

Substituting equation (7.14) and (7.15) into the flux equation, when no external forces are acting on the system and there is no pressure gradient gives

$$\mathbf{J}_i = -\rho \sum_{\substack{k=1 \\ k \neq i}}^{n} D_{ik} \nabla z_k - \rho z_i (1 - z_i) D_i^T \nabla T \tag{7.16}$$

The result is expressed in terms of the mole fractions. A similar derivation may be carried out for mass fractions. In the last case, the mass thermal diffusion parameters are obtained. Further, since $j \neq i$, we do not take into account the interaction between the same components, which in the case of thermal diffusion is equal to zero. The fact that the diffusion coefficients D_{ij} are equal to zero for $i = j$, makes the suggested approach very closely linked to the Stefan-Maxwell picture of the multicomponent transport [21].

7.2 Existing models for multicomponent mixtures

Several models for the calculation of the thermal diffusion factors exist, but most of them are only applicable to binary mixtures. We presented an extensive evaluation of the existing models in Chapter 4.

The models proposed by Kempers [52, 53] are also applicable for multicomponent systems. The model of Hasse [44] may be deduced by the same approach. Therefore, it is also possible to extend this model onto multicomponent mixtures. The model of Shukla and Firoozabadi [116] is of the same structure as the previous two models. We have also extended this model onto multicomponent systems using the same mathematical structure as for the models of Kempers and Haase.

The mentioned models can be generalized in the two ways. The first approach, suggested by Kempers, depends on a reference component:

$$\begin{aligned} &\textstyle\sum_{j=1}^{n-1} \left(\frac{1}{a_i} \frac{\partial \mu_i}{\partial z_j} - \frac{1}{a_n} \frac{\partial \mu_n}{\partial z_j} \right) z_j (1 - z_j) \alpha_j^T \\ &= \frac{E_n - E_n^0}{a_n} - \frac{E_i - E_i^0}{a_i} + RT \left(\frac{\alpha_i^{0,T}(1 - z_i)}{a_i} - \frac{\alpha_n^{0T}(1 - z_n)}{a_n} \right) \end{aligned} \quad (i = 1, .., n-1) \tag{7.17}$$

The second approach suggested by Kempers, is more symmetric:

Table 7.1: Possible substitutions for a_i and E_i for the general model, equations (7.17) and (7.18)

Equation	E Energy parameter	a_i variable
Kempers model	h_i	v_i
Haase Model	h_i	M_i
Sukla and Firoozabadi model	u_i	v_i/τ_i
h_i = partial molar enthalpy M_i = molecular weight u_i = partial internal energy v_i = partial molar volume τ_i = 4		

$$\sum_{j=1}^{n-1} \frac{\partial \mu_i}{\partial z_j} z_j(1-z_j)\alpha_j^T = \frac{a_i}{a}(E-E^0) - (E_i - E_i^0) + RT(1-z_i)\alpha_i^{0,T} \ (i=1,..,n) \quad (7.18)$$

Equations (7.17) are defined only for $n-1$ components. The thermal diffusion factor for the last component is estimated from the relation $\sum \alpha_i^T z_i(1-z_i) = 0$. Equations (7.18) are defined for n components, however, only $n-1$ of them are independent.

If a_i is the molecular weight and E_i the partial molar enthalpy, equation (7.17) is reduced to the Haase model. Similarly, if E_i is the partial molar enthalpy and a_i the partial molar volume, then we obtain the second model of Kempers. In some cases the contribution for the ideal gas part is neglected and then the second term of the right hand side of equations (7.17) and (7.18) is equal to zero. If we then substitute the partial molar volumes for a_i and the partial molar enthalpies for E_i, we obtain the first model of Kempers [52]. If E_i is equal to u_i/τ_i and a_i to v_i, the model of Shukla and Firoozabadi is derived. It can easily be proven that this expression is simplified to equation (2.50) for binary systems. The values of τ_i are already discussed in Chapter 2. They will be assumed to be equal to 4. The values a and E represent the properties for the entire mixture and are determined as: $a = \sum_{i=1}^{n} z_i a_i$, $E = \sum_{i=1}^{n} z_i E_i$. Table 7.1 summarizes possible interpretations of equations (7.17) or (7.18). Other interpretations are also possible.

A different approach for estimating the thermal diffusion factor in multicomponent systems was presented by Firoozabadi et al. [35, 39] Their approach was based on relation (7.10), where the transport coefficients were defined with respect to a reference component. The following equation for the thermal diffusion factor was obtained:

$$\alpha_i^T = \frac{M_i M_n}{MRTL_{ii}} \sum_{j=1}^{n-1} L_{ij} \left(\begin{array}{c} \left(\frac{u_n}{\tau_n M_n} - \frac{u_j}{\tau_j M_j}\right) \\ + \left(\frac{\sum z_k u_k/\tau_k}{\sum z_k V_k}\right)\left(\frac{V_j}{M_j} - \frac{V_n}{M_n}\right) \end{array} \right) \quad (i = 1, ..., n-1) \quad (7.19)$$

where L_{ij} are the phenomenological coefficients, calculated from:

$$\sum_{l=1}^{n-1}\sum_{k=1}^{n-1} \frac{(M_k z_k + M_n z_n \delta_{lk})}{M_k} \frac{\partial \ln f_k}{\partial z_j} L_{li} = \frac{c M_n z_n}{R} D_{ij} \quad (i, j = 1, ..., n-1) \quad (7.20)$$

where f_k is the fugacity of component k in the mixture and D_{ij} the binary diffusion coefficient obtained from equation (7.20). The authors used the model of Kooijman and Taylor [60] to calculate the molecular diffusion coefficients. For the case of ideal mixtures the authors proposed the following expression:

$$\alpha_i^T = \frac{M_i M_n}{MRT}\left(\frac{u_n}{\tau_n M_n} - \frac{u_i}{\tau_i M_i} + \frac{\sum z_k u_k/\tau_k}{\sum z_k V_k}\left(\frac{V_i}{M_i} - \frac{V_n}{M_n}\right)\right) \quad (i = 1, ..., n-1) \quad (7.21)$$

7.3 Comparison of different models

Let us compare different models for estimation of the thermal diffusion factor in multicomponent mixtures. For evaluation we selected a ternary system of alcanes. We evaluated the performance of different models for a simple system of n-Butane + n-Hexane + n-Decane under normal thermodynamic conditions.

A second comparison was carried out between the thermal diffusion factors predicted by the models and obtained by molecular dynamic simulations for the mixture

Methane + nPentane + n-Decane. The molecular dynamic simultaions are reported in [37].

We tested four different approaches in the framework of equation (7.17): the models of Kempers, both from 1989 [52] and 2002 [53]; the Haase model [44]; the Shukla and Firoozabadi expression [116] incorporated according to Kempers approach as shown in Table 7.2. At last, we incorporated the original expression of Firoozabadi, equation (7.21). Table (7.2) summarizes the equations evaluated.

7.3.1 n-Butane + n-Hexane + n-Decane

Figures 7.1, 7.3 and 7.2 show the results obtained for the six expressions presented in Table 7.2. The results are plotted as functions of the n-Hexane mole fraction. Each line represents different mole fractions of n-Decane. Figure 7.1 presents the thermal diffusion factor for n-Butane, Figure 7.3 for n-Hexane and Figure 7.2 for n-Decane. In each figure, plot (a) shows the results obtained with the Haase model, plots (b) and (c) with the first and second model of Kempers, and, finally, plots (d) and (e) show the results obtained with the Shukla and Firoozabadi model and the Firoozabadi et al. approach correspondingly.

From Figure 7.1 it may be observed that the Haase model is significantly different from other models. It predics positive values of the thermal diffusion factor for n-Butane. This is contrary to expectations, since small molecules are expected to go to the hot region, exhibiting negative thermal diffusion factors. On the other hand, this is what it is predicted by the rest of the models shown in Figure 7.1. Comparing the results obtained by both models of Kempers with those given by Shukla and Firoozabadi, we see that only the absolute values of the thermal diffusion factors differ. The model of Firoozabadi et al. shows a slight difference in the behavior.

Figure 7.2 shows thermal diffusion factors for n-Decane. Again, the models of Kempers, Shukla and Firoozabadi and Firoozabadi et al. predict positive thermal diffusion factors, as expected, while the Haase model predicts negative factors.

Finally, Figure 7.3 shows the thermal diffusion factor for the intermediate component, n-Hexane. In this case, the Haase model and the Firoozabadi et al. model exhibit positive thermal diffusion factor for the whole range of molar fractions, in

Table 7.2: Thermal diffusion expressions evaluated for multicomponent systems.

Model	Notation	Equation	Reference
Haase 1969	a_HAA69	$\sum_{j=1}^{n-1}\left(\frac{1}{M_i}\frac{\partial\mu_i}{\partial z_j}-\frac{1}{M_n}\frac{\partial\mu_n}{\partial z_j}\right)z_j(1-z_j)\alpha_j^T = \frac{h_n-h_n^0}{M_n}-\frac{h_i-h_i^0}{M_i}+RT\left(\frac{\alpha_i^{0,T}(1-z_i)}{M_i}-\frac{\alpha_n^{0T}(1-z_n)}{M_n}\right)$ $(i=1,..,n-1)$	[44]
Kempers 1989	a_KEM89	$\sum_{j=1}^{n-1}\left(\frac{1}{v_i}\frac{\partial\mu_i}{\partial z_j}-\frac{1}{v_n}\frac{\partial\mu_n}{\partial z_j}\right)z_j(1-z_j)\alpha_j^T=\frac{h_n-h_n^0}{v_n}-\frac{h_i-h_i^0}{v_i}$ $(i=1,..,n-1)$	[52]
Kempers 2002	a_KEM02	$\sum_{j=1}^{n-1}\left(\frac{1}{v_i}\frac{\partial\mu_i}{\partial z_j}-\frac{1}{v_n}\frac{\partial\mu_n}{\partial z_j}\right)z_j(1-z_j)\alpha_j^T = \frac{h_n-h_n^0}{v_n}-\frac{h_i-h_i^0}{v_i}+RT\left(\frac{\alpha_i^{0,T}(1-z_i)}{v_i}-\frac{\alpha_n^{0T}(1-z_n)}{v_n}\right)$ $(i=1,..,n-1)$	[53]
Shukla and Firoozabadi	a_SHF98	$\sum_{j=1}^{n-1}\left(\frac{1}{\tau_i v_i}\frac{\partial\mu_i}{\partial z_j}-\frac{1}{\tau_n v_n}\frac{\partial\mu_n}{\partial z_j}\right)z_j(1-z_j)\alpha_j^T=\frac{U_n-U_n^0}{\tau_n v_n}-\frac{U_i-U_i^0}{\tau_i v_i}$ $(i=1,..,n-1)$	[116]
Firoozabadi et al. 2000	a_FIR00	$\alpha_i^T=\frac{M_iM_n}{MRT}\left(\left(\frac{u_n}{\tau_nM_n}-\frac{u_i}{\tau_iM_i}\right)+\left(\frac{\sum z_k u_k/\tau_k}{\sum z_k V_k}\right)\left(\frac{V_i}{M_i}-\frac{V_n}{M_n}\right)\right)$ $(i=1,...,n-1)$	[35, 39]
$\tau_i = 4$ for $i = (1,..,n)$			

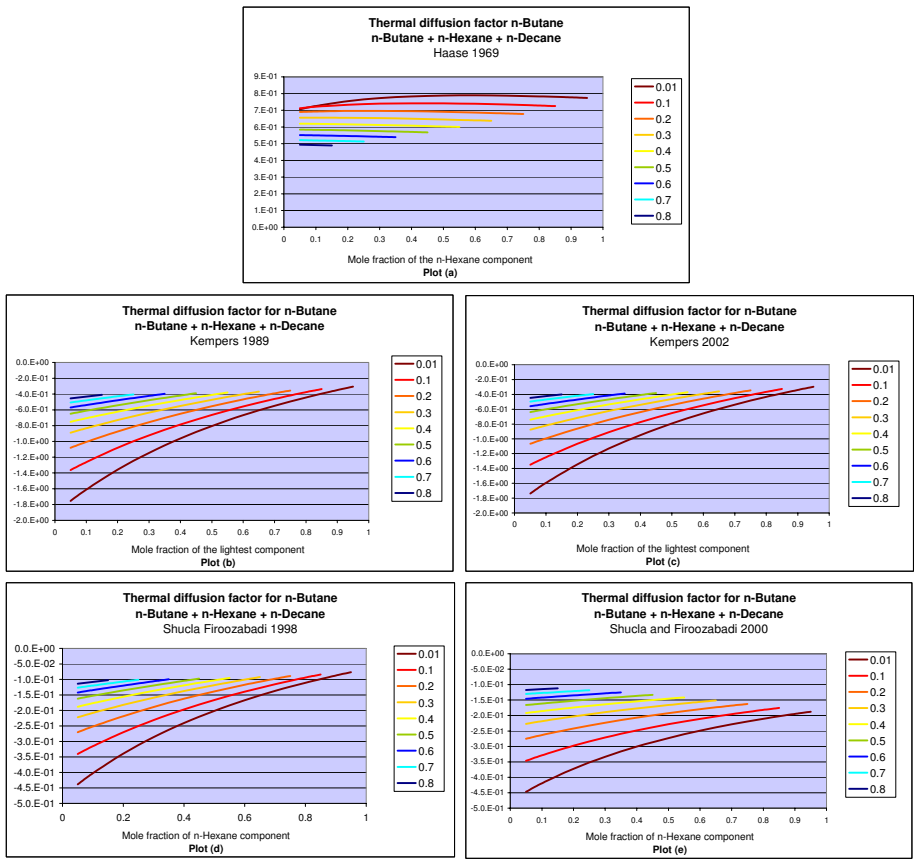

Figure 7.1: Thermal diffusion factor for n-Butane in the mixture n-Butane + n-Hexane + n-Decane under normal conditions. Plots (a) show the results obtained for the Haase model, Plots (b) and (c) show the results for the first and second model of Kempers correspondingly and Plots (d) and (e) show the results for the model of Shukla and Firoozabadi and the Firoozabadi et al. apporach.

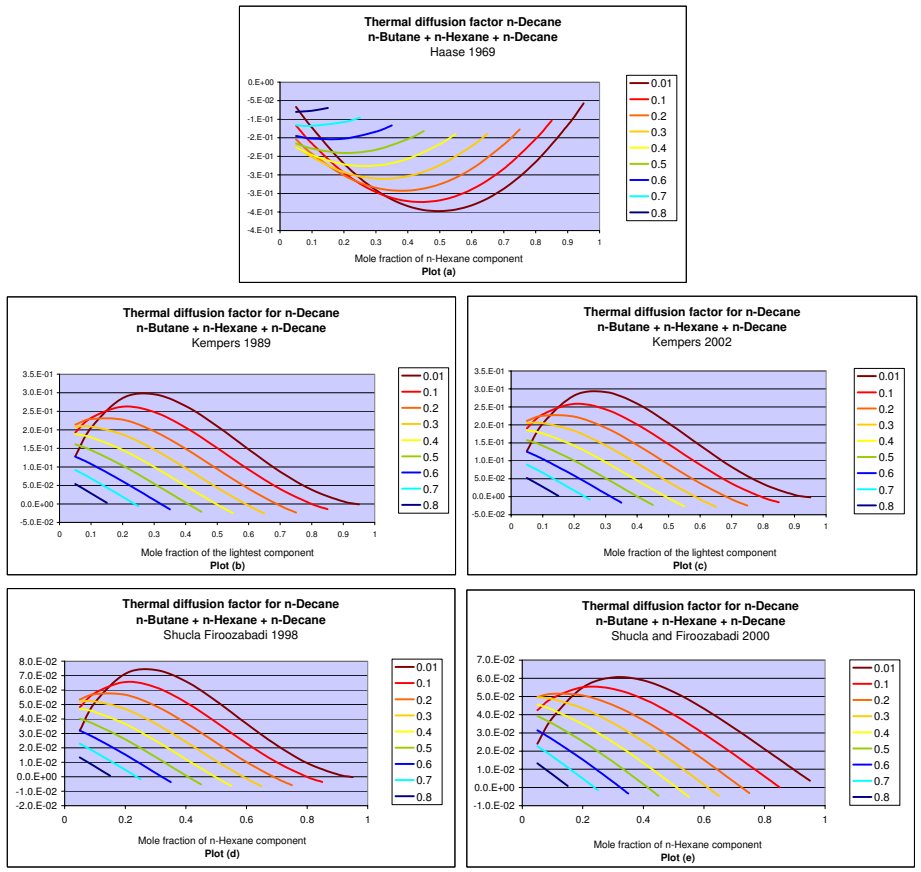

Figure 7.2: Thermal diffusion factor for n-Decane in the mixture n-Butane + n-Hexane + n-Decane under normal conditions. Plots (a) show the results obtained for the Haase model, Plots (b) and (c) show the results for the first and second model of Kempers correspondingly and Plots (d) and (e) show the results for the model of Shukla and Firoozabadi and the Firoozabadi et al. apporach.

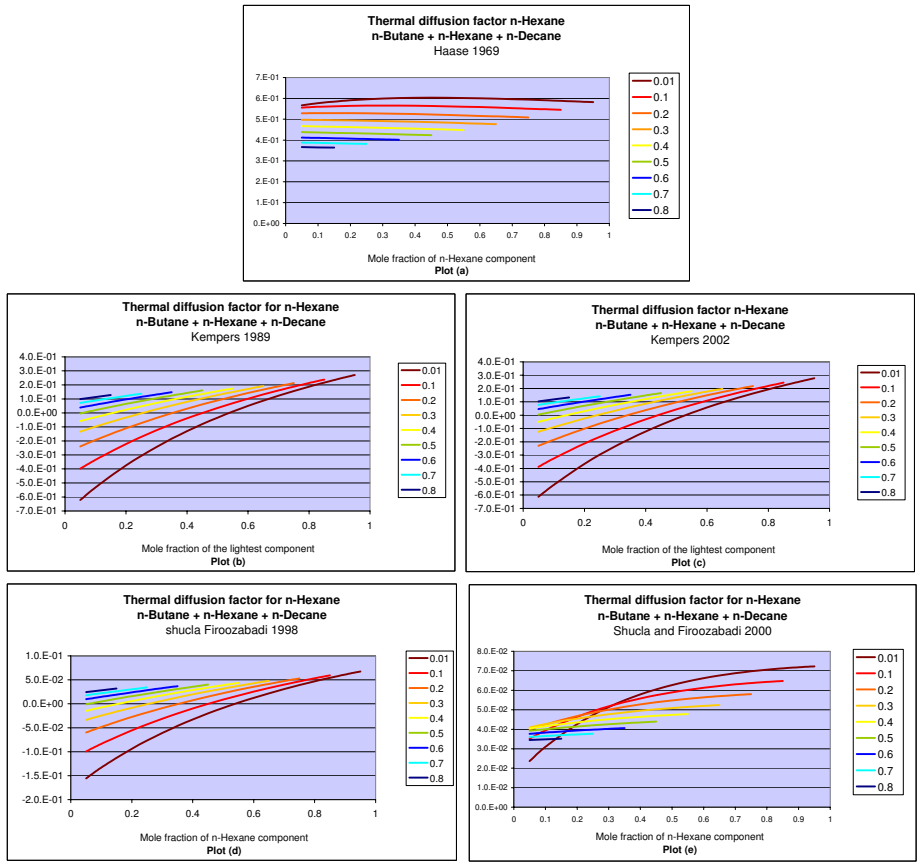

Figure 7.3: Thermal diffusion factor for n-Hexane in the mixture n-Butane + n-Hexane + n-Decane under normal conditions. Plots (a) show the results obtained for the Haase model, Plots (b) and (c) show the results for the first and second model of Kempers correspondingly and Plots (d) and (e) show the results for the model of Shukla and Firoozabadi and the Firoozabadi et al. apporach.

contradiction to other models. As to the rest of the models, change of sign is observed in relation not only with the concentration of n-Hexane, but also with the concentration of n-Decane. The thermal diffusion factor is mainly positive for high concentrations of n-Decane.

In conclusion, both approaches of Kempers and the extension of the Shukla and Firoozabadi model give most reasonable results. Change of the sign of the thermal diffusion factor for the intermediate component is exhibited as a function of composition. Similar behavior was also observed for ideal gas mixtures in Chapter 6.

7.3.2 Methane + n-Pentane + n-Decane

Molecular dynamics calculations of the thermal diffusion factor in binary and ternary alcane mixtures close to the critical point are described in [37]. Here we test the models in comparison with the data obtained in [37]. These data are obtained for constant reduced properties: $T^r = 2.273$, $\rho^r = 0.4227$, and $P^r = 1.018$.

To estimate the real temperature and pressure needed for calculations we used the following definitions:

$T^r = \frac{k_B T}{\varepsilon_x}$; $\rho^* = \frac{N\sigma_x^3}{V}$; $P^* = \frac{P\sigma_x^3}{\varepsilon_x}$;

where T^r, ρ^r and P^r are the reduced temperature, reduced density and reduced pressure correspondingly, k_B is the Boltzmann constant, N is the number of particles, V is the volume of the simulation box, σ_x is the typical atomic diameter of the studied mixture, and ε_x is the potential parameter. The last two variables were calculated by the van der Walls one-fluid approximation, applying equations (6.31) and (6.32). The evaluated data points are presented in Table 7.3.

The thermal diffusion factor was estimated for each component in the mixture, as in the previous example. The results are plotted as functions of the mole fraction of Methane. Figure 7.4 shows the results presented in the literature for the thermal diffusion factor obtained for Methane by molecular dynamic simulations. Figure 7.5 presents the results obtained by six different models described in Table 7.2.

Table 7.3: Data points for the evaluation of the thermal diffusion factor near the critical point

T (K)	P (atm)	$z_{Methane}$	$z_{nPentane}$	$z_{nDecane}$
887.75	213.59	0.07	0.47	0.47
825.62	217.19	0.17	0.42	0.42
722.40	225.08	0.33	0.33	0.33
619.84	236.78	0.50	0.25	0.25
518.50	255.92	0.67	0.17	0.27
419.92	292.78	0.83	0.08	0.08
363.98	337.27	0.93	0.03	0.03

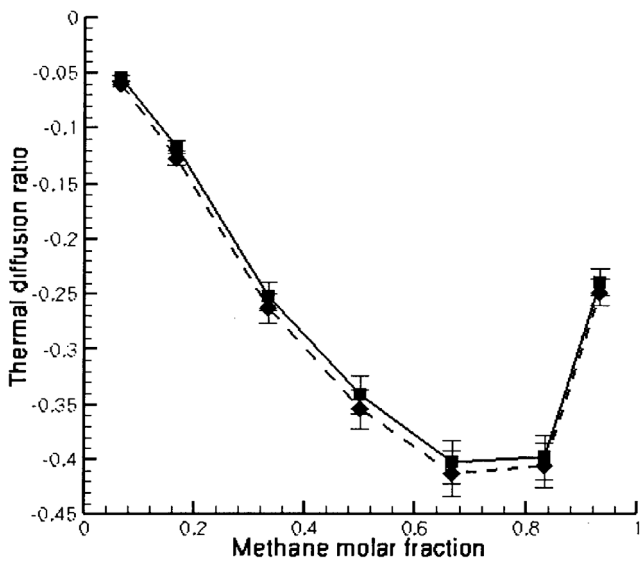

Figure 4. Methane thermal diffusion ratios for various methane molar fractions in a ternary methane–*n*-pentane–*n*-decane mixture (■) and in an 'equivalent' binary mixture (◆) at $T^* = 2.273$ and $\rho^* = 0.4227$.

Figure 7.4: Results obtained by molecular dynamics simulation for the thermal diffusion factor for Methane in the ternary mixture Methane + n-Pentane + n-Decane. Reproduced from [37].

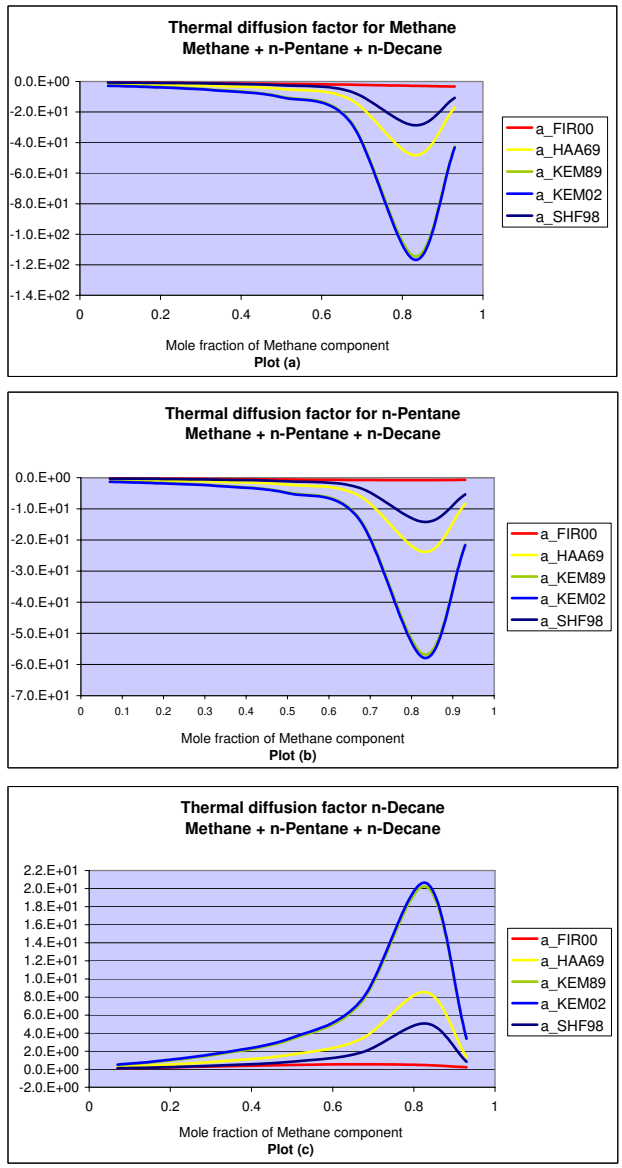

Figure 7.5: Thermal diffusion factor for the ternary mixture Methane + n-Pentane + n-Decane near the critical point. Plot (a) presents the thermal diffusion factor for Methane, Plot (b) for n-Pentane and correspondingly Plot (c) for n-Decane. The Haase model by *a_HAA69*; the Shukla and Firoozabadi model by *a_SHF98*; the Firoozabadi et al. model by *a_FIR*00; the Kempers model from 1989 by *a_KEM*89; and finally the Kempers model from 2002 by *a_KEM02*.

It may be observed that the thermal diffusion factor is negative both for Methane and n-Pentane, while for n-Decane it has a positive value. For small mole fractions of Methane the thermal diffusion coefficient is quite small and starts increasing when its concentration increases. A maximum (or minimum) value is observed for $z_{Methane} = 0.83$. The models based on equation (7.17) show trends similar to the molecular dynamic simulation data. A minimum value for the thermal diffusion factor for Methane exists in both cases. However, the decreasing slope is much smaller for the simulations. The Firoozabadi expression, equation (7.21), does not exhibit the same type of behavior.

7.4 Conclusions

We presented the problems that appear when studying the thermal diffusion effect in multicomponent mixtures. Study of the transformation from mass fraction to mole fraction has resulted in the conclusion that in multicomponent systems the mass thermal diffusion factors and the molar thermal diffusion factors are not equal and should be defined separately. Different parameters used for describing the thermal diffusion effect were presented for this type of mixtures.

Most of the existing models for calculating the thermal diffusion factor are of the same mathematical structure, except for the approach given by Firoozabadi et al. [35]. A general formula was presented, from which different approximations may be derived. Different models were compared on the example of an alcane mixture under normal thermodynamic conditions. The general formula exhibited a change of sign when working with volume coordinates. The model using the mass framework predicted oposite values to those obtained with the volume reference. The same models were also compared with the results of molecular dynamic simulations. It was observed that the trend for the thermal diffusion factor for the lightest component was qualitatively reproduced by all the models derived from the general equations (7.17) and (7.18). However, the absolute values differ largely from those obtained by molecular simulations.

Chapter 8

Conclusions and Recommendations for Future Work

We have presented a comparison between different models available in the literature and the reported experimental data for binary mixtures, much more extensive than similar comparisons, which may be found in the literature. The analysis led to the conclusion that, although none of the models can correctly describe the thermal diffusion factor for all the mixtures, we can use the Haase expression as a first estimation. This model predicted the correct sign for 70% of the mixtures. The model of Shukla and Firoozabadi in some cases gives better approximations than the Haase approach; however, it was observed that in such cases the Haase approach does not differ largely from the previous model. The Kempers models, on the other hand, are capable to correctly predict the sign of the thermal diffusion factor as well as the Shukla and Firoozabadi approach; however, they overestimate the thermal diffusion factors compared to the experimental data. The standard errors of the models are in general very large, with only some exceptions. Even the orders of magnitude and the signs cannot be trusted.

The thermal diffusion factors are extremely sensitive to the values of the partial molar properties and, thus, to the EoS selected. There is a need for improving the existing equations of state in such a way that they are not only capable to predict the phase equilibria, but also the partial molar properties with a high degree of accuracy. This is a well-known limitation for the presently available EoS.

Our work was complicated by the fact that the experimental data on thermal diffusion coefficients are not always reliable. For the same systems the experimental values reported may present large deviations. This is due to the fact that in the measurement of the thermal diffusion effect, it is difficult to avoid convection. Several techniques have been suggested to avoid convection, but only in the past years researchers had achieved to reproduce the experimental data using different setups. Unfortunately, these data is very scarce and it will take some years to measure and collect reliable experimental data. Experiments in microgravity conditions may help to establish what corrections are needed (for convection perturbations), when measuring the thermal diffusion effect on the Earth.

It was the goal of the new approach presented in Chapter 5 to provide a solid theoretical base for estimating the transport coefficients. General properties of the thermal diffusion coefficients were established in the framework of this theory. Diffusion coefficients have been shown to give very good approximations with respect to experimental values once the coefficients of the penetration length were estimated. Based on those results, we believed that it is possible to obtain equally good results for the thermodiffusion. However, further modeling work is required in order to provide realistic predictable evaluation of these coefficients. The theory should further be tested with regard to the agreement with the basic observations and empirical laws, which have been reported for the thermal diffusion coefficients.

When studying thermodiffusion in multicomponent systems, several inconsistencies arise. First, we estimated the thermal diffusion ratio for ideal gas mixture. The expressions for the thermal diffusion coefficients, both for binary and multicomponent mixtures, were presented by Hirschfelder et al. Comparison between the models and the experiments for binary mixtures, drove us to the conclusion that the pseudo-binary formulation applied to multicomponent systems gave very good approximations to the experimental points. However, the consistency requirement could not be satisfied by the multicomponent formulations. Unfortunately, no experimental data was found for multicomponent gas mixtures, in order to check the results. It may be concluded that thermodiffusion in multicomponent systems is not described correctly by the formulae shown in Hirschfelder et al. Therefore we

recommend a careful application of these formulae and implementation of one of the pseudo-binary formula instead.

The theory for non-ideal multicomponent systems also contains some inconsistencies. Two different thermal diffusion coefficients have been defined: a mass thermal diffusion factor and a molar thermal diffusion factor. For binary systems these coefficients are equal. An alternative definition of the thermal diffusion coefficients was suggested, very closely linked to the Stefan-Maxwell picture of the multicomponent transport.

Generalized formulae for calculating the thermal diffusion factors in multicomponent systems were derived. Different models were obtained from these formulae according to the framework used (mass or volume) and according to different expressions for heats of transport. Comparison between the models showed that a reasonable behavior was obtained when working with the volume framework, for which the intermediate component exhibited a change of sign for the thermal diffusion factor, while the heaviest component went to the cold region and the lightest component to the hot region. Opposite results were obtained for the mass framework. In comparison with the results of molecular dynamic simulations, similar trends were obtained with different expressions derived from the general formulation. Both the thermodynamic models and the molecular dynamic simulations showed a minimum around the same mole fraction. However, the absolute values of the thermal diffusion factors differed largely from each other.

Comparing the results obtained for binary and for multicomponent systems, we conclude that only the Shukla and Firoozabadi model is most likely to give the best approximation. However, due to the lack of experimental data, we can not make any definite statement. The sensitivity of the thermodynamic models to the EoS used and possible inaccuracy of the EoS with regards to thermodynamic properties remains the main problem there. Therefore, we believe that the main direction of modeling of the thermal diffusion coefficients should be associated with development of the thermodynamic equations of state providing reliable and stable evaluation of the partial molar properties and their derivatives. Furthermore, more experimental data is required for the mixtures both for simple binary mixtures and for ternary

systems. As was already mentioned, the new approach should be further tested with regards to derivatives and the equations of state used. And, finally, a careful revision of the theoretical basis for the thermal diffusion effect for multicomponent systems is required.

List of Symbols

C_i Molecular velocity for component i

c_k Mass fraction of component k

CN_k Coordination number for component k

cp_k Heat capacity for component k

D_{kj} Binary isothermal diffusion coefficient for components k and j

D_k^T Thermal diffusion coefficient for component k

E_k^{vap} Vaporization energy for component k

$\mathbf{f}$ Thermodynamic matrix

f_k Fraction of nearest neighbors for component k

F_k External forces over the component k

g Gravity constant

$\mathbf{G}$ System of coordinates matrix

H Molar enthalpy of the mixture

h_k Partial molar enthalpy for component k

h_0 Reference enthalpy

J_c Mass exchange flux due to chemical reaction

J_k Mass flux of component k

J_q Heat flux

J_k^q Mass flux due to Soret effect

J_q^k Heat flux due to Dufour effect

k_k^T Thermal diffusion ratio for component k

$\mathbf{L}$ Diffusion Matrix

L_D Diffusion matrix for binary mixture

L_{DT} Thermal diffusion matrix for binary mixture

L_{ij} Phenomenological coefficients

$\mathbf{L_N}$ Diffusion matrix

$\mathbf{L_{UN}}$ Thermally induce mass transfer matrix

$\mathbf{L_{NU}}$ Convective energy transfer matrix

$\mathbf{L_{UU}}$ Energy transfer matrix

M Total mass of the mixture

M_k Molecular weight of component k

m_k Mass of component k

Nah Avogadro's number

N_k Mole density of component k

n_k Number of moles of component k

Om Accentric factor

P Pressure of the system

P_C Critical pressure

P^r Reduce pressure

Q_k^* Heat transported by component k - Heat of transport

R Gass constant

S Total entropy of the system

s Specific entropy of the system

s_o Reference entropy

S^T Soret coefficient

t Time variable

T Mean temperature of the mixture

T_C Critical temperature

T^r Reduce temperature

U Internal energy of the system

u Specific internal energy

Ua_k Activation energy for component k

Ue Excess internal energy

u_k Partial internal energy for component k

V Total volume of the system

v Specific volume of the system

v_k Partial molar volume

$\mathbf{v}$ Velocity vector

X_k Force associated to flux J_k

X_u Force associated to flux J_q

Z_k Molecular penetration length for component k

Z_u Energy penetration length

z_k Mole fraction for component k

Greek Letters

α^T Thermal diffusion factor

α^{0T} Thermal diffusion factor in ideal gas mixtures

χ_{ij} Matrix form by the derivatives of the internal energy

Δhf_k Enthalpy of formation of component k

Δsf Entropy of formation of component k

ϕ_i Activation energy

η Viscosity of the mixture

μ_k Chemical potential of component k

μ_0 Reference chemical potential

ρ Density of the mixture

ρ^r Reduce density

υ_k Rate of reaction

ψ_k Volume ratio of component k

Abbreviations

$2Chamber$ Two chamber cell

CPA Cubic Plus Association equation of state

$C-TGC$ Concentric Thermogravitational column

EoS Equation of state

$Diph-cell$ Diaphragma cell

LDV Laser Doppler Velocimeter

$P - Diaph - cell$ Pressure Diaphragma cell

$P - TGC$ Parallel Thermogravitational column

$Pk - cell$ Packed Thermodiffusion cell

$Pk - TGC$ Packed Thermogravitational column

PR Peng-Robinson equation of state

SRK Soave - Redlich-Kwong equation of state

$TDFRS$ Thermal Diffusion Force Rayleigh Scattering

$ThFFF$ Thermal Field Flow Fractionation

Appendix A

Input data for pure components

Table A.1: Input data used in the calculations

Component	M_i (kg/mol)	om (-)	T_C (K)	P_C (bar)	σ (Å)	ε/k (K)	T_{br} (K)	Ref.
Methane	16.040	0.0110	190.40	46.00	3.758	148.60	111.60	[96]
Water	18.015	0.3440	647.30	221.20	2.641	809.10	373.20	[96]
Methanol	32.040	0.5560	512.60	80.90	3.626	481.80	337.70	[96]
Diethylamine	73.130	0.3115	496.50	37.10	5.433[a]	374.72[a]	328.60	[96]
Ethanol	46.070	0.6440	513.92	61.40	4.530	362.60	351.40	[96]
n-Butane	58.123	0.1990	425.20	38.00	4.687	531.40	272.70	[96]
2 Propanol	60.100	0.6650	508.30	47.60	5.039[a]	383.62[a]	355.40	[96]
n-Pentane	72.150	0.2510	469.70	33.70	5.784	341.10	309.20	[96]
2butanol	74.123	0.5770	536.10	41.80	5.356[a]	404.60[a]	372.70	[96]
n-Butyl alcohol	74.120	0.5930	563.10	44.20	5.345[a]	424.98[a]	390.90	[96]
Carbon Disulfide	76.131	0.1090	552.00	79.00	4.483	467.00	319.00	[96]
Benzene	78.114	0.2120	562.16	48.90	5.349	412.30	353.20	[96]
Cyclohexane	84.160	0.2120	553.50	40.70	6.182	297.10	353.80	[96]
n-Hexane	86.178	0.2990	507.50	30.10	5.949	399.30	341.90	[96]
2 Methylpentane	86.178	0.2780	497.50	30.10	5.829[a]	375.47[a]	333.40	[96]
2,2 Dimethylbutane	86.178	0.2320	488.80	30.80	5.751[a]	368.91[a]	322.80	[96]
2,3 Dimethylbutane	86.178	0.2470	500.00	31.30	5.763[a]	377.36[a]	331.10	[96]
3 Methylpentane	86.178	0.2720	504.50	31.20	5.787[a]	380.75[a]	336.40	[96]
Toluene	92.141	0.2630	591.80	41.00	5.572[a]	446.64[a]	383.80	[96]
Isobutyl Chloride	92.570	0.2487[b]	504.53	37.59	5.438[a]	380.78[a]	327.91	[132]
n-Butyl Chloride	92.570	0.2180	542.00	36.80	5.609[a]	409.06[a]	351.60	[96]
[a] Lennard-Jones potentials calculated according to Chung et al. method [96]								
[b] Accentric factor calculated according to Reid et al. [96]								

Component	M_i (kg/mol)	om (-)	T_C (K)	P_C (bar)	σ (Å)	ε/k (K)	T_{br} (K)	Ref.
sec-Butyl Chloride	92.570	0.3000	520.60	39.50	5.405[a]	392.91[a]	341.40	[96]
tert-Butyl Chloride	92.570	0.1900	507.00	39.50	5.358[a]	382.64[a]	324.00	[96]
cis-Dichloroethylene	96.940	0.2219[b]	537.00	56.00	4.862[a]	405.28[a]	333.30	[96]
trans-Dichloroethylene	96.940	0.2320	513.00	48.10	5.037[a]	387.17[a]	321.90	[96]
1,1 Dichloroethane	98.960	0.2400	523.00	50.70	4.981[a]	394.72[a]	330.50	[96]
1,2 Dichloroethane	98.960	0.2780	566.00	53.70	5.017[a]	427.17[a]	356.70	[96]
Cyclohexanol	100.160	0.5280	625.00	37.50	5.845[a]	471.70[a]	434.30	[96]
i-Heptane	100.204	0.3290	530.40	27.30	6.152[a]	400.30[a]	363.20	[96]
n-Heptane	100.204	0.3490	540.30	27.40	6.182[a]	407.77[a]	371.60	[96]
Triethylamine	101.193	0.3200	535.00	30.30	5.959[a]	403.77[a]	362.50	[96]
Hexanol	102.170	0.5600	611.00	40.50	5.654[a]	461.13[a]	430.20	[96]
Ethylbenzene	106.167	0.3020	617.20	36.00	5.901[a]	465.81[a]	409.30	[96]
m-Xylene	106.167	0.3250	617.10	35.40	5.933[a]	465.74[a]	412.30	[96]
o-Xylene	106.167	0.3100	630.30	37.30	5.872[a]	475.70[a]	417.60	[96]
p-Xylene	106.167	0.3200	616.20	35.10	5.947[a]	465.06[a]	411.50	[96]
Chloro Benzene	112.559	0.2490	632.40	45.20	5.514[a]	477.28[a]	404.90	[96]
n-Octane	114.232	0.3980	568.80	24.90	6.493[a]	429.28[a]	398.80	[96]
nitroBenzene	123.110[b]	0.3364[b]	715.80	32.40	6.421[a]	540.23[a]	482.81	[110]
n-Nonane	128.260	0.4450	594.60	22.90	6.776[a]	448.75[a]	424.00	[96]
Tetrahydronaphtalene	132.200	0.3030	719.00	35.10	6.261[a]	542.64[a]	480.70	[96]
Isobutylbenzene	134.220	0.3800	650.00	31.40	6.283[a]	490.57[a]	445.90	[96]
n-Butyl Bromide	137.200	0.3389[b]	542.61	42.55	5.346[a]	409.51[a]	357.08	[132]
n-Decane	142.280	0.4890	617.70	21.20	7.042[a]	466.19[a]	447.30	[96]
Carbon Tetra Chloride	153.822	0.1926	556.35	45.00	5.947	322.70	349.90	[96]
Ethyl Iodide	155.967	0.1843[b]	554.00	47.00	5.208[a]	418.11[a]	345.60	[110]
Bromo Benzene	157.010	0.2510	670.00	45.20	5.621[a]	505.66[a]	429.20	[96]
1122-TetraChloroethane	167.850	0.3088[b]	661.20	58.40	5.138[a]	499.02[a]	419.40	[96]
Dodecane (C12H26)	170.330	0.5750	658.20	18.20	7.567[a]	496.75[a]	489.50	[96]

n-Butyl Iodide	184.200	0.2680^{b}	588.27	37.92	5.707^{a}	443.98^{a}	384.06	[132]
1,2 dibromo ethane	187.860	0.7950	646.00	53.50	5.250^{a}	487.55^{a}	404.70	[96]
n-Tetradecane	198.390	0.5810	693.00	14.40	8.324^{a}	523.02^{a}	526.70	[96]
n-Pentadecane	212.410	0.7060	707.00	15.20	8.230^{a}	533.58^{a}	543.80	[96]
n-Hexadecane	226.440	0.7420	722.00	14.10	8.498^{a}	544.91^{a}	560.00	[96]
n-Octadecane	254.490	0.7900	748.00	12.00	9.073^{a}	564.53^{a}	589.50	[96]
Carbon Tetra Bromide	331.630	0.4954^{b}	757.88	96.31	4.552^{a}	571.98^{a}	483.69	[132]
1122-Tetrabromoethane	345.650	0.5384^{b}	770.42	66.97	5.166^{a}	581.45^{a}	511.2	[132]
n-Octadecane								
Carbon Tetra Bromide								

Appendix B
Results of the calculations for non-ideal binary mixtures

The Appendix is found on the attached CD.

Appendix C

Third approximation for k^T in binary ideal gas

$$S_{00} = \begin{vmatrix} s_{-2-2} & s_{-2-1} & s_{-21} & s_{-22} \\ s_{-1-2} & s_{-1-1} & s_{-11} & s_{-12} \\ s_{1-2} & s_{1-1} & s_{11} & s_{12} \\ s_{2-2} & s_{2-1} & s_{21} & s_{22} \end{vmatrix}$$

$$S_{01} = \begin{vmatrix} s_{-2-2} & s_{-2-1} & s_{-20} & s_{-22} \\ s_{-1-2} & s_{-1-1} & s_{-10} & s_{-12} \\ s_{1-2} & s_{1-1} & s_{10} & s_{12} \\ s_{2-2} & s_{2-1} & s_{20} & s_{22} \end{vmatrix}$$

$$S_{0-1} = \begin{vmatrix} s_{-2-2} & s_{-20} & s_{-21} & s_{-22} \\ s_{-1-2} & s_{-10} & s_{-11} & s_{-12} \\ s_{1-2} & s_{10} & s_{11} & s_{12} \\ s_{2-2} & s_{20} & s_{21} & s_{22} \end{vmatrix}$$

$$s_{00} = 8\frac{M_1 M_2 \Omega_{12}^{(1,1)*}}{(M_1 + M_2)^2}$$

$$s_{01} = s_{10} = 8\frac{\sqrt{2M_1} M_2^2 \left(\frac{5}{4}\Omega_{12}^{(1,1)*} - \frac{3}{2}\Omega_{12}^{(1,2)*}\right)}{(M_1 + M_2)^{\frac{5}{2}}}$$

$$s_{20} = s_{02} = 4\frac{\sqrt{2M_1}M_2^3}{(M_1+M_2)^{\frac{7}{2}}}\left(\frac{35}{8}\Omega_{12}^{(1,1)*} - \frac{21}{2}\Omega_{12}^{(1,2)*} + 6\Omega_{12}^{(1,3)*}\right)$$

$$s_{-10} = s_{0-1} = -\left(\frac{M_1}{M_2}\right)^{\frac{3}{2}} s_{01}$$

$$s_{0-2} = s_{-20} = -\left(\frac{M_1}{M_2}\right)^{\frac{5}{2}} s_{02}$$

$$s_{11} = -\frac{8M_2}{(M_1+M_2)^3}\left(\frac{5}{8}(6M_1^2+5M_2^2)\Omega_{12}^{(1,1)*} - \left(\frac{15}{2}\Omega_{12}^{(1,2)*} - 6\Omega_{12}^{(1,3)*}\right)M_2^2 + 2M_1M_2\Omega_{12}^{(2,2)*}\right)$$
$$+4\Omega_{12}^{(2,2)*}\sqrt{\frac{2M_2}{M_1+M_2}}\left(\frac{\sigma_{11}}{\sigma_{12}}\right)^2\frac{z_2}{z_2}$$

$$s_{21} = s_{12} = \frac{8M_2^2}{(M_1+M_2)^4}\begin{pmatrix} \frac{35}{32}(12M_1^2+5M_2^2)\Omega_{12}^{(1,1)*} \\ -\frac{63}{16}(4M_1^2+5M_2^2)\Omega_{12}^{(1,2)*} \\ +\frac{57}{2}M_2\Omega_{12}^{(1,3)*} - 15M_2^2\Omega_{12}^{(1,4)*} \\ +7M_1M_2\Omega_{12}^{(2,2)*} \\ -8M_1M_2\Omega_{12}^{(2,3)*} \end{pmatrix}$$
$$+\sqrt{\frac{2M_2}{M_1+M_2}}\left(7\Omega_{11}^{(2,2)*} - 8\Omega_{11}^{(2,3)*}\right)\left(\frac{\sigma_{11}}{\sigma_{12}}\right)^2\frac{z_1}{z_2}$$

$$s_{-21} = s_{1-2} = -\frac{8\sqrt{M_1^5M_2^3}}{(M_1+M_2)^3}\begin{pmatrix} \frac{595}{32}\Omega_{12}^{(1,1)*} - \frac{567}{16}\Omega_{12}^{(1,2)*} - \frac{57}{2}\Omega_{12}^{(1,3)*} \\ -15\Omega_{12}^{(1,4)*} - 7\Omega_{12}^{(2,2)*} + 8\Omega_{12}^{(2,3)*} \end{pmatrix}$$

$$s_{22} = \frac{8M_2^2}{(M_1+M_2)^5}\begin{pmatrix} \frac{35}{128}(40M_1^4+168M_1^2M_2^2+35M_2^4)\Omega_{12}^{(1,1)*} \\ -\frac{21}{16}M_2^2(84M_1^2+35M_2^2)\Omega_{12}^{(1,2)*} \\ +\frac{3}{4}M_2(108,M_1^2+133M_2^2)\Omega_{12}^{(1,3)*} - 105M_2^4\Omega_{12}^{(1,4)*} \\ +45M_2^4\Omega_{12}^{(1,5)*} + \frac{7}{2}M_1M_2(4M_1^2+7M_2^2)\Omega_{12}^{(2,2)*} \\ -56M_1M_2^3\Omega_{12}^{(2,3)*} + 40M_1M_2^3\Omega_{12}^{(2,4)*} + 12M_1^2M_2^2\Omega_{12}^{(3,3)*} \end{pmatrix}$$
$$+\sqrt{\frac{2M_2}{M_1+M_2}}\left(\frac{77}{4}\Omega_{11}^{(2,2)*} - 28\Omega_{11}^{(2,3)*} + 20\Omega_{11}^{(2,4)*}\right)\left(\frac{\sigma_{11}}{\sigma_{12}}\right)^2\frac{z_1}{z_2}$$

$$s_{2-2} = s_{-22} = \frac{8(M_1 M_2)^{\frac{5}{2}}}{(M_1 + M_2)^5} \begin{pmatrix} \frac{8505}{128}\Omega_{12}^{(1,1)*} - \frac{2499}{16}\Omega_{12}^{(1,2)*} \\ +\frac{723}{4}\Omega_{12}^{(1,3)*} - 105\Omega_{12}^{(1,4)*} + 45\Omega_{12}^{(1,5)*} \\ +\frac{77}{2}\Omega_{12}^{(2,2)*} + 56\Omega_{12}^{(2,3)*} \\ -40\Omega_{12}^{(2,4)*} - 12\Omega_{12}^{(3,3)*} \end{pmatrix}$$

Appendix D

Second approximation for D^T in ideal gas

$$L_{ii}^{00} = 0$$

$$L_{ij}^{00} = \frac{2z_1z_2}{A_{12}^*[\lambda_{ij}]_1} + \sum_{k\neq i}\frac{2z_iz_jM_j}{M_iA_{12}^*[\lambda_{ij}]_1}\ i \neq j$$

$$L_{ii}^{01} = 5\sum_{k\neq i}\frac{z_iz_kM_k\left(\frac{6}{5}C_{ij}^* - 1\right)}{\left(M_i + M_j\right)A_{ik}^*[\lambda_{ij}]_1}$$

$$L_{ij}^{10} = \frac{M_i}{M_j}L_{ij}^{01}$$

$$L_{ii}^{11} = -\frac{4z_i^2}{[\lambda_i]_1} - \sum_{k\neq i}\frac{2z_iz_k\left(\frac{15}{2}M_i^2 + \frac{25}{4}M_k^2 - 3M_k^2B_{ik}^* + 4M_iM_kA_{ik}^*\right)}{(M_i+M_k)^2A_{ik}^*[\lambda_{ik}]_1}$$

$$L_{ij}^{11} = \frac{2z_iz_j\left(\frac{55}{4} - 3B_{ij}^* - 4A_{ik}^*\right)}{(M_i+M_j)^2} \quad i \neq j$$

Appendix E

Third approximation for D^T in ideal gas

$$Q_{ij}^{00} = 8\sqrt{\frac{\pi RT}{2}} \begin{pmatrix} \sum_j \frac{z_i z_j \Omega_{ij}^{(1,1)*} \sigma_{ij}^2}{\sqrt{M_i+M_j}} \left(\delta_{ik}\sqrt{\frac{M_j}{M_i}} - \delta_{kj}\right) \\ -\frac{z_k}{z_i}\sqrt{\frac{M_k}{M_i}} \sum_j \frac{z_i z_j \Omega_{ij}^{(1,1)*} \sigma_{ij}^2}{\sqrt{M_i+M_j}} \left(\sqrt{\frac{M_j}{M_i}} - \delta_{ij}\right) \end{pmatrix}$$

$$Q_{ij}^{01} = 8\sqrt{\frac{\pi RT}{2}} \sum \frac{z_i z_j \sigma_{ij}^2 \left(\frac{5}{4}\Omega_{12}^{(1,1)*} - \frac{3}{2}\Omega_{12}^{(1,2)*}\right)}{(M_i+M_j)^{\frac{3}{2}}} \left(\delta_{ij} M_j \sqrt{\frac{M_j}{M_i}} + \delta_{kj} M_i\right)$$

$$Q_{ij}^{10} = Q_{ij}^{01}$$

$$Q_{ij}^{02} = 4\sqrt{\frac{\pi RT}{2}} \sum z_i z_j \sigma_{ij}^2 \delta_{ik} \sqrt{\frac{M_j^5}{M_i(M_i+M_j)^5}} \left(\frac{35}{4}\Omega_{12}^{(1,1)*} - \frac{14}{3}\Omega_{12}^{(1,2)*} + \Omega_{ij}^{(1,3)*}\right)$$

$$Q_{ij}^{20} = Q_{ij}^{02}$$

$$Q_{ij}^{11} = 8\sqrt{\frac{\pi RT}{2}}\sum_j \frac{z_i z_j M_i M_j \sigma_{ij}^2}{(M_i+M_j)^{\frac{5}{2}}} \begin{pmatrix} \frac{\delta_{ij}}{\sqrt{M_i^3 M_j}} \begin{pmatrix} \frac{5}{6}(6M_i^2+5M_2^2)\Omega_{ij}^{(1,1)*} \\ -M_j^2\left(\frac{10}{3}\Omega_{ij}^{(1,2)*}+\Omega_{ij}^{(1,3)*}\right) \\ +4M_iM_j\Omega_{ij}^{(2,2)*} \end{pmatrix} \\ -\delta_{ij}\begin{pmatrix} \frac{55}{4}\Omega_{ij}^{(1,1)*}-\frac{10}{3}\Omega_{ij}^{(1,2)*} \\ +\Omega_{ij}^{(1,3)*}-4\Omega_{ij}^{(2,2)*} \end{pmatrix} \end{pmatrix}$$

$$Q_{ij}^{12} = 8\sqrt{\frac{\pi RT}{2}}\sum_j \frac{z_i z_j \sigma_{ij}^2}{(M_i+M_j)^{\frac{7}{2}}} \begin{pmatrix} \delta_{ij}\sqrt{\frac{M_j}{M_i^5}} \begin{pmatrix} \frac{35}{32}(12M_i^2+5M_2^2)\Omega_{ij}^{(1,1)*} \\ -\frac{63}{16}\left(4M_i^2+5M_j^2\right)\Omega_{12}^{(1,2)*} \\ +\frac{57}{2}M_j^2\Omega_{ij}^{(1,3)*}+15M_iM_j\Omega_{ij}^{(1,4)*} \\ +7M_iM_j\Omega_{ij}^{(2,2)*}-6M_iM_j\Omega_{ij}^{(2,3)*} \end{pmatrix} \\ -\delta_{ij}M_i^2M_j\begin{pmatrix} \frac{595}{32}\Omega_{ij}^{(1,1)*}-\frac{567}{16}\Omega_{ij}^{(1,2)*} \\ +\frac{57}{2}\Omega_{ij}^{(1,3)*}-15\Omega_{ij}^{(1,4)*} \\ +7\Omega_{ij}^{(2,2)*}-8\Omega_{ij}^{(2,3)*} \end{pmatrix} \end{pmatrix}$$

$$Q_{ij}^{21} = Q_{ij}^{12}$$

$$Q_{ij}^{22} = 8\sqrt{\frac{\pi RT}{2}}\sum_j \frac{z_i z_j (M_iM_j)^2\sigma_{ij}^2}{(M_i+M_j)^{\frac{9}{2}}}$$

$$\begin{pmatrix} \frac{\delta_{ij}M_j}{(M_iM_j)^{\frac{5}{2}}} \begin{pmatrix} \frac{35}{128}(40M_i^4+168M_i^2M_j^2+35M_j^4)\Omega_{ij}^{(1,1)*} \\ -\frac{21}{16}M_j^2(84M_i^2+35M_j^2)\Omega_{ij}^{(1,2)*} \\ -\frac{3}{4}M_j^2(108M_i^2+133M_j^2)\Omega_{ij}^{(1,3)*} \\ -105M_j^4\Omega_{ij}^{(1,4)*}+45M_j^4\Omega_{ij}^{(1,5)*} \\ -\frac{7}{2}M_iM_j(4M_i^2+7M_j^2)\Omega_{ij}^{(2,2)*}-56M_iM_j^3\Omega_{ij}^{(2,3)*} \\ +40M_iM_j^3\Omega_{ij}^{(2,4)*}+12M_i^2M_j^2\Omega_{ij}^{(3,3)*} \end{pmatrix} \\ -\delta_{ij}\begin{pmatrix} \frac{8505}{128}\Omega_{ij}^{(1,1)*}-\frac{2499}{16}\Omega_{ij}^{(1,2)*} \\ +\frac{723}{4}\Omega_{ij}^{(1,3)*}-105\Omega_{ij}^{(1,4)*} \\ +45\Omega_{ij}^{(1,5)*}-\frac{77}{2}\Omega_{ij}^{(2,2)*}+56\Omega_{ij}^{(2,3)*} \\ -40\Omega_{ij}^{(2,4)*}+12\Omega_{ij}^{(3,3)*} \end{pmatrix} \end{pmatrix}$$

$$R_i = \frac{15}{4} z_i \sqrt{\frac{2k_B T}{m_i}}$$

Bibliography

[1] C. Allain, P. Lallemand, C.R. Hebd. (1977). Principle of a method to determine the thermal diffusion ratio using forced Rayleigh scattering . Seanc. Acad. Sci. Paris, **285**(8), 187-190

[2] S. Alves, G. Demouchy, A. Bee, D. Talbot, A. Bourdon, A.M. Figueiredo Neto. (2003). Investigation of the sign of the Soret coefficient in different ionic and surfacted magnetic colloids using forced Rayleigh scattering and single-beam Z-scan techniques. Philosophical Magazine, **83**, (17-18), 2059-2066

[3] N. Arnaud, J. Georges. (2001). On the analytical use of the Soret-enhanced thermal lens signal in acqueous solutions. Analytical Chimica Acta, **445**, 239-244

[4] S. Barta. (1996). Thermodiffusion and thermo-electric phenomena in condensed systems. Int. J. Heat Mass Transf., **39**, (16), 3531-3542

[5] R.J. Bearman, J.G. Kirkwood, M. Fixman. (1958). Statistical-Mechanical theory of transport processes. 10. The heat transport in binary liquid solutions. Advances in Chemical Physics, **1**, 1-13

[6] P. S. Belton, H. J. V. Tyrrell. (1971). Thermal diffusion in mixtures of alcohol and aromatic hydrocarbons. Z. Naturforsch, **26a**, 48-51

[7] L.B. Benano-Melly, J.P. Caltagirone, B. Faissat, F. Montel, P. Costeseque. (2001). Modelling Soret coefficient measurement experiments in porous media considering thermal and solutal convection. International Journal of Heat and Mass Transfer, **44**, 1285-1297

[8] M.M. Bou-Ali, O. Ecenarro, J.A. Madariaga, C.M. Santamaria, J.J. Valencia. (1999). Soret coefficient of some binary liquid mixtures. J. Non-Equilibrium Thermodynamics, **24**, 228-233

[9] M.M. Bou-Ali, J.J. Valencia, J.A. Madariaga, C. Santamaria, O. Encenarro, J.F. Dutrieux. (2003). Determination of the thermodiffusion coefficient in three binary organic liquid mixtures by the thermogravitational method (Contribution of the Universidad del Pais Vasco, Bilbao, to the benchmark test). Philosophical Magazine, **83**, (17-18), 2011-2015

[10] D. Braun, A. Libchaber. (2002). Trapping of DNA by thermophoretic depletion and convection. Physical review letters, **89**, (19), 188103-1 - 188103-4

[11] C. Ceballo, R. Martinez, A. Escalona. (1999). Characterization of petroleum asphaltenes by thermal field flow fraction using modied mobile phases. Petroleum Science and Technology, **17**, (7-8), 783-810

[12] R. Cerbino, A. Vailati, M. Giglio. (2003). Fast-onset Soret-driven convection in a colloidal suspension heated from above. Philosophical Magazine, **83**, (17-18), 2023-2031

[13] J. Chan, J.J. Popov, S. Kolisnek-Kehl, D.G. Leaist. (2003). Soret coefficients for aqueous polyethylene glycol solutions and some test of the segmental model of polymer thermal diffusion. J. of Solution Chemistry, **3e**(3), 197-214

[14] S. Chapman, T.G. Cowling. (1970). The Mathematical Theory of Non-Uniform Gases, 3rd edn. (Cambridge)

[15] K. Chen, H. Jiang, J. Chen., D. Yin. (1997). Thermal diffusion of vortices ans self-organized criticality. Solid State Communications, **101**, (1), 67-70

[16] K. Clusius, M. Huber. (1955). Das Trennrohr.14. Die Trennschaukel-Thermodiffusions-Faktoren im system CO2/H2. Z. Naturforsch. Teil A, **10**, (3), 230- 238

[17] J. Colombani, J. Bert. (1999). Convection Thermohaline et effect Soret dans le Chlorure de Lithium Aqueux Concentré. Entropie, **218**, 35-38

[18] P. Costeseque. (1982). PhD thesis: Sur la migration selective des isotopes et des elements par thermodiffusion dans les solutions. Application de l'effect thermogravitationnel, Universite Paul Sabatier, Tolouse, France.

[19] P. Costeseque, J.C. Loubet. Measuring the Soret coefficient of binary hydrocarbon mixtures in packed thermogravitaional columns (Contribution of Toulouse University to the benchmark test). Philosophical Magazine, 83, (17-18), 2017-2022

[20] P. Costeseque, S. Gaillard, Y. Gachet, Ph. Jamet. Determination of the apparent negative Soret coefficient of water-10% alcohol solutions by experimental and numerical methods in packed cells. Philosophical Magazine, 83, (17-18), 2039-2044

[21] E.L. Cussler. (2000). Diffusion Mass Transfer in fluid systems. Second edition, Cambridge.

[22] B.J. de Gans, R. Kita, S. Wiegand, J. Luettmer-Strathmann. (2003). Unusual thermal diffusion in polymer solutions. Physical Review Letters, **91**, (24), 245501-1 - 245501-4

[23] S.R. de Groot. (1952). Thermodynamics of Irreversible Processes. (Amsterdam)

[24] DSSC proyect. Diffusion and Soret coefficients measurement for improvement of oil recovery. (2002). Carried out by Microgravity Research Centre, Université Libre de Bruxelles, Belgique

[25] K.G. Denbigh, (1951). The Thermodynamics of the Steady State, London: Methuen & Co. LDT.

[26] J. K. G. Dhont. (2004). Thermodiffusion of interacting colloids. I. A statistical thermodynamic approach. J. Chem. Phys., **120**, (3), 1632-1641

[27] E.L. Dougherty, H.G. Drickamer. (1955). A theory of thermal diffusion in liquids. J. Chem. Phys., **23**, (2), 295-309

[28] E.L. Dougherty, H.G. Drickamer. (1955). Thermal diffusion and molecular motion in liquids. J. Chem.Phys., **59**, 443-449

[29] P. J. Dunlop, C. M. Bignell. (1995). Prediction of gaseous diffusion coefficients from thermal diffusion measurements an other experimental data. J. Chem. Phys., **102**, 5781-5784

[30] J.F. Dutrieux, J.K. Platten, G. Chavepeyer, M.M. Bou-Ali. (2002). On the measurement of positive Soret coefficients. J. Phys. Chem. B, **106**, 6104-6114

[31] O. Encenarro, J.A. Madariaga, J.L. Navarro, C.M. Santamaria, J.A. Carrion, J.M. Saviron. (1993). Thermogravitational separation and the thermal diffusion factor near critical points in binary liquid mixtures. J. Physical Condens. Matter, **5**, 2289-2294

[32] ESA. http://www.estec.esa.nl/spaceflight/map/map/oilrecov.htm

[33] G. Eshel. (). http://geosci.uchicago.edu/~gidon/geosci245/thermohal/thermohaline.html

[34] K. H. Simmrock, R. Janowsky, A. Ohnsorge. (1986). Critical data of pure substances - Chemistry Data Series. Vol. II, Part 1.

[35] A. Firoozabadi, K Ghorayeb, K Shukla. (2000). Theoretical model of thermal diffusion factors in multicomponent mixtures. AIChE Journal, **46**, (5), 892-900

[36] M. Franko, C. D. Tran. (1989). Temperature effect on photothermal lens phenomena in water: photothermal defocousing and focousing. Chem. Phys. Letters, **158**, (12), 31-36

[37] G. Galliero, B. Duguay, J.P. Caltagirone, F. Montel. (2003). Philosophical Magazine, **83**, (17-18), 2097- 2108

[38] Ph. Georis, F. Montel, S. Van Vaerenbergh, Y. Decroly, J.C. Legros. (1998). Measurement of the Soret coefficient in crude oil. SPE International, 50573, 57-66

[39] K. Ghorayeb, A. Firoozabadi. (2000). Molecular, pressure and thermal diffusion in non-ideal multicomponent mixtures. AIChE Journal, **46**, (5), 883-891

[40] M. Giglio, A. Vendramini. (1974). Thermal lens effect in a binary liquid mixture: A new effect. Applied Physics Letters, **25**, (10), 555-557

[41] M. Gonzalez-Bagnoli, A. Shapiro, O.O. Medvedev, E.H. Stenby. (2004). Submitted for publication at The European Physical Journal E (EPJE). Proceeding of the 6th International Meeting on Thermodiffusion.

[42] M. Gonzalez-Bagnoli, A. Shapiro, E.H. Stengby. (2003). Evaluation of the thermodynamics models for the thermal diffusion factor, Philosophical Magazine, **83**, (17-18), 2171-2183

[43] H. Guo, F. Liu, G.J. Smallwood, Ö. Gülder. (2004). A numerical investigation of thermal diffusion influence on soot formation in Ehylene/Air diffusion flames. International Journal of Computational Fluid Dynamics, **18**,(2), 139-151

[44] R. Haase. (1969). Thermodynamics of Irreversible Processes, Addison Welsey Publishing Company. London.

[45] R. Haase, H.W. Borgmann, K.H. Dücker, W.P. Lee. (1971). Thermodiffusion in critical evaporation range of binary systems. Z. Naturf (a), **26**, (7), 1224-&

[46] J.M. Hellemans, J. Kestin, S.T. RO. (1974). Physica, 71, 1-

[47] J.O. Hirschfelder, C.H. Curtis, R.B. Bird. (1967). Molecular Theory of Gases and Liquids, 4th. edn. John Wiley & Sons. New York.

[48] A.E. Humphreys, E.A. Mason. (1970). Intermolecular forces: Thermal diffusion and diffusion in Ar-Kr. The Physics fo Fluids, **13**, (1), 65-70

[49] International Critical Tables, McGraw-Hill Book Company Inc., New York

[50] Ph. Jamet, D. Fargue, P. Costeseque. (1996). Determination of the effective transport coefficients for the separation of binary mixtures of organic compounds into packed thermal diffusion columns. Chemical Engineering Science, **51**, (19), 4463-4475

[51] J. Janca. (2003). Micro-thermal field-flow fractionation: new challenge in experimental studies of thermal diffusion of polymers and colloidal particles. Philosophical Magazine, **83**, (17-18), 2045-2058

[52] L.J.T.M. Kempers. (1989). A thermodynamic theory of the Soret effect in a multicomponent liquid. J. Chem. Phys., **90**, (11), 6541-6548

[53] L.J.T.M. Kempers. (2001). A comprehensive thermodynamic theory of the Soret effect in a multicomponent gas, liquid or solid. J. of Chem. Phys. **15**, (11), 6330-6341

[54] J.M. Kincaid, E.G.D. Cohen, M. Lopez de Haro. (1987). The Enskog theory for multicomponent mixtures. IV. Thermal diffusion. J. Chem. Phys., **86**, (2), 963-975

[55] J.M. Kincaid, M. Lopez de Haro, E.D.G. Cohen. (1983). The Enskog theory for multicomponent mixtures. II. Mutual diffusion. J. Chem Phys., **79**, (9), 4509-4521

[56] N. Kobayashi, Y. Enokida, I. Yamamoto. (2001). Isotopic approximation to thermal diffusion factor and ordinary diffusion coefficients in a mixture of more than 4 components. J. Nucl. Sci. Technol., **38**, (8), 682-688

[57] W. Kohler. (1993). Thermodiffusion in polymer solutions as observed by forced Rayleigh scattering. J. Chem. Phys., **98**, (1), 660-668

[58] K.J. Kolb, H.V. Frey, S.E.H. Sakimoto. (2003). A model for near-surface groundwater on Mars. http://academy.gsfc.nasa.gov/2003/ra/kolb/poster-details.pdf

[59] G. M. Kontogeorgis, E. C, Voutsas, I.V. Yakaumis, D.P. Tassios. (1996). An equation of state for associating fluids. Ind. Eng. Chem. Res., **35**, 4310-4318

[60] H.A. Kooijman, R. Taylor. (1991). Estimation of Diffusion coefficients in multicomponent liquid systems. Ind. Eng. Chem. Res., **30**, 1217-...

[61] C. Korte, J. Janek, H. Timm. (1997). Transport processes in temperature gradients. Thermal diffusion and Soret effect in crystalline solids. Solid State Ionics, **101-103**, 465-470

[62] H. Korsching. (1969). Soret-Koeffizienten von gemischen aus n-alkanen und cyclischen kohlenwasserstoffen. Z Naturforsch, **24a**, 444-446

[63] J.P. Larre, J. K. Platten, G. Chavepeyer. (1997). Soret effects in ternary systems heated from below. Int. J. heat mass transfer, **40**, (3), 545-555

[64] J. C. Legros, W. A. Van Hook, G. Thomaes. (1968). Thermal diffusion in $CHBr_2 \bullet CHBr_2$-$CHCl_2 \bullet CHCl_2$ solutions. Chem. Phys. Letters, **2**, (4), 251-252

[65] J. C. Legros, D. Rasse, G. Thomaes. (1970). Convection and thermal diffusion in a solution heated from below. Systems CCl_4- C_6H_{12}; H_2O- CH_3OH; H_2O - C_2H_5OH. Chem. Phys. Letters, **4**, (10), 632-634

[66] J. C. Legros, D. Rasse, G. Thomaes. (1972). Thermal diffusion in a flowing layer with normal and adverse temperature gradients in the CCl_4-C_6H_6system. Physica, **57**, 585-593

[67] J. C. Legros, P. Potty, G. Thomaes. (1973). Thermal diffusion in the two-component fluid Benard problem. Physica, **64**, 481-496

[68] J. C. Legros, P. Goemaere, J. K. Platten. (1985). Soret coefficient and the two-component Benard convection in the benzene-methanol system. Physica, **32**, (3), 1903-1905

[69] C. Leppla, S. Wiegand. (2003). Investigation of the Soret effect in binary liquid mixtures by thermal-diffusion-forced Rayleigh scattering (contribution to the Benchmark test). Philosophical Magazine, **83**, (17-18), 1989-1999

[70] D. Longree, J. C. Legros, G. Thomaes. (1977). Soret coefficient of liquified simple gases at low temperatures: the Kr-CH_4 system. Z. Naturforsch., **32**, 1061-1062

[71] D. Longree, J. C. Legros, G. Thomaes. (1980). Measured Soret coefficients for simple liquified gas mixtures at low temperature. J. Phys. Chem., **84**, 3480-3483

[72] M. Lopez de Haro, E.G.D. Cohen, J.M. Kincaid. (1983). The Enskog theory for multicomponent mixtures. I. Linear transport theory. J. Chem. Phys., **78**, (5), 2746-2759

[73] M. Lopez de Haro, E.G.D. Cohen. (1984). The Enskog theory for multicomponent mixtures. III. Transport properties of dense binary mixtures with one tracer component. J.Chem. Phys., **80**, (1), 408-415

[74] O.O. Medvedev, A.A. Shapiro. (2004). Modeling diffusion coefficients in binary mixtures. Accepted for publication in Fluid Phase Equilibria.

[75] J.Mollerup, M. Michaelsen. (2004). Thermodynamics Models: Fundamentals and Computational Aspects, 1st edn. Copenhagen.

[76] F. Montel, P.L. Gouel. (1985). Prediction of compositional grading in a reservoir fluid column. SPE 14410.

[77] F. Montel. (1993). Phase equilibria needs for petroleum exploration and production industry. Fluid Phase Equilibria, **84**, 343-367

[78] F. Montel, J. Bickert, J. Hy-Billiot, M. Royer. (2003). Pressure and compositional gradients in reservoirs. Annual SPE International Technical Conference and Exhibition in Abuja, Nigeria, August 4-6, (2003)

[79] H.A.W. Mubarek, P. Ashburn. (2003). Reduction of boron thermal diffusion in silicon by high energy fluorine implantation. Applied Physical letters, **83**, (20), 4134-4136

[80] A. K. Mukherjee, S. K. Sanyal. (1989). Thermal diffusion of acqueous alcohols. Can. J. Chem., **67**, 867-870

[81] NASA, http://liftoff.msfc.nasa.gov/shuttle/usmp4/

[82] M. Nguyen, R. Beckett, L. Pille, D.H. Solomon. (1998). Determination of thermal diffusion coefficients for polydisperse polymers and microgels by ThFFF and SEC-MALLS. Macromolecules, **31**, 7003-7009

[83] Penoloux, Rauzy. (1982).

[84] A. Perronace, C. Leppla, F. Leroy, B. Rousseau, S. Wiegand. (2002). Soret and mass diffusion measurements and molecular dynamics simulation of n-Pentane - n-Decane mixtures. J. Chem. Phys., **116**, (9), 3718-3729

[85] R. Piazza. (2003). Thermal diffusion in ionic micellar solutions. Philosophical Magazine, **83**, (17-18), 2067-2085

[86] J.K. Platten, M.M. Bou-Ali, J.F. Dutrieux. (2003). Precise determination of the Soret, thermodiffusion and isothermal diffusion coefficients of binary mixtures of dodecane, isobutylbenzene and 1,2,3,4-Tetrahydronaphtalene (contribution of the university of Mons to the Benchmark test). Philosophical Magazine, **83**, (17-18), 2001-2010

[87] J.K. Platten, M.M. Bou-Ali, P. Costeseque, J.F. Dutrieux, W. Kohler, C. Leppla, S. Wiengard, G. Wittko. (2003). Benchmark values for the Soret, thermal idffusion and diffusion coefficients of the three binary organic liquid mixtures. Philosophical Magazine, **83**, (17-18), 1965-1971

[88] Platten. (2004). Presentation in IMT6, Varenna, Italy

[89] M. Pons, S. Nonell, I. Garcia-Moreno, A. Costela, R. Sastre. (2004). Thermal diffusion coefficients of solid polymeric laser dye solutions: A time-resolved thermal lens study. http://www.photobiology.com/photobiology2000/nonell

[90] J.P. Praizey, S. Van Vaerenbergh, J.P. Garandet. (1995). Thermomigration experment on board EURECA. Adv. Space Res., **16**, (7), (7)205-(7)214

[91] J. Prausnitz, R. N. Lichtenthaler, E. Gomes de Azevedo. (1999). Molecular Thermodynamics of fluid-phase equilibria, 3rd edn.

[92] I. Prigogine. (1967). Introduction to Thermodynamics of Irreversible Processes, 3rd edn. (Interscience Publishers)

[93] I. Prigogine, L. de Brouckere, R. Amand. (1950). Recherches sur la thermodiffusion en phase liquide (premiere communication). Physica, **XVI**, (7-8), 577-598

[94] I. Prigogine, L. de Brouckere, R. Amand. (1950). Recherches sur la thermodiffusion en phase liquide (2e communication). Physica, **XVI**, (11-12), 851-860

[95] A.S. Rao. (2001). A unique model invoking soret effect for the origin of the deformed Proterozoic anorthositic massifs and the associated Fe-Ti oxide deposits. Eleventh Annual V.M. Goldschmidt Conference.

[96] R. Reid, J.M. Prausnitz, B.E. Poling. (1987). The Properties of Gases and Liquids, 4th edn. (Mc Graw Hill)

[97] W. J. Roos, W. M. Rutherford. (1969). Experimental verification, with Krypton, of the theory of the thermal-diffusion column for multicomponent systems. J. Chem. Phys., **50**, (1), 424-429

[98] W. M. Rutherford, H.G. Drickamer. (1954). Theory of themal diffusion in liquids and the use of pressure to investigate the theory. J. of Chem.Phys., **22**, (7), 1157-1165

[99] W. M. Rutherford, H.G. Drickamer. (1954). The effect of pressure on themal diffusion in n-paraffin hydrocarbon - CS_2 mixtures. J. of Chem.Phys., **22**, (8), 1284-1287

[100] W. M. Rutherford, E. L. Dougherty, H. G. Drickamer. (1954). Thermal diffusion in binary mixtures of CS_2 and hexane isomers. J. of Chem.Phys., **22**, (8), 1289-1292

[101] W. M. Rutherford, J.G. Roof. (1959). Thermal diffusion in Methane - n-Butane mixtures in the critical region. AIChE Journal, **63**, 1506-1511

[102] W. M. Rutherford. (1982). Numerical evaluation of thermal diffusion column coefficients. Computer & Chemical Engineering, **6**, (2), 111-114

[103] W. M. Rutherford. (1984). Effect of mass distribution on the isotopic thermal diffusion of substituted benzenes. J. Chem. Phys., **81**, (12), 6136-6139

[104] W. M. Rutherfored. (1987). Isotopic thermal diffusion of carbon disulfide in the liquid phase. J. Chem. Phys., **86**, (1), 397-399

[105] W. M. Rutherfored. (1987). Effect of masss distribution on isotopic thermal diffusion of benzene. J. Chem. Phys., **86**, (9), 5217-5218

[106] W. M. Rutherford. (1989). Effect of carbon and hydrogen isotopic substitutions on the thermal diffusion of benzene. J. Chem. Phys., **90**, (1), 602-603

[107] A.G. Shashkov, A.F. Zolotukhina, T.N. Abramenko, B.P. Mathur, S.C. Saxena. (1979). Thermal diffusion factor for binary gas systems: Ar-N_2, Ar-CO_2, He-H_2, He-N_2O, Kr-N_2O, and He-NH_3. J. Phys. B: Atom. Molec. Phys., **12**, (21), 3619-3630

[108] R. L. Saxton, E. L. Dougherty, H.G. Drickamer. (1954). Thermal diffusion in binary liquid mixtures of molecules of simple symmetry. J. Chem. Phys., **22**, (7), 1166-1168

[109] R. L. Saxton, H. G. Drickamer. (1954). Thermal diffusion in mixtures of tetrachloroethane with normal paraffin hydrocarbons. J. Chem. Phys., **22**, (8), 1287-1288

[110] K. H. Simmrock, R. Janowsky, A. Ohnsorge. (1986). Critical data of pure substances - Chemistry Data Series. Vol. II, Part 1. DECHEMA, Frankfurt.

[111] A.A. Shapiro, E.H. Stenby. (1999). Applications - Non-equilibrium segregation in petroleum reservoirs. Entropie, **217**, (35), 55-60

[112] A.A. Shapiro, E. H. Stenby (2000). Factorization of transport coefficients in macroporous media. Transport in Porous media, **41**, (3), 305-323

[113] A.A. Shapiro. (2003). Evaluation of diffusion coefficients in multicomponent mixtures by means of the fluctuation theory. Physica, A 320, 211-234

[114] A.A. Shapiro. (2004). Fluctuation theory for transport properties in multicomponent mixtures: thermodiffusion and heat conductivity. Physica, A 332, 151-157

[115] J. Shieh. (1969). Thermal diffusion and segmental motion in binary n-alkane systems. J. Phys. Chem., **73**, (5), 1508-1513

[116] K. Shukla, A. Firozaabadi. (1998). A new model of thermal diffusion coefficients in binary hydrocarbon mixtures. Ind. Engng Chem., Res., **37**, 3331-3342

[117] W. L. Taylor. (1989). A critique of Trennschaukel Operation, E. G. & G. mound Applied Tehcnologies, Report MLM-3586.

[118] W. L. Taylor, J. J. Hurly. (1992). Thermal diffusion factors and intermolecular potentials for noble gas-SF_6 systems. J. Chem. Phys., **98**, (3), 2291-2297

[119] G. Thomaes (1956). Thermodiffusion en phase condensee. Nouveau dispositif experimental pour la mesure du coefficient de Soret. J. Chimie Physique et de physico-chemie biologique SERIAL. **53**, 407-411

[120] G. Thomaes. (1956). Thermal diffusion near the critical solution point. J. Chem. Phys., **25**, (1), 32-33

[121] L. J. Tichacek, W. S. Kmak, H.G. Drickamer. (1956). Thermal diffusion in liquids; the effect of non-ideality ans association. J. Phys. Chem., **60**, 660-665

[122] R.D. Trengove, H.L. Robjohns, M.L. Bell, M.L. Martin, P.J. Dunlop. (1981). Thermal diffusion factor at 300K for seven binary noble gas systems containing Helium or Neon. Physica, **108A**, 488-501

[123] R.D. Trengove, P.J. Dunlop. (1982). Diffusion coefficients and thermal diffusion factors for five binary systems of Nitrogen and a Noble gas. Physica, **115A**, 339-352

[124] D.J. Trevoy, H.G. Drickamer. (1949). Diffusion in binary liquid hydrocarbon mixtures. J. Chem. Phys., **17**, (11), 1117-1120

[125] D.J. Trevoy, H.G. Drickamer. (1949). Thermal diffusion in binary liquid hydrocarbon mixtures. J. Chem. Phys., **17**, (11), 1120-1124

[126] S. Van Vaerenbergh, J.C. Legros, J.C. Dupin. (1995). First results of Soret coefficients measurement experiment. Adv. Space Res., **16**, (8), (8)69-(8)81

[127] S. Van Vaerenbergh, S.R. Coriell, G.B. McFadden, B.T. Murray, J.C. Legros. (1995). Modification of morphological stability by Soret diffusion. Journal of Crystal Growth, **147**, 207-214

[128] S. Van Vaerenbergh, J.P. Garandet, J.P. Praizey, J.C. Legros. (1998). Reference Soret coefficients of natural isotopes and diluted alloys of tin . Phys. Rev. E., **58**, (2), 1866-1873

[129] H. Yamakawa, N. Kobayashi, Y. Enokida, I. Yamamoto. (2000). Thermal diffusion factor for diatomic gas mixtures in multicomponent system. J. Nucl. Sci. Technol., **37**, (4), 397-404

[130] G. Wittko, W. Kohler. (2003). Precise determination of the Soret, thermal diffusion and mass diffusion coefficients of binary mixtures of dodecane, isobutylbenzene and 1,2,3,4-tetrahydronaphtalene by a holographic grating technique. Philosophical Magazine, **83**, (17-18), 1973-1987

[131] F. Zeng. (2002). Thermophoresis of spherical and non-spherical particles: a review of theories and experiments. Advances in Colloid and Interface Science, **97**, 255-278

[132] www.pirika.com/chem/TCPEE/TCPE-htm

Mariana Gabriela Gonzalez Bagnoli

Modeling the Thermal Diffusion Coefficients

ISBN: 87-91435-14-5